

A NUMERICAL SENSITIVITY ANALYSIS OF STREAMLINE SIMULATION

A Thesis

by

FADY RUBEN CHABAN HABIB

Submitted to the Office of Graduate Studies of
Texas A&M University
in partial fulfillment of the requirements for the degree of

MASTER OF SCIENCE

December 2004

Major Subject: Petroleum Engineering

A NUMERICAL SENSITIVITY ANALYSIS OF STREAMLINE SIMULATION

A Thesis

by

FADY RUBEN CHABAN HABIB

Submitted to the Office of Graduate Studies of
Texas A&M University
in partial fulfillment of the requirements for the degree of

MASTER OF SCIENCE

Approved as to style and content by:

Akhil Datta-Gupta
(Chair of Committee)

Daulat D. Mamora
(Member)

Richard Gibson
(Member)

Stephen A. Holditch
(Head of Department)

December 2004

Major Subject: Petroleum Engineering

ABSTRACT

A Numerical Sensitivity Analysis of Streamline Simulation.

(December 2004)

Fady Ruben Chaban Habib, B.S., Universidad Bicentennial de Aragua, Venezuela

Chair of Advisory Committee: Dr. Akhil Datta-Gupta

Nowadays, field development strategy has become increasingly dependent on the results of reservoir simulation models. Reservoir studies demand fast and efficient results to make investment decisions that require a reasonable trade off between accuracy and simulation time. One of the suitable options to fulfill this requirement is streamline reservoir simulation technology, which has become very popular in the last few years. Streamline (SL) simulation provides an attractive alternative to conventional reservoir simulation because SL offers high computational efficiency and minimizes numerical diffusion and grid orientation effects. However, streamline methods have weaknesses incorporating complex physical processes and can also suffer numerical accuracy problems.

The main objective of this research is to evaluate the numerical accuracy of the latest SL technology, and examine the influence of different factors that may impact the solution of SL simulation models. An extensive number of numerical experiments based on sensitivity analysis were performed to determine the effects of various influential elements on the stability and results of the solution. Those experiments were applied to various models to identify the impact of factors such as mobility ratios, mapping of saturation methods, number of streamlines, time step sizes, and gravity effects. This study provides a detailed investigation of some fundamental issues that are currently unresolved in streamline simulation.

DEDICATION

To my adored mother, my dear father's memory, my forever love Ana, my precious sisters, brother, nephews and nieces, and my unconditional friends.

ACKNOWLEDGMENTS

Firstly, I'd like to thank God for giving me the persistence and patience in demanding moments.

My special gratitude is extended to my advisor and committee chair, Dr. Akhil Datta-Gupta, for his friendship, continuous support, and outstanding technical guidance.

I'd like to thank Dr. Mamora and Dr. Gibson for being a part of my evaluation committee.

My forever gratefulness to Dr. Sonia Embid for her friendship and priceless help to start my graduate program.

Thanks to PDVSA Intevap for the economic support provided.

I am very proud to belong to the splendid (MCERI) research group in the Petroleum Engineering Department of Texas A&M, and I would like to express my gratitude to all the guys but especially to Dayo Oyerinde and Eduardo Jimenez for their unconditional technical support, fellowship and effort during the development of this work.

Thanks to the Harold Vance Department faculty and staff, and my new family at Texas A&M. It's been a fantastic experience to share with this entire amazing group of people.

Thank you.

TABLE OF CONTENTS

	Page
ABSTRACT.....	iii
DEDICATION.....	iv
ACKNOWLEDGMENTS	v
TABLE OF CONTENTS.....	vi
LIST OF TABLES	vii
LIST OF FIGURES	viii
CHAPTER	
I INTRODUCTION	1
1.1. Objective of Study.....	2
II LITERATURE REVIEW	3
2.1 Historical Context.....	3
2.2 Streamline Method.....	5
2.2.1. Streamline Method Governing IMPES Equations.....	7
2.2.2. Coordinate Transform.....	8
2.2.3. Time Stepping.....	10
2.2.4. Tracing Streamlines.....	11
III INFLUENTIAL ELEMENTS IN ACCURACY OF STREAMLINE MODELS	17
3.1. Reservoir Model Heterogeneity.....	17
3.2. Saturation Mapping Methods.....	18
3.2.1. Line to Block Saturation Mapping Method.....	21
3.2.2. Line to Line Saturation Mapping Method.....	22
3.3. Mobility Ratio Changes.....	23
3.4. Material Balance Calculation.....	24
3.5. Time Step Size.....	25
3.6. Number of Streamlines	26
3.7. Gravity Effect.....	27
IV SENSITIVITY ANALYSIS FOR INFLUENTIAL ELEMENTS IN ACCURACY OF STREAMLINE MODELS	31
4.1 Model Description	31
4.2 Effects of Saturation Mapping Methods.....	33
4.3 Effects of Time Step Size.....	40
4.4 Effects of Mobility Ratios (0.2, 0.5 and 10).....	43
4.5 Effects of Number of Streamlines.....	47
4.6 Effects of Gravity in Streamline Solution.....	67

CHAPTER	Page
V CONCLUSIONS AND RECOMMENDATIONS	104
5.1. Conclusions.....	104
5.2. Recommendations.....	104
REFERENCES	107
VITA	110

LIST OF TABLES

TABLE		Page
4.1	First stage cases for analysis.....	32
4.2	Cases distribution for number of streamlines analysis.....	48
4.3	Cases distribution for gravity effect analysis.....	69
4.4	Gravity number (N_g) based in K_v/K_h for gravity effect analysis.....	71

LIST OF FIGURES

FIGURE	Page
2.1	Finite difference cell showing XYZ definitions 12
2.2	Schematic showing the computation of exit point and travel time in 2D 15
3.1	Line to block saturation mapping 21
3.2	Line to line saturation mapping 22
3.3	Gravity effect for streamline model 27
3.4	Phase velocities of multiphase flow in streamline model 27
3.5	Operator splitting method 29
3.6	Operator splitting steps for gravity effect in streamline model 30
4.1	Quarter of a five-spot grid model description 31
4.2	Permeability distribution for heterogeneous model 33
4.3	Saturation profile by saturation mapping for homogeneous case and $M=0.2$ 34
4.4	Saturation profile by saturation mapping for homogeneous case and $M=0.5$ 35
4.5	Saturation profile by saturation mapping for homogeneous case and $M=10$ 36
4.6	Saturation profile by saturation mapping for heterogeneous case and $M=0.2$ 36
4.7	Saturation profile by saturation mapping for heterogeneous case and $M=0.5$ 37
4.8	Saturation profile by saturation mapping for heterogeneous case and $M=10$ 38
4.9	Water MBE by saturation mapping for homogeneous, $\Delta t=5$ and $M=0.5$ 39
4.10	Oil MBE by saturation mapping for homogeneous, $\Delta t=1$ and $M=0.5$ 39
4.11	Pressure profile by saturation mapping for homogeneous case and $M=5$ 41
4.12	Pressure profile by saturation mapping for homogeneous case and $M=10$ 41
4.13	Pressure profile by saturation mapping for heterogeneous case and $M=0.5$ 42
4.14	Pressure profile by saturation mapping for heterogeneous case and $M=10$ 42

FIGURE	Page
4.15 Saturation profile based on mobility changes-homogeneous, $\Delta t=1$ day.....	44
4.16 Saturation profile based on mobility change-homogeneous, $\Delta t=20$ days.....	44
4.17 Saturation profile based on mobility changes-heterogeneous, $\Delta t=1$ day.....	45
4.18 Saturation profile based on mobility changes-heterogeneous, $\Delta t=20$ days	46
4.19 Total oil production varying mobility ratios for homogeneous, $\Delta t=20$ days.	47
4.20 Line to block saturation mapping for 0.01, 0.05, 0.1 and 0.3 fractions of streamlines number and $M=0.5$ for homogeneous, $\Delta t=1$ day at 300 days.....	49
4.21 Line to block saturation mapping for 0.5, 0.8 and 1 fractions of streamlines number and $M=0.5$ for homogeneous, $\Delta t=1$ day at 300 days.....	50
4.22 Line to block mapping for 0.01 fraction of streamlines number and $M=0.5$ for homogeneous using different time step sizes at 300 days.....	51
4.23 Line to block mapping for 0.1 fraction of streamlines number and $M=0.5$ for homogeneous using different time step sizes at 300 days.....	51
4.24 Line to block mapping for 0.5 fraction of streamlines number and $M=0.5$ for homogeneous using different time step sizes at 300 days.....	52
4.25 Saturation mapping comparison by number of streamlines in homogeneous model for $\Delta t=1$ day	53
4.26 Saturation mapping comparison by number of streamlines in homogeneous model for $\Delta t=20$ days	54
4.27 Mobility comparison by streamlines number for line to block in homogeneous model at time step size of 1 day.....	56
4.28 Mobility comparison by streamlines number for line to block in homogeneous model at time step size of 20 days.....	57
4.29 Mobility comparison by streamlines number for line to line in homogeneous model at time step size of 1 day.....	58
4.30 Comparison using different numbers of streamlines in homogeneous model at time step size of 1 day (0.01 and 0.1 fractions)	59
4.31 Comparison using different numbers of streamlines in homogeneous model at time step size of 1 day (0.5 and 1 fractions)	60
4.32 Line to block saturation mapping for 0.01, 0.05, 0.1 and 0.3 fractions of streamlines number and $M=0.5$ for heterogeneous, $\Delta t=1$ day at 300 days.....	61
4.33 Line to block saturation mapping for 0.5, 0.8, and 1 fractions of streamlines number and $M=0.5$ for heterogeneous, $\Delta t=1$ day at 300 days.....	62

FIGURE	Page
4.34 Comparison by mobility ratios using different numbers of streamlines (0.01 and 0.1 fractions) in heterogeneous model at time step size of 1 day	63
4.35 Comparison by mobility ratios using different numbers of streamlines (0.5 and 1 fraction) in heterogeneous model at time step size of 1 day.....	64
4.36 Comparison by time step size using different numbers of streamlines (0.01 and 0.1 fractions) in heterogeneous with $M=0.5$	65
4.37 Comparison by time step size using different numbers of streamlines (0.5 and 1 fractions) in heterogeneous with $M=0.5$	66
4.38 Homogeneous line to block case without gravity effect and $M=0.5$	70
4.39 Homogeneous line to block varying K_v/K_h using $\rho_o=\rho_w*0.8$ at $\Delta t=20$ days	71
4.40 Homogeneous line to block varying K_v/K_h using $\rho_o=\rho_w*0.9$ at $\Delta t=20$ days	72
4.41 Homogeneous line to block varying K_v/K_h and using $\rho_o=\rho_w*0.8$ at $\Delta t=5$ days	73
4.42 Homogeneous line to block varying K_v/K_h and using $\rho_o=\rho_w*0.9$ at $\Delta t=5$ days	74
4.43 Homogeneous line to block for $K_v/K_h=1$ using different ρ_o and varying Δt	75
4.44 Homogeneous line to block for $K_v/K_h=0.1$ using different ρ_o and varying Δt	75
4.45 Homogeneous line to block for $K_v/K_h=0.01$ using different ρ_o and varying Δt	76
4.46 Homogeneous line to block for $K_v/K_h=1$ using different SegIT and varying Δt	77
4.47 Homogeneous line to block for $K_v/K_h=1$ using different SegIT at $\Delta t=20$ days	77
4.48 Homogeneous line to block for $K_v/K_h=1$ varying SegIT and ρ_o at $\Delta t=20$ days	78
4.49 Homogeneous line to block general comparison for $\Delta t=20$ days	79
4.50 Homogeneous line to line varying K_v/K_h and using $\rho_o=\rho_w*0.8$ at $\Delta t=20$ days	80
4.51 Homogeneous line to line varying K_v/K_h and using $\rho_o=\rho_w*0.9$ at $\Delta t=20$ days	81

FIGURE	Page
4.52 Homogeneous line to line for $K_v/K_h=1$ and varying ρ_o and Δt	82
4.53 Homogeneous line to line for $K_v/K_h=0.01$ and varying ρ_o and Δt	82
4.54 Homogeneous line to line for $K_v/K_h =0.01$ at different Δt	83
4.55 Homogeneous saturation mapping comparison varying SegIT	84
4.56 Homogeneous with $q_{inj}=50$ Bbls/D varying K_v/K_h	85
4.57 Homogeneous with $q_{inj}=50$ Bbls/D varying K_v/K_h and $\rho_o=\rho_w*0.9$	86
4.58 Homogeneous with $q_{inj}=50$ Bbls/D varying time step size	87
4.59 Homogeneous with $q_{inj}=50$ Bbls/D varying time step size at $\rho_o=\rho_w*0.9$	88
4.60 Homogeneous with $q_{inj}=50$ Bbls/D varying SegIT value.....	89
4.61 Homogeneous line to line with $q_{inj}=50$ Bbls/D using different Δt	90
4.62 Homogeneous line to block at same PVI using $\Delta t=20$ days.	92
4.63 Homogeneous line to block at same PVI using $\Delta t=5$ days.	93
4.64 PermX distribution for heterogeneous model in gravity cases.	94
4.65 Heterogeneous line to block varying K_v/K_h and using $\rho_o=\rho_w*0.8$ at $\Delta t=20$ d.....	95
4.66 Heterogeneous line to block varying K_v/K_h and using $\rho_o=\rho_w*0.9$ at $\Delta t=20$ d.....	96
4.67 Heterogeneous line to block varying K_v/K_h and Δt	97
4.68 Heterogeneous line to block varying K_v/K_h and SegIT for $\Delta t=20$ days.	98
4.69 Heterogeneous line to block varying K_v/K_h and SegIT for $\Delta t=5$ days.	99
4.70 Heterogeneous line to block using $\rho_o=\rho_w*0.9$ and varying SegIT for $\Delta t=5$ d.	100
4.71 Heterogeneous saturation mapping comparison varying K_v/K_h	101
4.72 Heterogeneous saturation mapping comparison for a higher injection	102

CHAPTER I

INTRODUCTION

Reservoir simulation based on streamlines modeling has acquired more importance in the past few years. This allows numerical simulation the ability to model flow through complex reservoir geometry and reservoir characteristics.

Recent studies in streamline-based flow simulators have shown many of the applications of this reservoir simulation approach. It can be mentioned that this kind of simulators are now fully 3D and account for multiphase flow gravity and fluid mobility as well as compressibility effects. Another improvement is that the methodology can now account for changing well conditions due to rate changes, infill drilling, producer-injector conversions, and well abandonment.

The new advances in streamline (SL) methods are turning it into a common tool to assist in the modeling and forecasting of oil reservoir fields. With the passing of time this technology has grown in application and has been available to a larger group of practitioners in the oil industry.

Some of the fundamental issues for the streamline technique are related to the numerical accuracy provided by the simulator. These factors are associated with elements like saturation mapping, mobility changes, material balance error, time step size, number of streamlines used in the model, gravity effects and others.

Latest advances in streamline based flow simulation have overcome many of previous streamline and streamtube methods¹⁻². Now this technology has matured and has become very useful; but despite the improvements SL still has some elemental issues currently unresolved.

Oil industry continues searching for the most suitable use of streamlines methods and how to integrate them into the current exploration and exploitation projects of the companies. In future, we will see broadening of the application of the technology because all the advantages shown by streamline simulation.

1.1. Objective of Study

Because of the increasing interest in this technology our general objective in this research is to investigate the numerical accuracy and efficiency during streamline modeling for two phase fluid flow. The specific objectives are:

- To analyze the effects of saturation mapping methods during streamline simulation.
- To describe the impact of the mapping on material balance and solution accuracy.
- To generate conclusive results using sensitivity analysis with respect to various parameters in streamlines models to determine their effects in the reservoir performance.
- A detailed study of modeling gravity by operator splitting and its effectiveness.
- Compare the results with commercial finite difference simulators to examine the accuracy of all the involved calculations.

CHAPTER II

LITERATURE REVIEW

2.1 Historical Context

Nowadays, streamlines models are very popular and commonly applied in reservoir simulation studies; nevertheless this technology has been in the literature since Muskat and Wyckoff's 1934 paper and has received repeated attention since then.

We can mention that the current 3D streamline simulation technology originated from four previous methods to model convection-dominated flow in the reservoir:

1. Line Source/Sink Solutions: These methods have been widely used by the petroleum industry³⁻⁴. They use analytic solutions to the pressure and velocity distribution in the reservoir. The primary limitation of these methods is the requirement for homogeneous properties and constant reservoir thickness.

2. Streamtubes: Requires tracking of tube geometry. These methods are more general and have been applied successfully for field-scale modeling of waterflooding and miscible flooding⁵⁻⁷. Here the flow domain is divided into a number of streamtubes and fluid-saturation calculations are performed along these streamtubes. However, the need to keep track of the streamtube geometries can become quite cumbersome in three dimensions. Thus, application of streamtubes is for 2D or some hybrid approach and has the difficult to extend to 3-D.

3. Particle Tracking: These methods have been used by the oil industry to model tracer transport in hydrocarbon reservoirs and also for groundwater applications⁸. These methods track the movement of a statistically significant collection of particles along appropriate pathlines; while they generally work well near steep fronts, they do not work

as well for smooth profiles. Another drawback is the loss of resolution of the front with the progression of time and the statistical variance in the concentration response.

4. Front Tracking Methods: These methods involve complications arising from the topology of the fronts, difficult to extend to 3-D and introduce fluid fronts as a degree of freedom in computation⁸⁻⁹.

Later, streamline method's evolution has involved several improvements and advances mentioned below:

1. Fully three-dimensional, heterogeneous media (Pollock, 1988). Pollock¹⁰ proposed a linear interpolation of the velocity field within a grid block which significantly improved the original Runge-Kutta streamline tracing technique used by Shafer¹¹. Pollock tracing was successfully used in a number of streamline simulators where appropriate flow modeling along the streamlines allowed for simulation of first contact miscible displacements and evaluation of the effects of reservoir heterogeneity. Martin et al⁵. showed streamtube models failed predicting waterflood performance for an isolated five-spot pattern under favorable mobility ratio which highlighted the need to update the streamlines to accurately account for non-linear viscous effects.

Muskat³ gave an early description to the governing analytical equations that define the stream function and potential function in simple two dimensional domains for incompressible flow. A notable work with these definitions was by Fay and Pratts¹², who developed a numerical model to predict tracer and two-phase flow on a two-well homogenous 2D system.

2. Time of flight formulation (Datta-Gupta & King, 1995). Datta-Gupta & King¹³ introduced the concept of "time of flight" along a streamline. This idea shall be used in this research quite extensively. Datta-Gupta & King¹³ also presented a streamline model for 2D heterogeneous areal displacements of two well-tracer and waterflooding problems. Most of the current streamline based flow simulators use this concept of time of flight,

because of its simplicity and its decoupling effects, which splits a 3D problem into a series of 1D problems. This has been the most significant contribution in streamline simulation. The present research work also builds on this concept of ‘time of flight’.

3. Gravity effects and changing field conditions (Bratvedt et al⁹, 1996, Batycky et al¹⁴, 1997). Blunt et al¹⁵, extended the streamline method to three dimensional systems, accounting for longitudinal and transverse diffusion. Bratvedt⁹ introduced an operator splitting technique similar to that used in front tracking methods, allowing him to account for multiphase gravity effects.

With advances in SL methods, the technique has become a common tool to assist in the modeling and forecasting of field cases. This technology is now available to a large group of engineers and because of the increasing interest in this technology, one of the objective in this research is to provide insight why we think the method may be accurate in some cases.

2.2 Streamline Method

Streamline based flow simulators have made significant advances in the past years. Today’s simulators are fully 3D, and account for gravity as well as for complex well controls. SL simulation also allows for compressible flow and compositional displacements¹⁶⁻¹⁷. Streamline based simulation is an attractive alternative because of the fundamentally different approach in moving fluids. Instead of moving fluids cell to cell, SL breaks up the reservoir into 1D systems and it approximates 3D fluid-flow calculations by a sum of 1D solutions along streamlines. The choice of streamline directions for the 1D calculation makes the approach extremely effective for modeling convection-dominated flows in the reservoir¹⁸⁻¹⁹. This is typically the case when heterogeneity is the predominant factor governing flow behavior.

Streamline simulation involves the following basic steps:

1. Trace the streamlines on the basis of a velocity field, typically derived numerically with finite-difference or finite-element methods.
2. Compute particle travel time or time of flight along the streamlines. The time of flight coordinate provides a quantitative form of flow visualization that can have a variety of applications in reservoir characterization/management.
3. Solve the transport equations (saturation and concentration) along streamlines. The transport calculations are performed in the time of flight coordinate, effectively decoupling heterogeneity effects and significantly simplifying calculations.
4. Periodically update the streamlines to account for mobility effects or changing field conditions. Once the streamlines are regenerated, recompute the time of flight along the new streamlines. Finally, saturation calculations are resumed with the updated time of flight. A critical step here is the mapping of information from the old streamlines to the new streamlines. This can be a potential source of error during streamline simulation.

The computational advantage of the streamline methods can be attributed to the following principal reasons: streamlines may need to be updated only infrequently; the transport equations along streamlines often can be solved analytically; also the 1D numerical solutions along streamlines are not constrained by the underlying geologic grid-stability criterion, thus allowing for larger time steps; and moreover for displacements dominated by heterogeneity, the computation time often scales nearly linearly with the number of gridblocks, making it the preferred method for fine-scale geologic simulations.

Additionally, the self-similarity of the solution along streamlines may allow us to compute the solution only once and map it to the time of interest. We also can mention as advantages of SL simulation that the subgrid resolution is very good and reduced numerical artifacts, such as artificial diffusion and grid orientation effects, because the

streamline grid used to solve the transport equations is effectively decoupled from the underlying static grid.

2.2.1. Streamline Method Governing IMPES Equations

Streamline simulators are based in Implicit Pressure Explicit Saturation (IMPES) approach to solve the governing conservation equation. Ignoring capillary and dispersion effects, the governing equation in terms of pressure P for incompressible multiphase flow in porous media is given by

$$\nabla \cdot \bar{k} \cdot (\lambda_f \nabla P + \lambda_g \nabla D) = 0 \quad (2.1)$$

Where the total mobility (λ_f) and the total gravity mobility (λ_g) are defined as

$$\lambda_f = \sum_{j=1}^{n_p} \frac{k_{rj}}{\mu_j} \quad \lambda_g = \sum_{j=1}^{n_p} \frac{k_{rj} \rho_j \mathbf{g}}{\mu_j} \quad (2.2)$$

D represents a depth below the datum. To determine the flow of the individual phases we also require a material balance equation for each phase j

$$\phi \frac{\partial S_j}{\partial t} + \vec{u}_t \cdot \nabla f_j + \nabla \cdot \vec{G}_j \quad (2.3)$$

The total velocity \vec{u}_t is derived from the 3D solution to the pressure field and the application of Darcy's Law. The phase fractional flow term is given by

$$f_j = \frac{k_{rj} / \mu_j}{\sum_{i=1}^{n_p} k_{ri} / \mu_i} \quad (2.4)$$

And the gravity term is given by

$$\vec{G}_j = \vec{k}g \nabla D f_j \sum_{i=1}^{n_p} k_{ri} / \mu_i (\rho_i - \rho_j) \quad (2.5)$$

In a conventional IMPES finite-difference (FD) simulator Eq. 2.3 is solved in its full three-dimensional form. With the streamline method, we decouple the 3D equation into multiple 1D equations that are solved along streamlines. For large problems, solving multiple 1D equations is much faster and more accurate than solving the full 3D problem.

2.2.2. Coordinate Transform

Streamlines are launched from grid block faces containing injectors. As the streamlines are traced from injectors to producers, we determine the time of flight along the streamline, which is defined as

$$\tau = \int_0^s \frac{\phi}{u_t(\zeta)} d\zeta \quad (2.6)$$

This equation gives the time required to reach a point s on the streamline based on the total velocity $u_t(\zeta)$ along the streamline. For orthogonal geometries it is possible to determine the coordinate transform rewriting equation 2.6 as

$$\frac{\partial \tau}{\partial s} = \frac{\phi}{|u_t|} \quad (2.7)$$

This can be rewritten as,

$$|u_t| \frac{\partial}{\partial s} \equiv \vec{u}_t \cdot \nabla = \phi \frac{\partial}{\partial \tau} \quad (2.8)$$

Substituting equation 2.8 into equation 2.3 gives

$$\frac{\partial S_j}{\partial t} + \frac{\partial f_j}{\partial \tau} + \frac{1}{\phi} \nabla \cdot \vec{G}_j = 0 \quad (2.9)$$

This equation is the governing pseudo-1D material balance equation for phase j transformed along a streamline coordinate. It is pseudo-1D since the gravity term is typically not aligned along the direction of a streamline.

To solve equation 2.9 we simply split the equation into two parts. First a convective step along the streamlines governed by

$$\frac{\partial S_j^c}{\partial t} + \frac{\partial f_j}{\partial \tau} = 0 \quad (2.10)$$

This includes boundary conditions at the wells, is taken to construct an intermediate saturation distribution S_j^c . Then, a gravity step is taken along the gravity lines and saturations are moved using

$$\frac{\partial S_j}{\partial t} + \frac{g}{\phi} \frac{\partial G_j}{\partial z} = 0 \quad (2.11)$$

For simplicity it is assumed that the gravity lines are aligned in the z coordinate direction. Equation 2.10 is solved numerically using single point upstream weighting scheme explicit in time. Equation 2.11 is solving using an explicit upstream weighting method. An additional advantage of decoupling equation 2.9 in this way is that equation 2.9 is only solved in flow regions where gravity effects are important. For example, in locations where fluids are completely segregated, equation 2.9 will not be solved, since $\partial G/\partial z = 0$

2.2.3. Time Stepping

Modeling field scale displacements considers that the streamline paths change with time due to the changing mobility field and/or changing boundary conditions. Thus the pressure field is updated periodically in accordance with these changes. By using numerical solutions along the recalculated streamline paths the method accounts for the non-uniform initial conditions now present along the recalculated paths.

To move the 3D solution forward in time from t^n to $t^{n+1}=t^n+\Delta t^{n+1}$ the following algorithm is used:

1. At the start of a new time step, t^{n+1} , solve for the pressure field P using equation 2.1 in the IMPES formulation. This equation may be solved using a standard seven-point finite difference scheme, with no-flow boundary conditions over the surface of the domain and specified pressure or rate at the wells.
2. Apply Darcy's law to determine the total velocity at grid block faces.
3. Trace streamlines from injectors to producers. For each streamline the following is performed: (a) while tracing a streamline, the current saturation information from each grid block that the streamline passes through is remembered. In this manner, a profile of saturation versus τ is generated for the new streamline; (b) Move the saturations forward by Δt^{n+1} by solving equation 2.10 numerically in 1D. Map the new saturation profile back to the original streamline path.
4. Average all the streamline properties within each grid block of the 3D domain to determine the saturation distribution at t^{n+1}
5. If $G_j \neq 0$ include gravity step that traces gravity lines from the top of the domain to the bottom of the domain along \vec{g} . For each gravity line the following is done (a) While tracing a gravity line, the saturation distribution calculated in the convective step

as a function of z is remembered; (b) The saturations are moved forward by Δt^{n+1} using equation 2.11. The new saturation profile is mapped back to the original gravity line.

6. If $G_j \neq 0$ average all gravity line properties within each grid block of the 3D domain to determine the final saturation distribution at t^{n+1} .
7. Return to step 1.

The fundamental reason for large speedup factors in the streamline method is the fact that Δt , the time step size for a convective, can be larger than the time step size in conventional simulators. This is a result of eliminating the global CFL (Courant-Freidrichs-Lewy) condition by decoupling fluid movement from the underlying grid.

Streamline methods are not restricted by the global CFL condition, but rather local CFL along each streamline. As a result they have an advantage over conventional finite difference IMPES simulators, allowing less frequent pressure updates. Also SL models suffer less numerical dispersion than conventional FD models.

An important consideration in field simulations is that the time step size in the streamline method can be limited by the need to honor changing well conditions. Thus is expected that speedup factors will be smaller for simulation that must honor historical production information since the pressure field is recomputed every time the well conditions change, as opposed to using the method in a forecast mode.

2.2.4. Tracing Streamlines (Pollock's interpolation approach)¹⁰

The average linear velocity component across each face in a particular cell (Fig. 2.1) is obtained by dividing the volume flow rate across the face by the cross sectional area of the face and the porosity (Eq. 2.12)

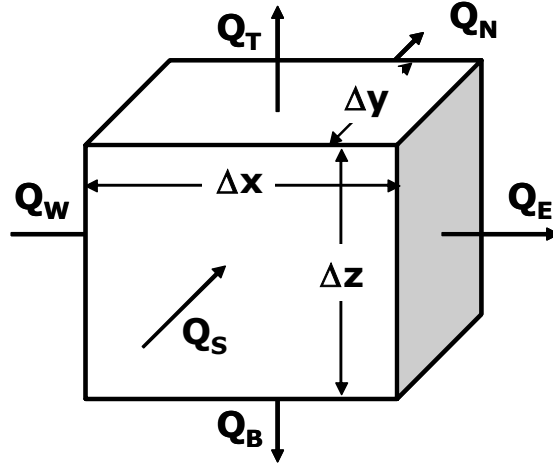


Fig. 2.1 Finite difference cell showing XYZ definitions

$$\begin{aligned}
 V_E &= \frac{Q_E}{\phi \cdot \Delta y \cdot \Delta z}, V_W = \frac{Q_W}{\phi \cdot \Delta y \cdot \Delta z} \\
 V_N &= \frac{Q_N}{\phi \cdot \Delta x \cdot \Delta z}, V_S = \frac{Q_S}{\phi \cdot \Delta x \cdot \Delta z} \\
 V_T &= \frac{Q_T}{\phi \cdot \Delta x \cdot \Delta y}, V_B = \frac{Q_B}{\phi \cdot \Delta x \cdot \Delta y}
 \end{aligned} \tag{2.12}$$

Where Q is a volume flow rate across a cell face, and Δx , Δy , and Δz are the dimensions of the cell in the respective coordinate directions. If flow to internal sources or sinks within the cell is specified as Q_s , the following mass balance equation can be written for the cell,

$$\frac{(\phi V_E - \phi V_W)}{\Delta x} + \frac{(\phi V_N - \phi V_S)}{\Delta y} + \frac{(\phi V_T - \phi V_B)}{\Delta z} = \frac{Q_s}{\Delta x \cdot \Delta y \cdot \Delta z} \tag{2.13}$$

The left hand side of this equation represents the net volume rate of outflow per unit volume of the cell, and the right hand side represents the net volume rate of production per unit volume due to internal sources and sinks.

In order to compute path lines, it is required to compute values of the principal components of the velocity vector at every point in the flow field based on the inter-cell

flow rates from the finite difference model. Pollock's method uses a simple linear interpolation to compute the principal velocity components at points within a cell, the principal velocity components can be expressed in the form,

$$\begin{aligned} V_x &= A_x(x - x_1) + V_W \\ V_y &= A_y(y - y_1) + V_N \\ V_z &= A_z(z - z_1) + V_T \end{aligned} \quad (2.14)$$

Where A_x , A_y , and A_z are constants that correspond to the components of the velocity gradient within the cell and are given by,

$$\begin{aligned} A_x &= \frac{(V_W - V_E)}{\Delta x} \\ A_y &= \frac{(V_N - V_S)}{\Delta y} \\ A_z &= \frac{(V_T - V_B)}{\Delta z} \end{aligned} \quad (2.15)$$

Linear interpolation of the six cell face velocity components results in a velocity vector field within the cell that automatically satisfies the differential conservation of mass equation at every point inside the cell. This is correct only if it is assumed that the internal sources or sinks are considered to be uniformly distributed within the cell.

The fact that the velocity vector field within each cell satisfies the differential mass balance equation assures that path lines will distribute liquid throughout the flow field in a way that is consistent with the overall movement of liquid in the system as indicated by the solution of the finite-difference flow equations.

In order to find the position of the particle, its movement through a three-dimensional finite-difference cell must be considered. Let's start with the rate of change in the particle's x -component of velocity as it moves through the cell, this is given by,

$$\left(\frac{dV_x}{dt}\right)_p = \left(\frac{dV_x}{dx}\right)\left(\frac{dx}{dt}\right)_p \quad (2.16)$$

The subscript, p , is used to indicate that a term is evaluated at the location of the particle denoted by the x - y - z coordinates (x_p, y_p, z_p) . The term $(dx/dt)_p$ is the time rate of change of the x -location of the particle. By definition,

$$V_{xp} = \left(\frac{dx}{dt}\right)_p \quad (2.17)$$

Where V_{xp} is the particle's x -velocity-component. Differentiating the principal velocity components (Eq. 2.14) with respect to x yields the additional relation,

$$\left(\frac{dV_x}{dx}\right) = A_x \quad (2.18)$$

Substituting equations (2.17) and (2.18) into equation (2.16.) gives,

$$\left(\frac{dV_x}{dt}\right)_p = A_x V_{xp} \quad (2.19)$$

This equation can be rearranged to the form,

$$\frac{1}{V_{xp}}(dV_x)_p = A_x dt \quad (2.20)$$

This equation can be integrated and evaluated for times t_1 and t_2 leading to,

$$\ln\left(\frac{V_{xp}(t_2)}{V_{xp}(t_1)}\right) = A_x \Delta t \quad (2.21)$$

By taking the exponential of each side of the equation and substituting the velocity components in equation (2.14) the x -position of the particle can be evaluated using the next expression,

$$x_p(t_2) = x_1 + \frac{1}{A_x} [V_{xp}(t_1)e^{A_x \Delta t} - V_{x1}] \quad (2.22)$$

The velocity components of the particle at time t_1 are known functions of the particle's coordinates; consequently, the coordinates of the particle at any future time t_2 can be computed directly from equation (2.22).

For steady-state flow, the direct integration method described above can be imbedded in a simple algorithm that allows a particle's exit point from a cell to be determined directly given any known starting location within the cell. To illustrate the method, consider the two-dimensional example shown in Fig. 2.2 cell (i,j) is in the x - y plane and contains a particle, p , located at (x_p, y_p) at time t_p .

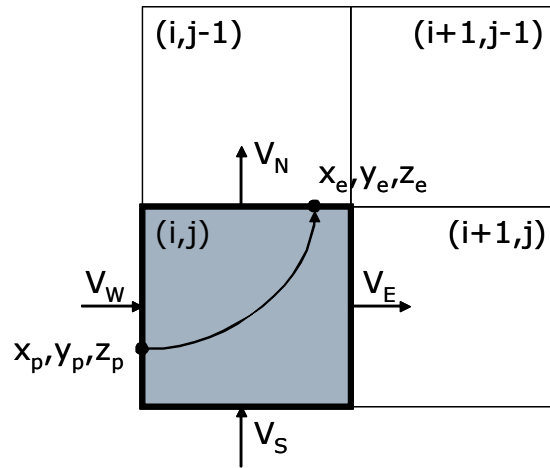


Fig. 2.2 Schematic showing the computation of exit point and travel time in 2D

The first step is to determine the face across which the particle leaves cell (i,j) . For the present example, this is accomplished by noting that the velocity components at the four faces require that the particle leave the cell through either the north or the east

face. Consider the x -direction first. From equation (2.14) V_{xp} can be calculated at the point (x_p, y_p) , since we also know V_x equals V_E at the east face, equation (2.21) can be used to determine the time that would be required for the particle to reach the east face. An analogous calculation can be made to determine the time required for the particle to reach the north face. If Δt_x is less than Δt_y , the particle will leave the cell across the east face and enter cell $(i+1, j)$. Conversely, if Δt_y is less than Δt_x , the particle will leave the cell across the north face and enter cell $(i, j-1)$.

The length of time required for the particle to travel from point (x_p, y_p) to a boundary face of cell (i, j) is taken to be the smaller of Δt_x and Δt_y , and is denoted as Δt_e . The value Δt_e is then used in equation (2.22) to determine the exit coordinates (x_e, y_e) for the particle as it leaves cell (i, j) ,

$$\begin{aligned} x_e &= x_1 + \frac{1}{A_x} \left[V_{xp}(t_p) e^{A_x \Delta t_e} - V_{x1} \right] \\ y_e &= y_1 + \frac{1}{A_y} \left[V_{yp}(t_p) e^{A_y \Delta t_e} - V_{y1} \right] \end{aligned} \quad (2.23)$$

The time at which the particle leaves the cell is given by: $t_e = t_p + \Delta t_e$. This sequence of calculations is repeated, cell by cell, until the particle reaches a discharge point. The approach can be generalized to three dimensions in a straight forward way by performing all of the calculations for the z -direction in addition to the x - and y -directions.

Tracing streamlines in 3D using time of flight means a truly 3D, rather than 2D as in the streamtube methods of the 70's and 80's. Streamlines correctly account for the previously missing vertical component of the flow description and are therefore fundamental to the current success of the technology²⁰. Practically, the use of 3D streamlines no longer requires geological models to be transformed into pseudo 2D areal models. Thus, streamlines are no longer tied to individual layers, but are truly 3D lines that can cut across simulation layers.

CHAPTER III

INFLUENTIAL ELEMENTS IN ACCURACY OF STREAMLINE MODELS

The initial approach to this research is to study the elements affecting the accuracy in the streamlines models. Therefore this investigation considers some of the most important factors affecting the accuracy and efficiency in streamline solution. In this group we can include saturation mapping method, mobility changes, time step size, number of streamlines used, gravity effects and phases presents. In this chapter we presente an analysis of the influence of those elements in streamline models.

3.1. Reservoir Model Heterogeneity

Detailed description of reservoir heterogeneity can improve the accuracy of fluid-flow models, but it can cause computer limitations problems. However, using streamline models can help to reduce significantly those limitations. The streamlines formulation incorporates variable mobility ratios, permeability trends, closed or open boundaries, gravity effects, etc.

Most heterogeneous models predictions using streamlines agree extremely well with field results and, also provide a good estimation of vertical and areal sweep efficiency. Additionally, the computer time requirement of streamline models is relatively low compared with that required by conventional 3D finite difference models representing the same level of detail²¹⁻²².

The streamline technique decomposes a heterogeneous 3D domain into a number of one-dimensional (1D) streamlines along which all fluid flow calculations are done. Streamlines represent a natural, dynamically changing grid for modeling fluid flow. This approach allows us to decouple the physics describing the displacement from the size of the grid used to model the reservoir geology²³⁻²⁴. The simplicity and speed of the approach makes it an ideal method to simulate large geological models without the need of substantial upscaling. Also the method works for strongly heterogeneous systems that

have well-defined flow paths. The fact of repeatedly propagating the 1D solution along updated streamlines causes small errors compared with the uncertainty in the performance due to the statistics derived from limited data describing the reservoir.

Most of the previous works have shown that streamline solutions are in agreement with the finite-difference solutions, are able to minimize the impact of numerical diffusion, and can be significantly faster. Numerical diffusion in finite-difference formulations can interact with reservoir heterogeneity to substantially mitigate mobility differences and lead to optimistic recovery predictions.

Likewise, the streamline approach produces fast and robust solutions to displacements dominated by reservoir heterogeneity, capturing the impact of heterogeneity on the flow field.

3.2. Saturation Mapping Methods

Streamtubes models were used until streamlines model. These models have the advantageous feature of being able to explicit account for the fluid volumes during saturation calculations.

The numerical experiments performed in this research are associated with models that involve waterflooding process, and are mathematically described by the fractional flow equation and the frontal advance theory. For horizontal flow, the fractional flow reduces to the equation 3.1 below,

$$f_w(s_w) = \frac{1}{1 + \frac{\mu_w k_{ro}}{k_{rw} \mu_o}} \quad (3.1)$$

and the frontal displacement theory that describes the rate at which a saturation front advances is given by the equation (3.2) below.

$$\left. \frac{dx}{dt} \right|_{sw} = \frac{q}{A\phi} \frac{\partial fw}{\partial sw} \quad (3.2)$$

In the derivation of equation 3.1, the effect of capillary pressure is neglected. This results in a sharp displacement front when combined with the equation 3.1 to derive a saturation profile of an injection process.

Capillary pressure effect results in a dispersion of the saturation front. Hence, in a displacement process that does not take into account of capillary pressure, it is expected that the displacement front would be just as modeled by the frontal advance theory²⁵.

In numerical simulation, the numerical approximation of the analytical solution provided by the mathematical principles governing fluid dynamics results in a dispersion due to the inherent data truncation. Hence, however insignificant the capillary effects are, the solution presents dispersion at the front.

In streamline simulation, this dispersion results from the numerical approximation involved in the saturation transport calculations. Saturation is determined from the time of flight equation which is presented below

$$\frac{\partial Sw}{\partial t} + \frac{\partial fw}{\partial \tau} = 0 \quad (3.3)$$

In cases of uniform initial saturation distribution, the saturation is determined by a direct analytic solution of the equation 3.3 above once the fractional flow tables have been generated. In the more common case of non-uniform saturation distribution, it is necessary to solve for saturation using the equation 3.4 which represents the numerical approximation to the equation 3.3.

$$Sw_i^{n+1} = Sw_i^n + \frac{\Delta t}{\Delta \tau} (fw_{i+1/2} - fw_{i-1/2}) \quad (3.4)$$

The term $\left(\frac{\Delta t}{\Delta \tau}\right)$ in the equation represents the CFL number, and hence a constraint on the size of time step that can be taken.

One of the advantages of streamline simulation derives from the speed with which it evaluates the saturation profile. This proves to be advantageous because the generated streamlines cluster around the fast flow paths. The streamlines mainly change when there is a remarkable change in the reservoir conditions be due to an infill well or change in production.

In the case of Finite Difference simulation however, the saturation is obtained by solving some modification of the equation 3.5 below.

$$\phi \frac{\partial S_w}{\partial t} + \nabla u_w = \text{Source} / \text{Sink} \quad (3.5)$$

This is done after obtaining the pressure solution. Equation 3.5 is solved at each time step after evaluating the pressure solution. The solution to the equation 3.5 is often time consuming, particularly is there are small grid cells. The need to solve the equation 3.5 above results in high computational time for finite difference solutions compared to the streamline simulation approach that considers a solution to the equation 3.4 which is less time consuming and only requires to be solved when there is a change in the general orientation of the streamlines.

There are two common approaches to mapping saturation between streamlines when streamlines are updated. These are: streamline to block (line to block) and streamline to streamline (line to line).

3.2.1. Line to Block Saturation Mapping Method

Tracing of streamlines with this method for mapping saturation property involves a grid block based approach, tracing the streamlines through every grid block in the domain to an injector. The time of flight (τ) to the grid block is then known and used to calculate grid block saturation. The grid saturation block is calculated based on the multiple streamlines that pass through the grid block.

This method uses the average of saturations of all streamline segments inside a grid block. Averaging is performed regardless of the location of the streamlines in the block. Fig. 3.1 shows an example of how the streamlines are crossing through a grid block.

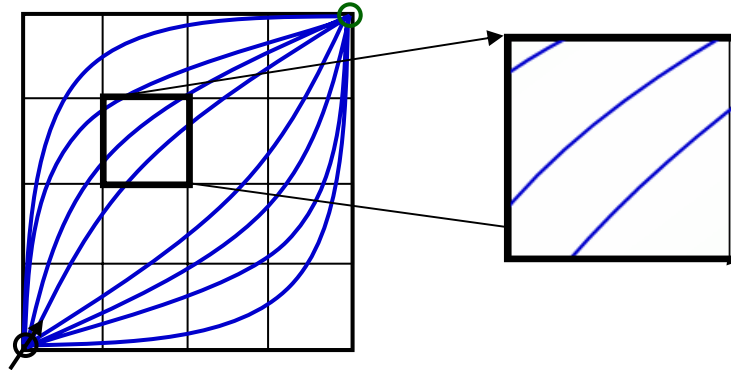


Fig. 3.1 Line to block saturation mapping

Considering the pore volume $V_{pi} = q_i \Delta \tau_i$ where q_i is the flux associated of the streamline and $\Delta \tau_i$ is the time of flight in the grid block, the average saturation (S_{avg}) for the streamlines passing over the grid block is,

$$S_{avg} = \frac{\sum_{i=1}^n \Delta \tau_i S_i q_i}{\sum_{i=1}^n \Delta \tau_i q_i} \quad (3.6)$$

where n is the number of streamlines crossing the grid block and S_i is the saturation in the streamline fragment. Then this average saturation is assigned to the grid block. Then, S_{avg} is assigned to the new streamlines resulting from pressure updating and that are crossing the grid block.

This method may be considered unfavorable because the averaging of saturation leads to numerical dispersion. But to validate this assumption we will present many cases in the following chapters. This procedure could result in mapping errors and faster sweep of the block with end effects.

3.2.2. Line to Line Saturation Mapping Method

Another method for saturation mapping using SL methodology is the sampling of saturation from streamlines to streamlines (Bratvedt, 1996⁹). This approach intends to preserve the saturation fronts inside the grid blocks using the saturation values on the fragments of the streamline inside a grid block. Then those values are traced again perpendicularly to the segments of the new streamlines. This perpendicular projection is considered as the shortest distance to the adjacent streamline. The next figure 3.2 will show a graphic view of the method.

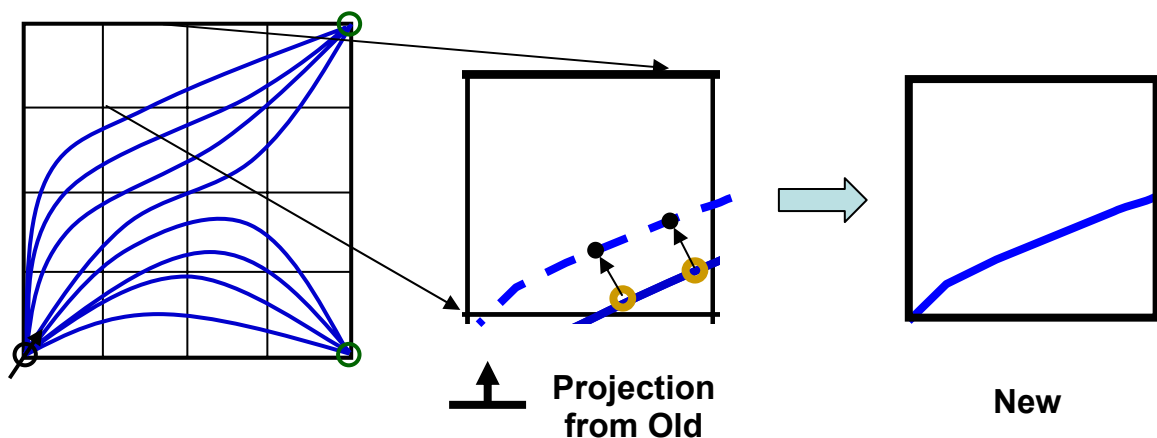


Fig. 3.2 Line to line saturation mapping

Now the saturation front from the old streamline is transferred to the new streamline. This approach is considered because it can minimize numerical dispersion and preserve the subgrid resolution in saturation but is computationally more demanding. It can also lead to mass balance errors arising from the repositioning of the front because of saturation assignments based on a non-conservative approach.

3.3. Mobility Ratio Changes

A mobility ratio changes is another element to evaluate for accuracy in the streamlines solution. Some numerical experiments based in last experience²⁶ have addressed the issue of taking into account mobility ratio effects. The results demonstrate the impact of transverse flux on the accuracy of the solution across a range of mobility ratios.

It is expected that the streamline paths change with time due to the changing mobility field. Thus the pressure field is updated periodically in accordance with these changes.

Martin et al.⁵ showed streamtube models failed predicting waterflood performance for an isolated five-spot pattern under favorable mobility ratio which highlighted the need to update the streamlines to accurately account for non-linear viscous effects. End point mobility ratio (M) is expressed as

$$M = \frac{\mu_o k_{rw}(S_{or})}{\mu_w k_{ro}(S_{wc})} \quad (3.7)$$

where $k_{rw}(S_{or})$ is the relative permeability to water at residual oil and $k_{ro}(S_{wc})$ is the relative permeability to oil at critical water saturation.

Martin et al.⁵ found that the streamtube method failed for a favorable mobility ratio less than M=0.1 and produced poor results for mobility ratios greater than 100. Thus,

they concluded that the changes in mobility occurred over a shorter distance, increasing the nonlinearity of the displacement. So, it was proposed to recalculate the streamtube paths periodically, obtaining good results. But recalculating streamline paths introduces non-uniform initial conditions along new streamlines. Martin et al⁵. used a numerical approach to move saturations along updated paths, calculating the value of the stream function (ψ) numerically on a 2D domain. This process allows the streamfunction to define the streamtubes updating the streamtubes to honor the changing mobility field. The original saturations are then mapped to the new streamtube locations.

As a general idea, it is necessary to update the streamlines periodically, to account for mobility effects or changing field conditions. Once the streamlines are regenerated, the time of flight along the new streamlines is recomputed.

3.4. Material Balance Calculation

Material balance represents an important factor that can judge the accuracy and applicability of streamline technology. Some of the causes of the material balance error (MBE) are: the non-conservative equation formulation, saturation mapping, residuals in iterative matrix solving methods, nonlinear equation coefficients, and roundoff errors.

The numerical mapping method for grid block saturations can introduce MBE. The process of mapping using line to block saturation and then determining average grid block saturations using this method does not ensure that mass is conserved. The remapping technique to assign grid block average fluid properties does not guarantee mass conservation because during saturation calculation we do not account for phase volume explicitly.

Mapping saturations from an underlying background grid to the streamlines, moved forward in time and then mapped from the streamlines to the background grid, introduce smearing and mass balance errors. When streamlines are updated frequently, the mapping error limits the accuracy of the streamline method.

Some causes of large MBE are related with the displacement front of the injected fluid. This is because the front is sharp, irregular and not closely aligned with the grid. If the flow is aligned with the grid or the saturation field is smooth, then mass balance errors will generally be smaller. The saturation mapping is not significantly improved by adding more streamlines since those additional streamlines tend to cluster in the same way. To solve this problem Mallison et al²⁷. proposed a strategy to improve the MBE, It consists of assigning a influx to each streamline and include this flux to determine the weights. If the flux reflects the clustering of streamlines correctly then the MBE can be improved. Those authors also suggest using kriging in computing the weights, improving the accuracy of the mapping to the background grid taking into account the correlation between streamline segments when computing the weights. This Leads to a Kriging interpolation scheme.

When the number of time steps is increased then the standard mappings to and from streamlines introduce numerical smearing of saturation fronts and MBE. Likewise, TOF weighting of streamline segments introduces large errors when streamlines become clustered.

Additional research will be required to reduce the MBE that arise streamlines when the streamlines are updated, due to changing well conditions or gravity.

3.5. Time Step Size

The efficiency of streamline simulation is based in their ability to take larger time steps with less pressure solution in the IMPES formulation. Unlike conventional Finite-difference simulators there is, however no available a guideline for the choice of time step and velocity updates. This has remained uncontrolled approximation and managed by engineering judgment or time consuming time step size sensitivities studies in projects. Osako et al²⁶. assumed that this is related to the lack of understanding of numerical stability and error estimates during the solution. They showed a useful

approach using heterogeneous and homogeneous experiments with particular focus in low mobility ratio displacements during streamline simulation modeling. The results achieved validate the importance of transverse flux correction on the accuracy of the solution and on the suitable choice of time step, across a range of mobility ratios. Osako et al²⁶. ran some experiments and it may be deduced that if the changes in boundary conditions are significant, then the time step size for flow simulation must honor this changes.

One advantage of the streamline models is that the stability constraint of the underlying grid is effectively decoupled from the solutions solved along streamlines. That is why very large convective time steps can be taken. The ability to take this large convective time steps and only update the streamline paths periodically are the factors which led to a faster method than the conventional ones. The maximum time step size which can be taken before the pressure field needs to be updated is dependent on the nonlinearities of the displacement.

3.6. Number of Streamlines

The number of streamlines used in the model is another factor that can affect the results from streamline method, there is a dependency based on the number of streamlines traced in a model. Greater number of streamlines launched in a model results in fewer number of grid blocks missed with the streamlines. For highly heterogeneous flows a large number of streamlines may be needed to trace from the injectors in order to intersect all grid blocks. However, recall that any missed grid block can be assigned a saturation based on tracing streamlines backwards in the velocity field from a missed grid block to one containing multiple streamlines. The number of streamlines launched does not effect the calculation of grid block phase saturations. The number of streamlines traced from injector to producer affects the resolution of the injected phase concentration at the producer. This is because the fluid cut at a producer is calculated based on the phase flux of arriving streamlines.

3.7. Gravity Effect

Gravity effect is another fundamental factor that can be accounted during streamline method. Streamlines follow the total velocity field rather than individual phase velocities; modeling gravity effects when mapping analytical solutions to the streamlines has been a discussion in earliest technical investigations. Blunt et al¹⁵. comment that the method works best for cases where the principal flow directions are dominated more by heterogeneity than by gravity.

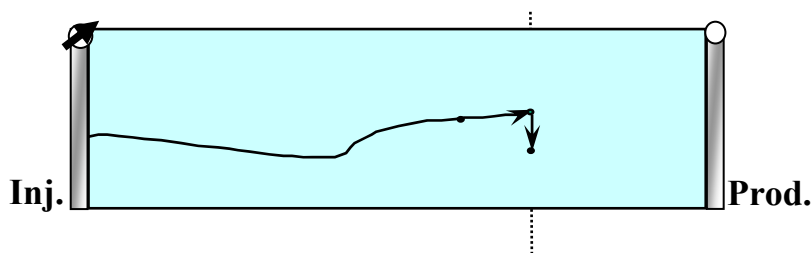


Fig. 3.3 Gravity effect for streamline model

Figure 3.3 shows how streamlines can be affected by gravity effect, this effect is an additional nonlinearity that alters the pressure field through time, and hence the streamline paths. The presence of gravity does require additional pressure solves over a given time interval to reach a converged solution. Also, as it was mentioned before, during multiphase flow, individual phase velocities may not be aligned with the total fluid velocity as show in Fig. 3.4:

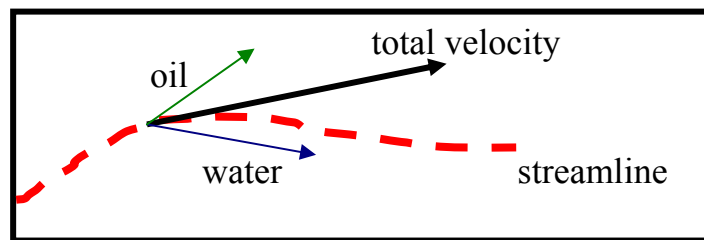


Fig. 3.4 Phase velocities of multiphase flow in streamline model

Gravity effects in FCM displacements could successfully be modeled over a large range of gravity numbers. Two-phase gravity problems are more difficult to model with

the streamline method. However, by separating the governing equation into a convective step and a gravity step (operator-splitting) the streamline method now accounts for gravity effects in multiphase flow²⁸.

In comparisons with conventional simulation methods, the streamline method still retains significant speedups and reasonable accuracy. The magnitude of the speedup depends on the size of the gravity number, the model size, and the type of displacement process.

Gravity effects in the streamline method are modeled using an operator splitting technique, which corrects fluid positions in the vertical direction after they have been moved convectively along streamlines. Conceivably, any other mechanism that is deemed important at the field scale simulators could be accounted using a similar operator splitting approach and viewed as a corrective step. Operator splitting relies on the consistency of treating the convective flux independently from the gravity flux within a given time step of the simulation. For small time steps the operator splitting approximation is fairly accurate whereas large time steps may lead to significant errors in the approximation²⁵.

Bratvedt et al⁵. presented a similar front tracking method as that of Glimm²⁹, but extended the method to full 3D systems with multiple wells. Their ideas were implemented in the commercial code FRONTSIM²⁹.

Gravity effects are accounted for by operator splitting such that fluids are moved convectively along streamlines then vertically due to gravity effects.

$$\frac{\partial \mathcal{S}_j}{\partial t} + \frac{\partial \mathcal{F}_j}{\partial \tau} + \frac{1}{\phi} \nabla \cdot \vec{G}_j = 0 \quad (3.8)$$

Then, this equation is solved with a two-step approach (operator-splitting):

First, saturations are transported along streamlines, ignoring any gravity effects. Next, saturations are then allowed to segregate because of density differences. Recently, this technology has been extended to, compressible and compositional flows³⁰.

Gravity and capillary forces are often important in the description of the dynamics of flow and must be included in the reservoir model. For this purpose, operator splitting algorithms represents an efficient numerical method to solve the reservoir model equations.

After the streamlines are computed, the equation for saturation (eq. 3.8), is then solved. For this purpose the convective and gravity effects have to be treated differently. Thus the mentioned equation is divided into two parts and solved using the operator splitting technique. The first part is a one dimensional, non-linear, hyperbolic equation which includes the convective term and is solved along the streamlines. The second part is a non linear parabolic equation which includes the gravity effect and it is solved using finite differences over the three dimensional grid. See figures 3.5 and 3.6. Details of this method can be found in references (2, 31).

$$\frac{\partial S_W}{\partial t} \approx \frac{\partial S_W}{\partial t_C} + \frac{\partial S_W}{\partial t_G}$$

The diagram illustrates the operator splitting method. At the top, the equation $\frac{\partial S_W}{\partial t} \approx \frac{\partial S_W}{\partial t_C} + \frac{\partial S_W}{\partial t_G}$ is shown. The terms $\frac{\partial S_W}{\partial t_C}$ and $\frac{\partial S_W}{\partial t_G}$ are enclosed in yellow circles with blue borders. Below these circles are two green rectangular boxes with blue borders. The left box is labeled "Convective step" and has an arrow pointing up to the $\frac{\partial S_W}{\partial t_C}$ term. The right box is labeled "Gravity step" and has an arrow pointing up to the $\frac{\partial S_W}{\partial t_G}$ term.

Fig. 3.5 Operator splitting method

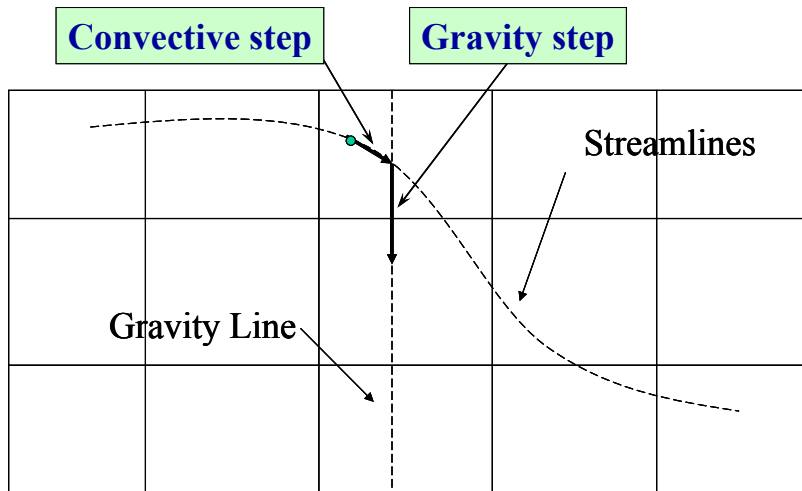


Fig. 3.6 Operator splitting steps for gravity effect in streamline model

CHAPTER IV

SENSITIVITY ANALYSIS FOR INFLUENTIAL ELEMENTS IN ACCURACY OF STREAMLINE MODELS

Sensitivity analysis is required to study the effects of the important elements in the accuracy of the streamlines models. It will be performed for a group of cases based on different scenarios to fulfill this propose.

The methodology for this analysis includes several stages, working separately on each of the factors affecting the precision in a streamline model. Also the reservoir model is changed depending on the element to be studied. All the cases are modeled in a commercial streamline based simulator FRONTSIM²⁹.

4.1 Model Description

For the first and second stage of this research, a 41x41x1 grid was generated to test the accuracy of the method. The flow is simulated for homogeneous and heterogeneous quarter five spot patterns. Thus, a water injector is located in the northeast corner and a producer in the southwest corner.

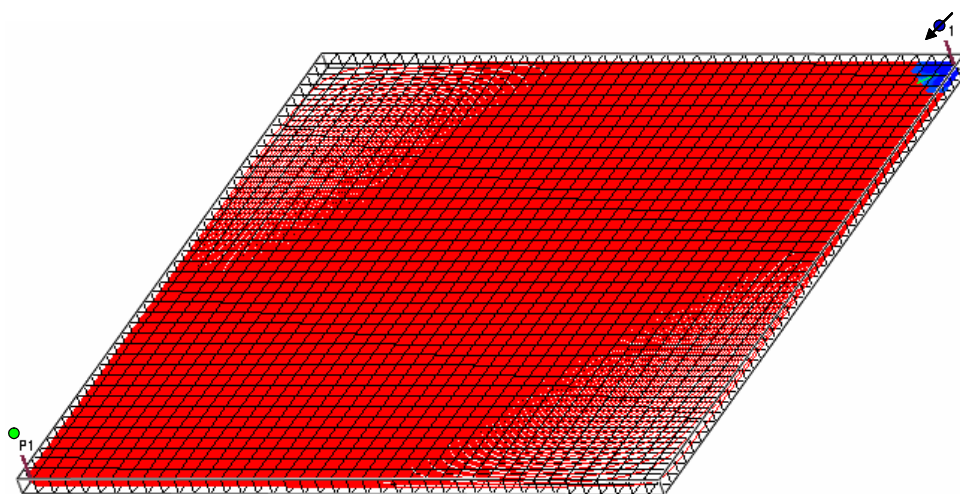


Fig. 4.1 Quarter of a five-spot grid model description.

Figure 4.1 shows the grid characteristics for the model analyzed in the first and second stage of this work.

The synthetic models start from the following premises:

- Homogeneous and Heterogeneous Reservoir Cases:
 - Grid: 41x41x1
 - 1 Oil producer well in the (1,41,1) grid location
 - 1 Water injector well in the (41,1,1) grid location
 - Saturation mapping methods:
 - Line to Block
 - Line to Line
 - Mobility: 0.2, 0.5 and 10
 - 2 Phase Flow
 - $\Delta t = 1, 5 \text{ \& } 20$ day.

Beginning from those premises, we created the scenarios for the analysis of the first group of influential factors, leading to obtain 36 simulations cases. The results of those runs can let us know which and how the mapping method, mobility and time step are affecting the reservoir performance and preciseness of solution. Table 4.1 shows the distributions of the cases run in this stage.

Table 4.1. First stage cases for analysis

Model	Mapping	Mobility ratio	Delt (days)
Homogeneous & Heterogeneous	Line to Line	0.2	1
	Line to Block		
	Line to Line		
	Line to Line	0.5	5
	Line to Block		
	Line to Line		
	Line to Line	10	20
	Line to Block		
	Line to Line		
	Line to Line	0.2	1
	Line to Block		
	Line to Line		
Line to Line	0.5	5	
Line to Block			
Line to Line			
Line to Line	10	20	
Line to Block			
Line to Line			

Figure 4.2 is a representation of the permeability distribution used in the heterogeneous cases.

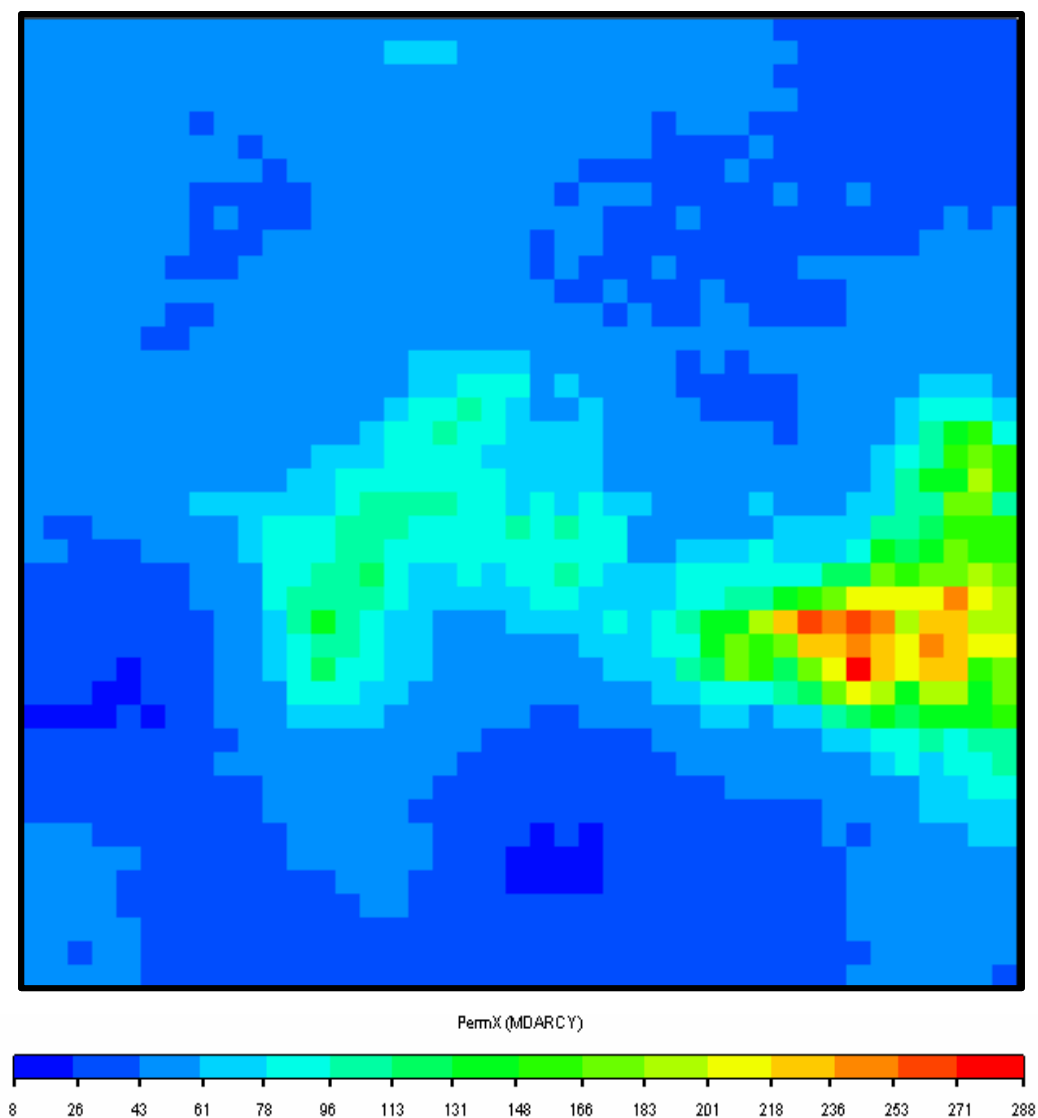


Fig. 4.2 Permeability distribution for heterogeneous model.

4.2 Effects of Saturation Mapping Methods

The sensitivities performed determine which of the mapping method preserves the front and reduces numerical dispersion and also define how the others parameters are affecting the reservoir performance, material balance, and the accuracy solution.

To represent the effects of saturation mapping during SL simulation, a waterflooding process is considered for the $\frac{1}{4}$ -five spot pattern model described in the last section (4.1).

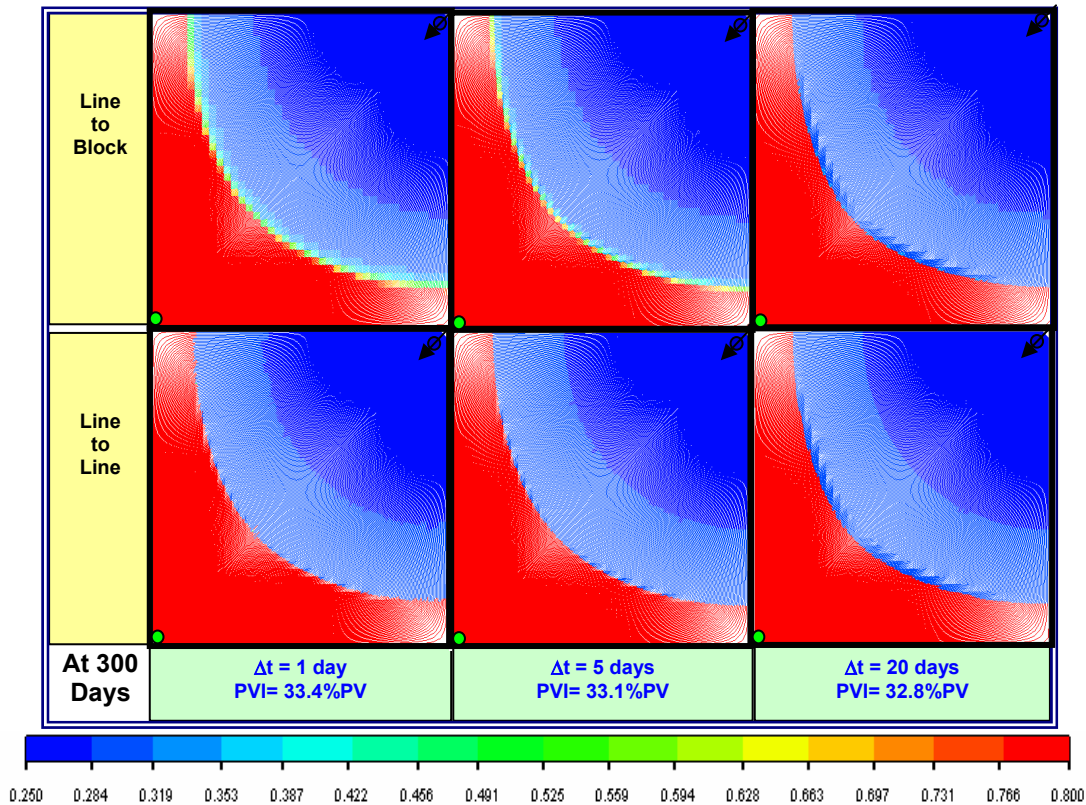


Fig. 4.3 Saturation profile by saturation mapping for homogeneous case and $M=0.2$.

Fig. 4.3 shows the results for the two mapping techniques: Line to Line and Line to Block during streamline simulation on a homogeneous model. The water saturation profile is shown at 300 days (0.33 PVI). The mobility ratio (M) in this case is 0.2 and we used different time step sizes of 1, 5, and 20 days for pressure updates and regeneration of streamlines.

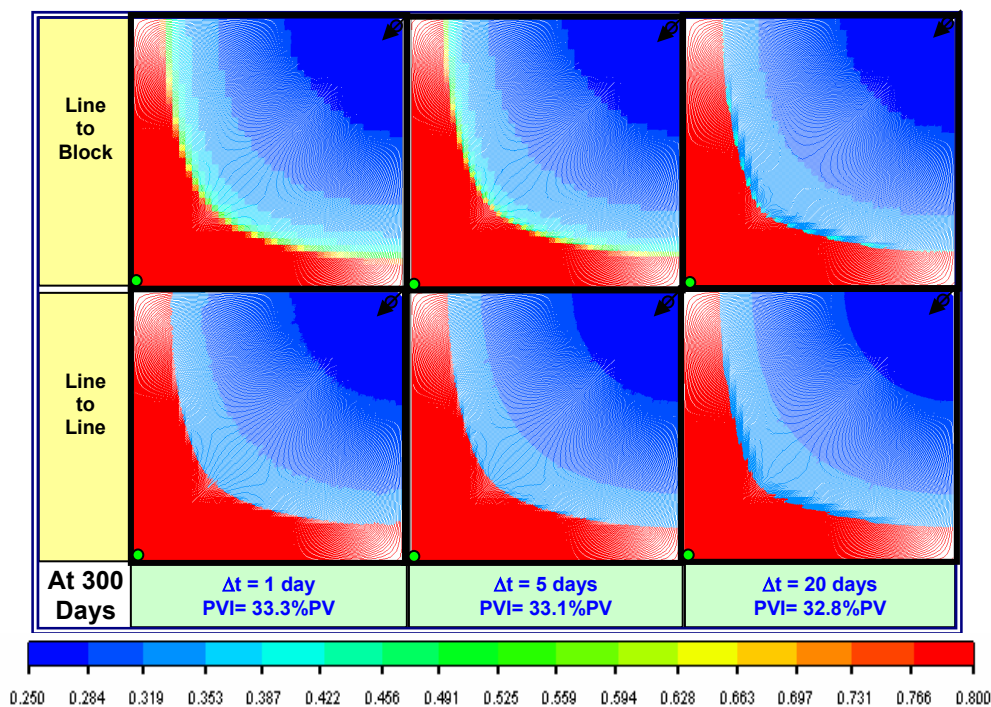


Fig. 4.4 Saturation profile by saturation mapping for homogeneous case and $M=0.5$.

In figure 4.4 using the same model but with $M=0.5$, we can see the same behavior shown in the $M=0.2$ cases, but with more signs of the numerical dispersion in the line to block method.

The next results presented in the figure 4.5 correspond to the cases of $M=10$. From these cases it is clear that the numerical smearing is higher in the line to block mapping and definitively, the line to line method better preserves the front by minimizing numerical dispersion effects.

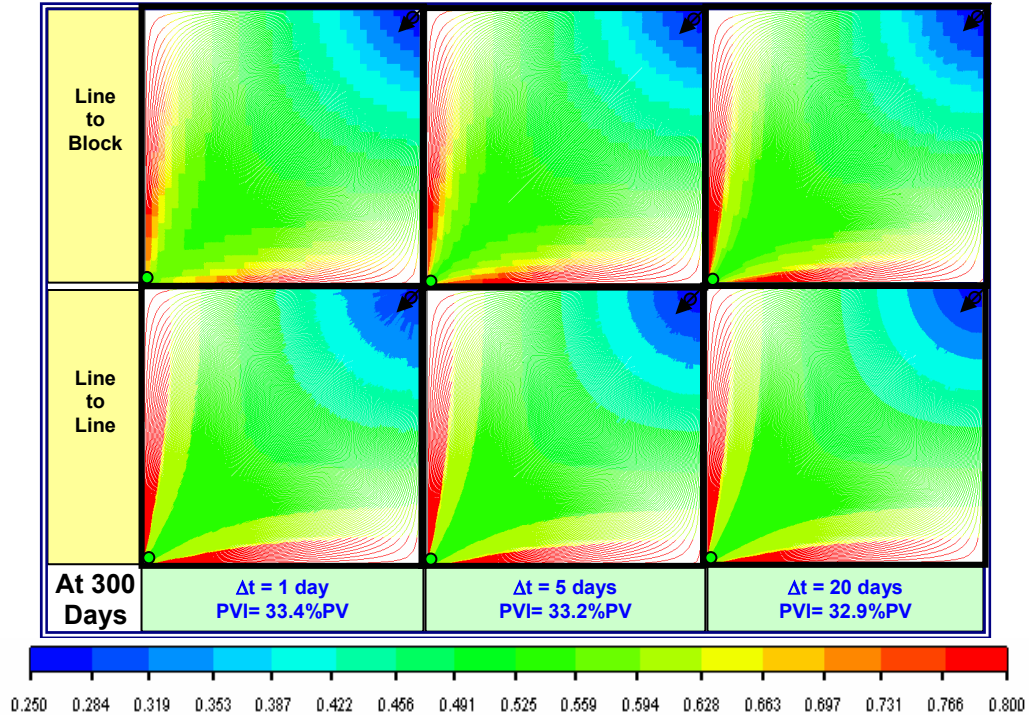


Fig. 4.5 Saturation profile by saturation mapping for homogeneous case and $M=10$.

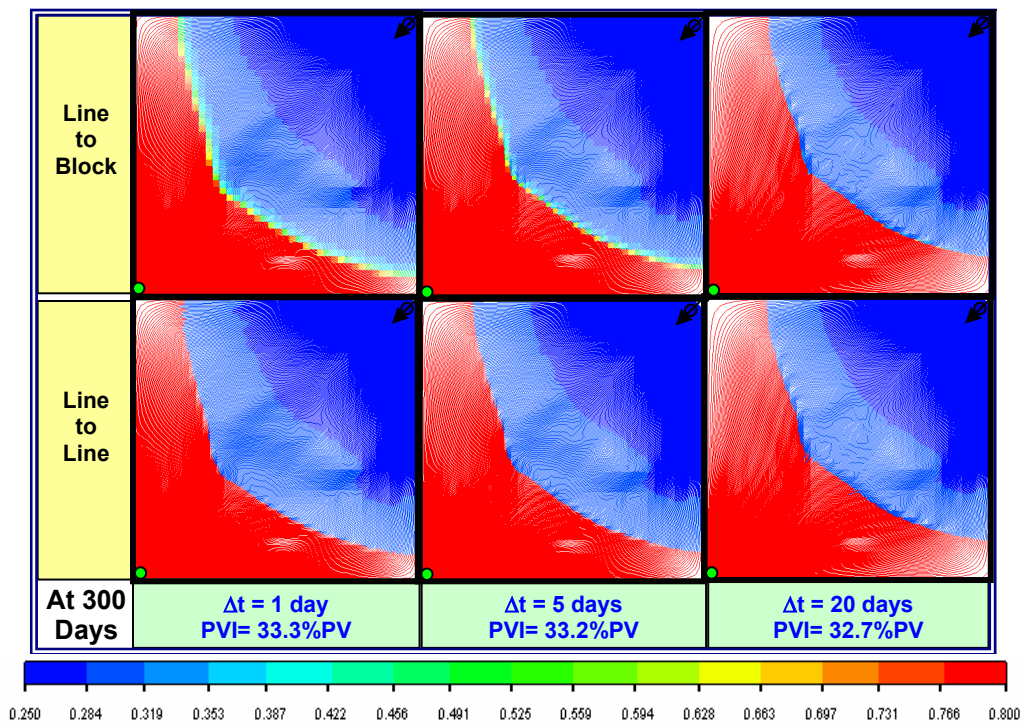


Fig. 4.6 Saturation profile by saturation mapping for heterogeneous case and $M=0.2$.

Figure 4.6 shows the same sensitive analysis as in the previous cases but considering a heterogeneous model. Similar behavior is seen as for the homogeneous case.

At this point, all the cases have exhibited smearing of the saturation front because of the Line to block mapping. Figures 4.7 and 4.8 also are results based on heterogeneous model using saturation mapping for $M=0.5$ and $M=10$ respectively.

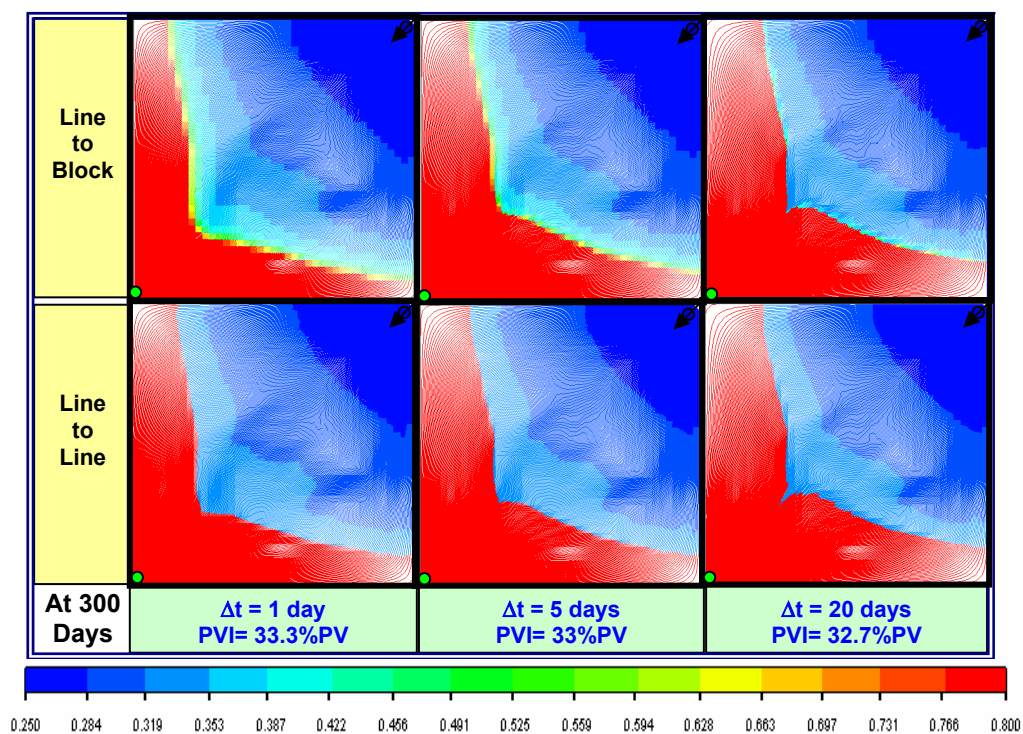


Fig. 4.7 Saturation profile by saturation mapping for heterogeneous case and $M=0.5$.

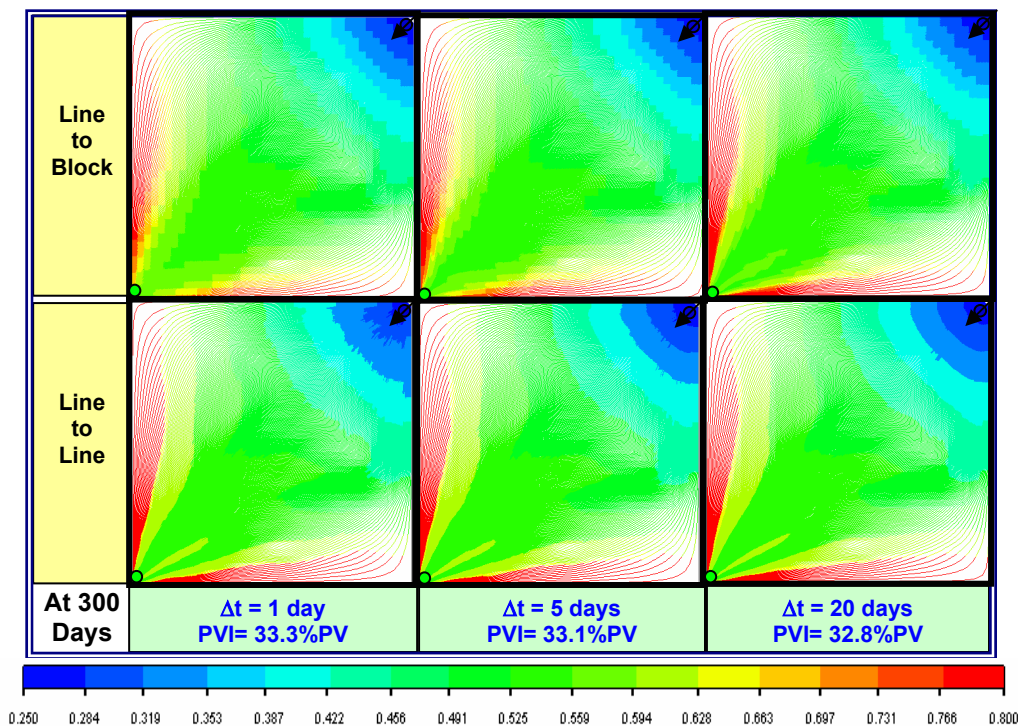


Fig. 4.8 Saturation profile by saturation mapping for heterogeneous case and $M=10$.

In the last figure 4.8, the comparison was performed based on the same saturation profiles for a pressure update time step of 1, 5, and 20 days. The mobility ratio used was 10, and it can be observed that the saturation profiles from line to line mapping shows very little effects of increased mapping. In contrast, line to block mapping shows considerably worse results due to numerical dispersion.

It can be mentioned that the relative permeability curves used for both water and oil phases in these calculations were based on a quadratic form. The results indicate that the line to block cases show a more numerical dispersion than the line to line. The smearing of the saturation front because of the Line to Block mapping is quite apparent in all the figures showed.

Based on the results obtained by the sensitivities analysis in this stage can be deduced some assumptions underling the fact that the line to block saturation mapping method shows more numerical dispersion than the line to line.

The smearing of the saturation front in Line to block mapping is quite apparent, it is supposed that this effect cause Material Balance but it is not, Although, the smearing of the saturation front is prevented, the material balance is not automatically preserved. Fig. 4.9 shows the performance of the water material balance error for each of the saturation methods in the homogeneous case using $M=0.5$ at time step size of 5 days.

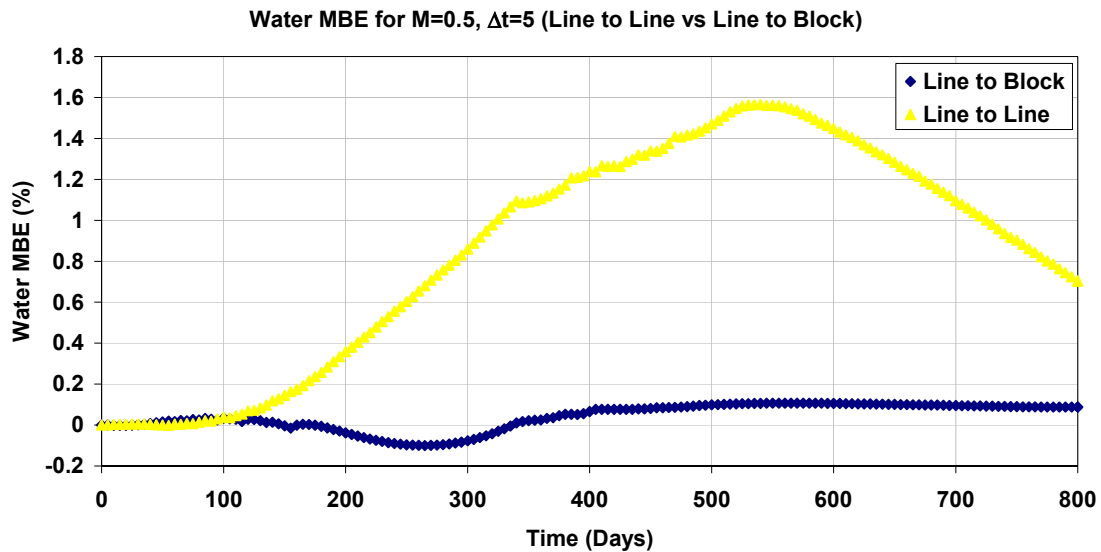


Fig. 4.9 Water MBE by saturation mapping for homogeneous, $\Delta t=5$ and $M=0.5$.

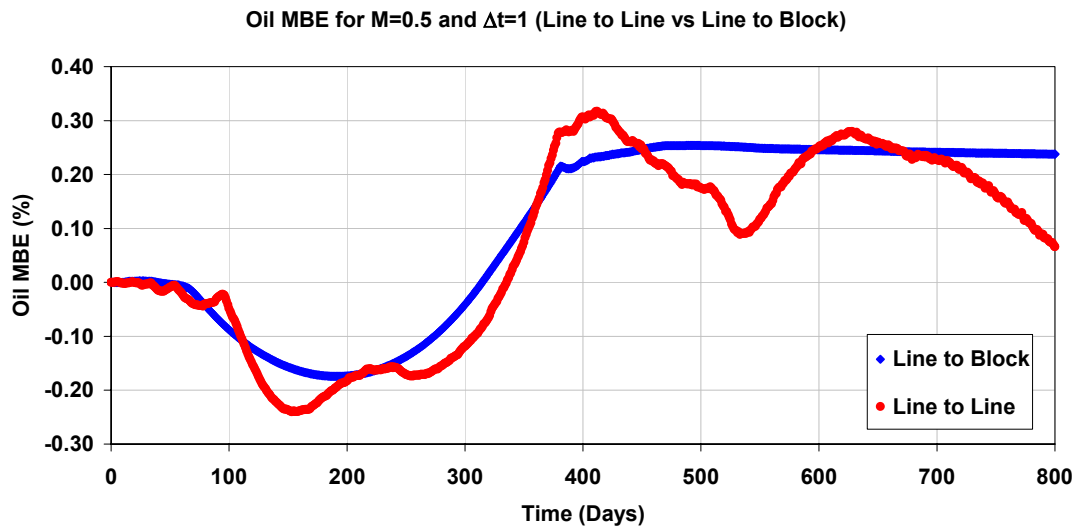


Fig. 4.10 Oil MBE by saturation mapping for homogeneous, $\Delta t=1$ and $M=0.5$.

Obviously, the last figures 4.9 and 4.10 validate that the Line to Line method produces higher MBE than the line to block.

4.3 Effects of Time Step Size

It is very known that streamlines models are efficient because their ability to take larger time steps with fewer pressure solution in IMPES formulation, in figures 4.3 to 4.8, we can see the effects of time step size in the saturation property based in streamline model, in those cases are observed some difference in accuracy for various time steps size using the same model.

Similar exercises were performed to observe the pressure profile, for Homogeneous and Heterogeneous case, changing the time step size, the results can see in figures 4.11 to 4.14.

In figure 4.11 is represented the pressure variation of the same homogeneous model with a mobility ratio of 0.5 at different time step sizes, larger time step introduces less preciseness in the model, likewise, the saturation mapping method affects the pressure calculation and distribution. Similar behavior is shown in figure 4.12 to figure 4.14.

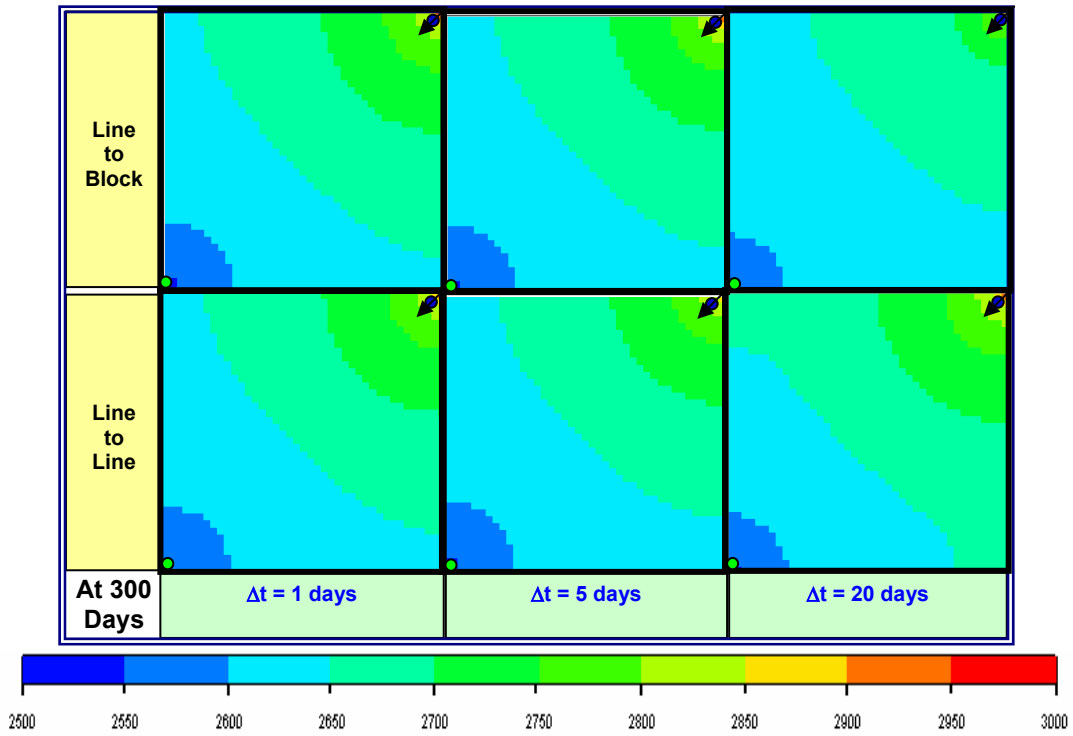


Fig. 4.11 Pressure profile by saturation mapping for homogeneous case and $M=5$.

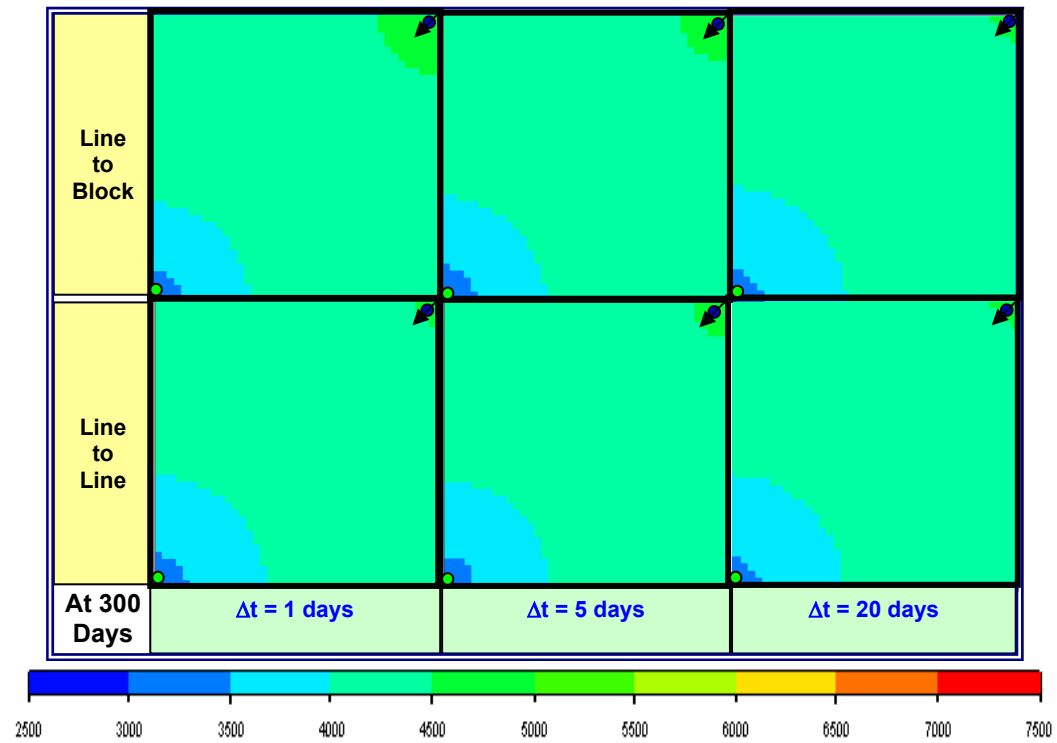


Fig. 4.12 Pressure profile by saturation mapping for homogeneous case and $M=10$.

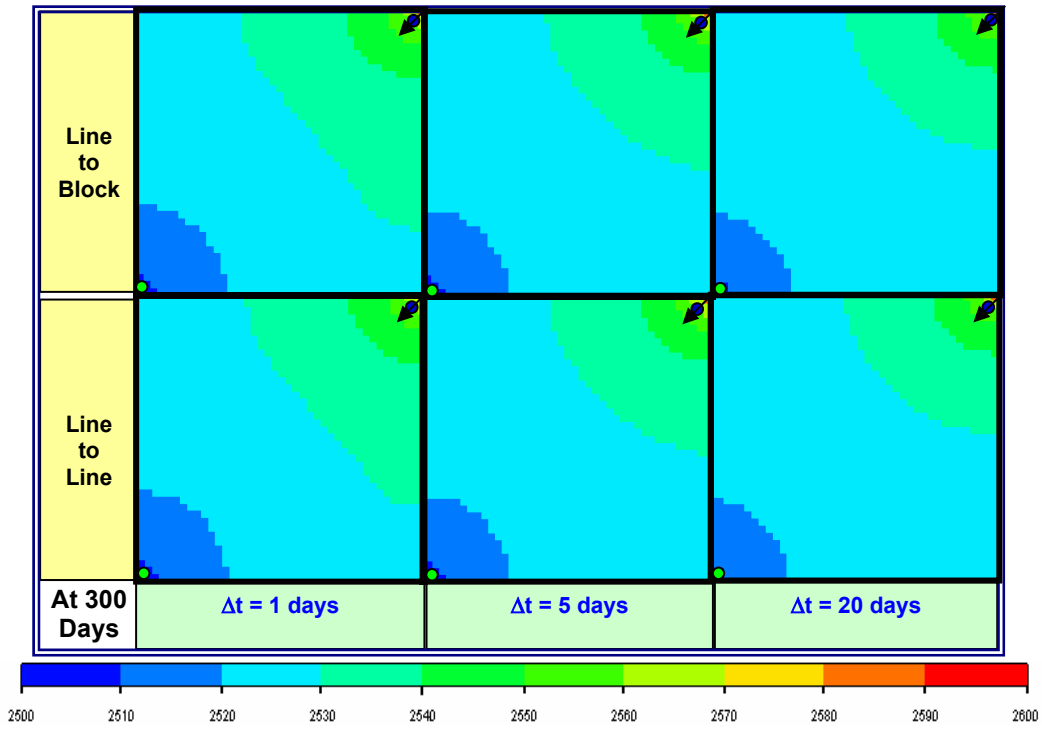


Fig. 4.13 Pressure profile by saturation mapping for heterogeneous case and $M=0.5$.

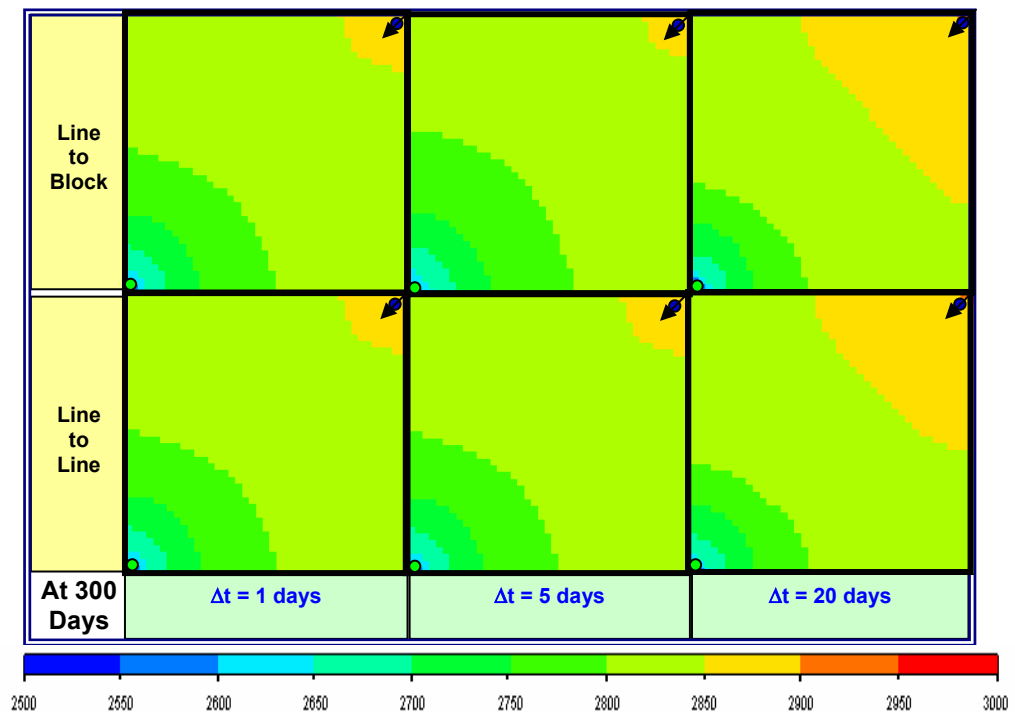


Fig. 4.14 Pressure profile by saturation mapping for heterogeneous case and $M=10$.

Definitively, time step size is an important element to consider in the accuracy of streamlines model, this element can affect the homogeneous and heterogeneous model solution in similar way. It is fundamental to optimize the number of pressure updates during streamline simulation not only to improve the computational efficiency but also to reduce the mapping errors. Details on how to improve the solution taking an ideal time step can be found in Osako et al reference.²⁶

4.4 Effects of Mobility Ratios (0.2, 0.5 and 10)

It was mentioned in the last chapter that the changes in mobility ratio affect the accuracy in the streamlines solution, the assumption indicates that the streamline paths change with time due to the changing mobility field. Thus the pressure field is updated periodically in accordance with these changes.

The sensitivities performed in the first stage lead us to determine the effect of the mobility ratio changes in the saturation streamline solution, figure 4.15 to 4.18 show the comparison of the results for each pressure update results by time step size (1 and 20 days) and varying the mobility ratios ($M=0.2, 0.5$ and 10) for homogeneous and heterogeneous cases.

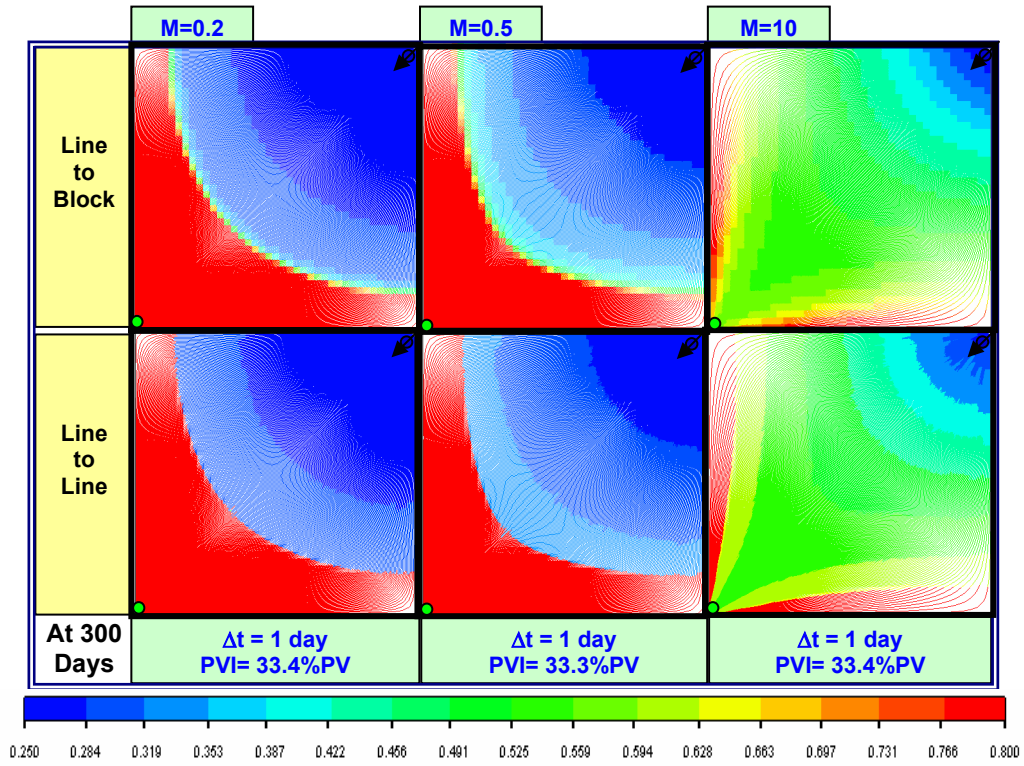


Fig. 4.15 Saturation profile based on mobility changes-homogeneous, $\Delta t=1$ day.

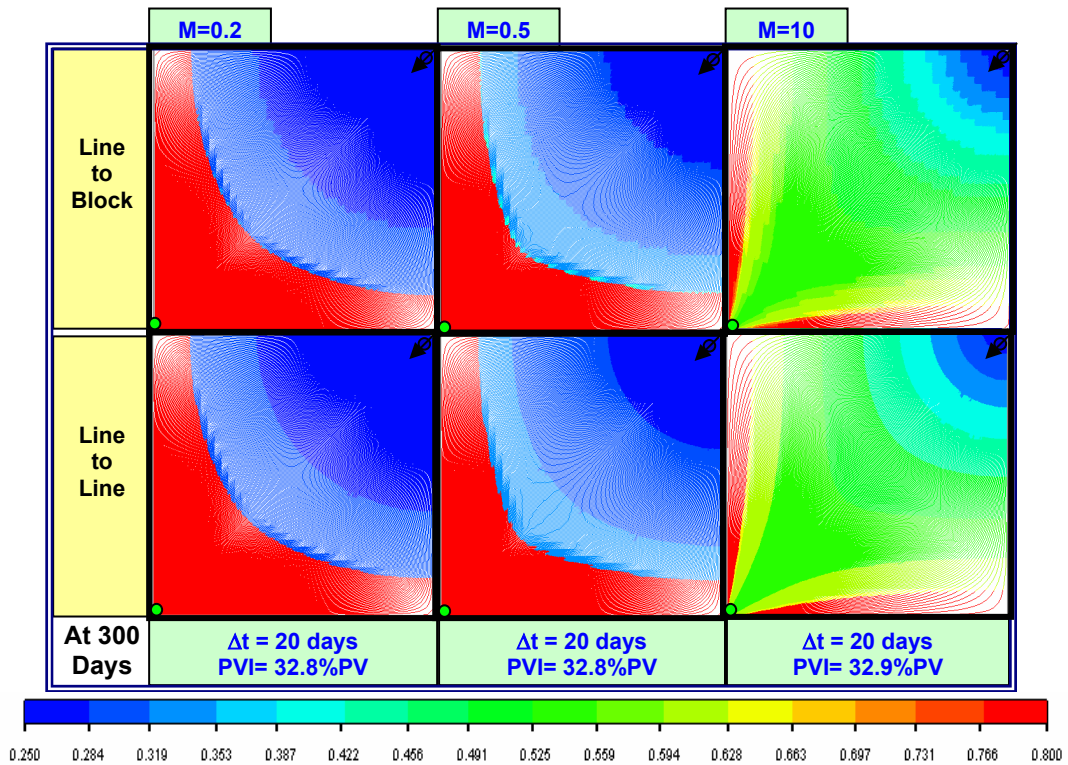


Fig. 4.16 Saturation profile based on mobility change-homogeneous, $\Delta t=20$ days.

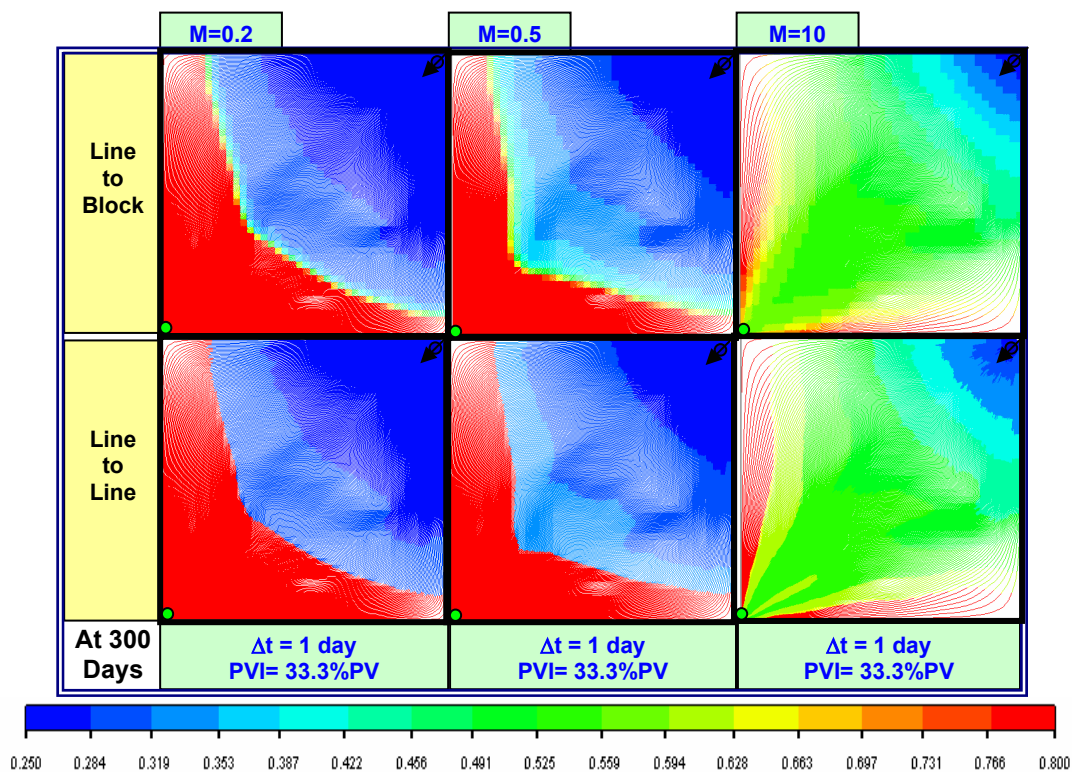


Fig. 4.17 Saturation profile based on mobility changes-heterogeneous, $\Delta t=1 \text{ day}$.

Line to Block mapping can also be observed in favorable mobility ratio displacements, in last Fig 4.17 we can see different displacements using mobility ratios of 0.2, 0.5 and 10, with a pressure update time step of 5 days.

Considering the saturation front, the effect of the mapping is not very significant in the favorable cases ($M=0.2$ and $M=0.5$), it is due to the heterogeneity that are repressed by the transverse fluxes because of the favorable mobility ratio.

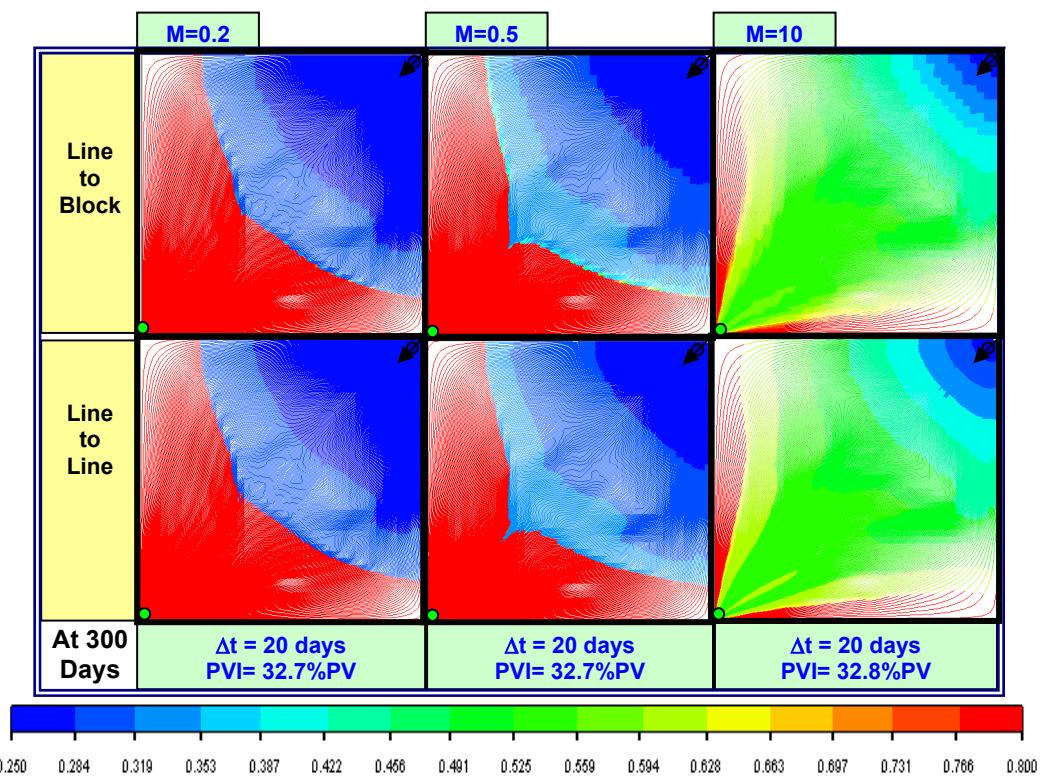


Fig. 4.18 Saturation profile based on mobility changes-heterogeneous, $\Delta t=20$ days.

Relatively high mobility in the oil zone results in relative uniform pressure in this region. In general, Buckley-Leverett³¹ theory predicts smaller mobility differences for unfavorable mobility ratios than for favorable ones.

The higher mobility ratio (unfavorable) in SL causes a decrease in the flow of oil to the producer, the low mobility ratios (favorable) causes the increasing of oil flow hence a better recovery is obtained. This assumption can be expressed in Fig. 4.19

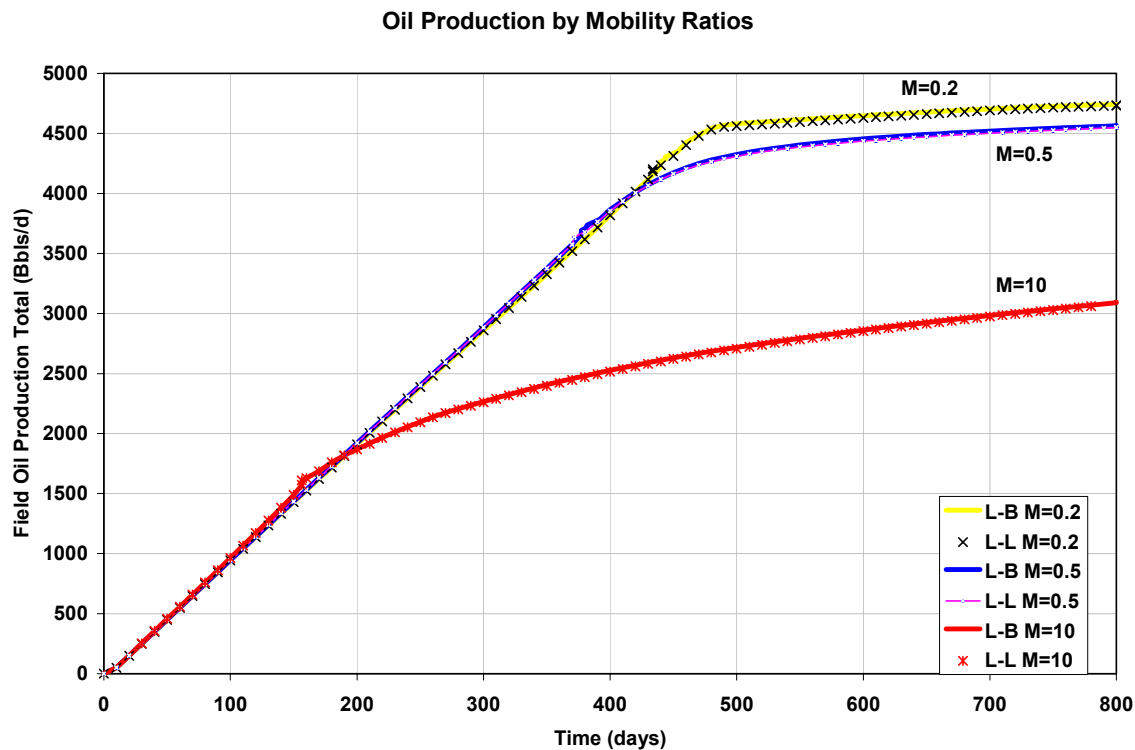


Fig. 4.19 Total oil production varying mobility ratios for homogeneous, $\Delta t=20$ days.

4.5 Effects of Number of Streamlines

For the second stage of this research, it is used the same synthetic $\frac{1}{4}$ -five spot pattern model from the first part (section 4.1) but considering some variations in the number of streamlines contemplated in the simulation model for the reservoir calculations. The default number of streamline provided by the commercial simulator is changed by: 0.01, 0.05, 0.1, 0.3, 0.5, and 0.8 fractions. This procedure leads to get 144 additional simulation cases and table 4.2 shows the cases distribution to be analyzed.

Table 4.2 Cases distribution for number of streamlines analysis

Model	Homogeneous & Heterogeneous											
Number of Streamlines (fraction)	M	Mapping Method	Delt (days)	Number of Streamlines (fraction)	M	Mapping Method	Delt (days)	Number of Streamlines (fraction)	M	Mapping Method	Delt (days)	
0.01 0.05 0.1 0.3 0.5 0.8	0.5	Line to Line	1	0.01 0.05 0.1 0.3 0.5 0.8	0.5	Line to Line	5	0.01 0.05 0.1 0.3 0.5 0.8	0.5	Line to Line	20	
0.01 0.05 0.1 0.3 0.5 0.8	10			0.01 0.05 0.1 0.3 0.5 0.8	10			0.01 0.05 0.1 0.3 0.5 0.8	10			
0.01 0.05 0.1 0.3 0.5 0.8	0.5	Line to Block		0.01 0.05 0.1 0.3 0.5 0.8	0.5	Line to Block		0.01 0.05 0.1 0.3 0.5 0.8	0.5	Line to Block		
0.01 0.05 0.1 0.3 0.5 0.8	10			0.01 0.05 0.1 0.3 0.5 0.8	10			0.01 0.05 0.1 0.3 0.5 0.8	10			

The number of streamlines during simulation determines the degree of transverse resolution. The computational advantage of streamline models is based on the decomposition of the 3-D saturation calculations into 1-D calculations along streamlines and this decomposition could lead to some problems in saturation mapping from 1-D streamlines to the 3-D, numerical accuracy and material balance errors³².

The discretization error in streamline simulation can be impacted by the number of streamlines. The spatial density of streamlines can vary depending on the heterogeneity, flow geometry and the proximity to the wells. This will lead to local as well global discretization errors during streamline simulation.

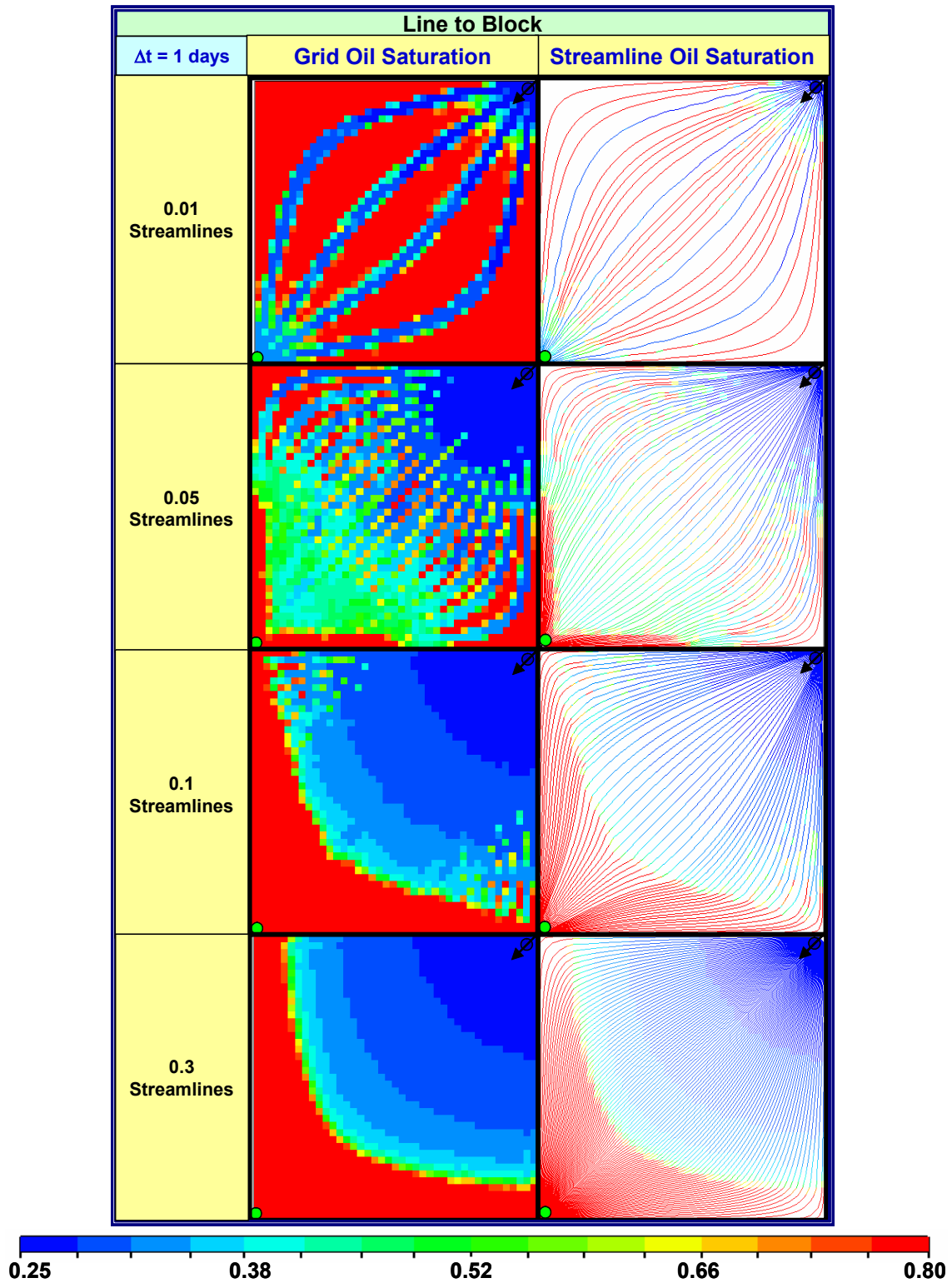


Fig. 4.20 Line to block saturation mapping for 0.01, 0.05, 0.1 and 0.3 fractions of streamlines number and $M=0.5$ for homogeneous, $\Delta t=1$ day at 300 days

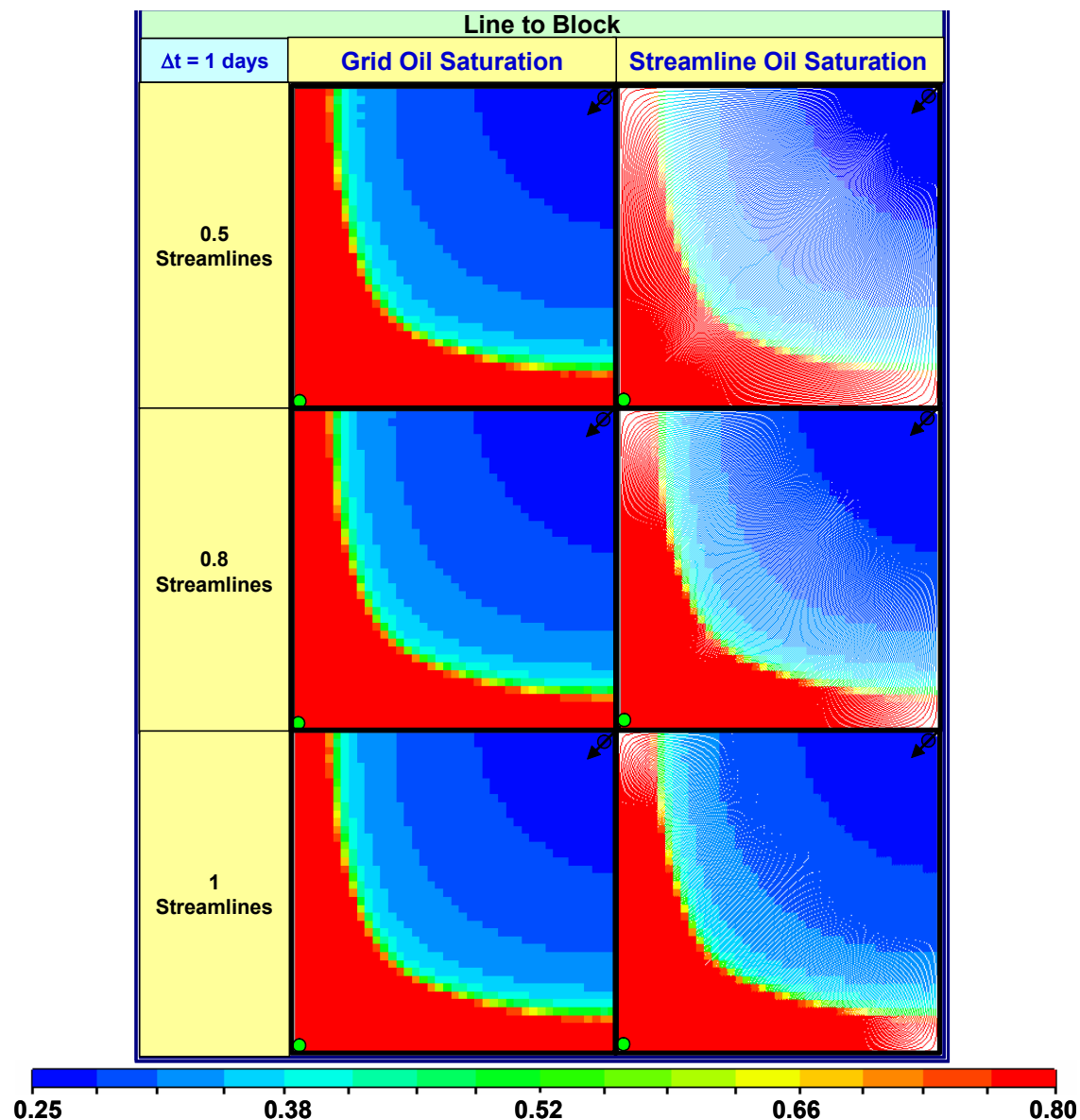


Fig. 4.21 Line to block saturation mapping for 0.5, 0.8 and 1 fractions of streamlines number and $M=0.5$ for homogeneous, $\Delta t=1$ day at 300 days

Figures 4.20 and 4.21 illustrate how the number of streamlines used can affect the solution of the model, more streamlines represent better results. Practically, increases the number of streamlines used by the saturation solver requires to increase approximately linearly the CPU and memory requirements. Although, the quality of the solution of the saturation equation is dependent on the number of streamlines used. If the grid has many areas with no flow (inactive cells), it might be necessary to increase the number of streamlines to capture the flow around barriers.

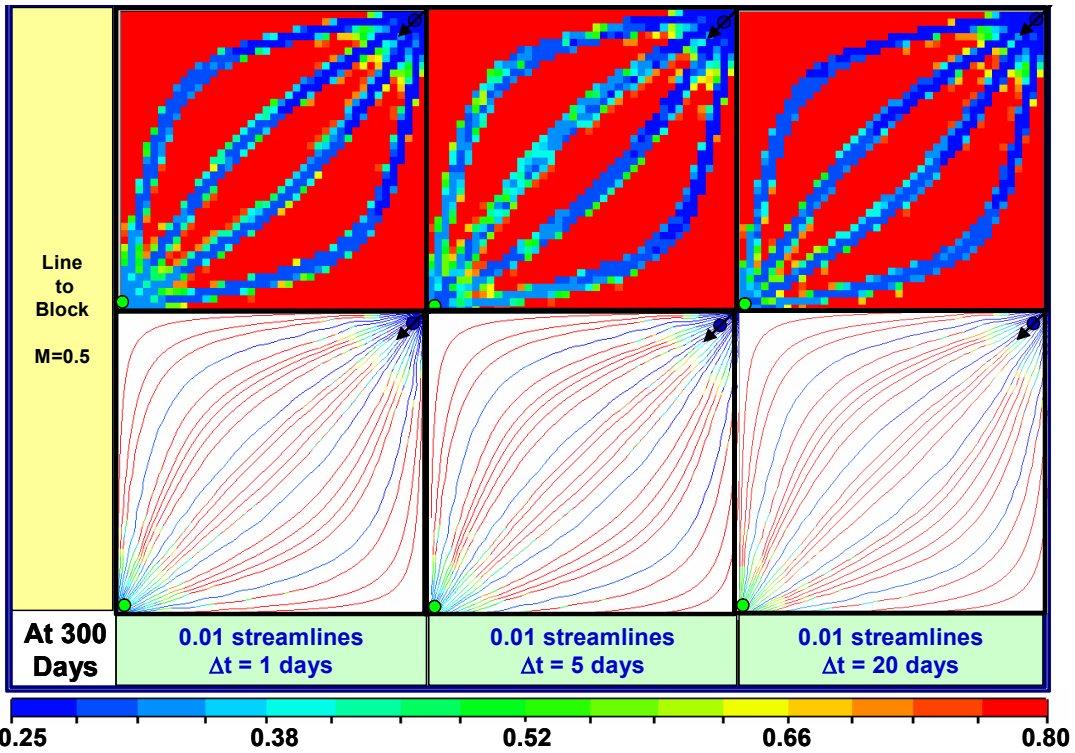


Fig. 4.22 Line to block mapping for 0.01 fraction of streamlines number and $M=0.5$ for homogeneous using different time step sizes at 300 days

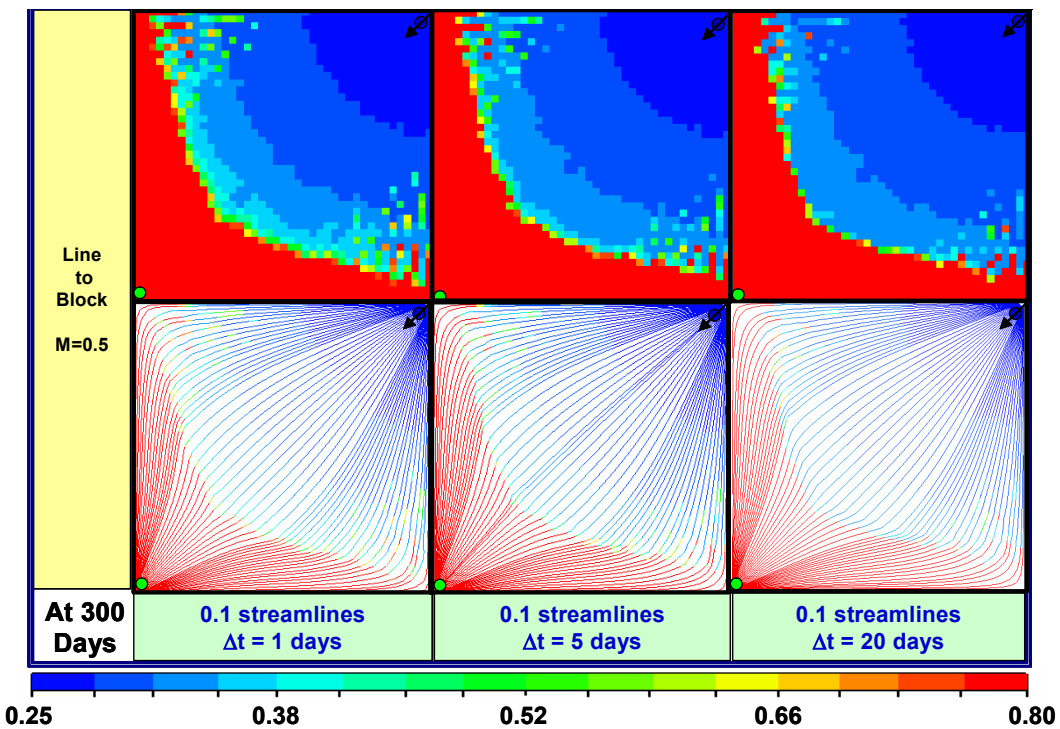


Fig. 4.23 Line to block mapping for 0.1 fraction of streamlines number and $M=0.5$ for homogeneous using different time step sizes at 300 days

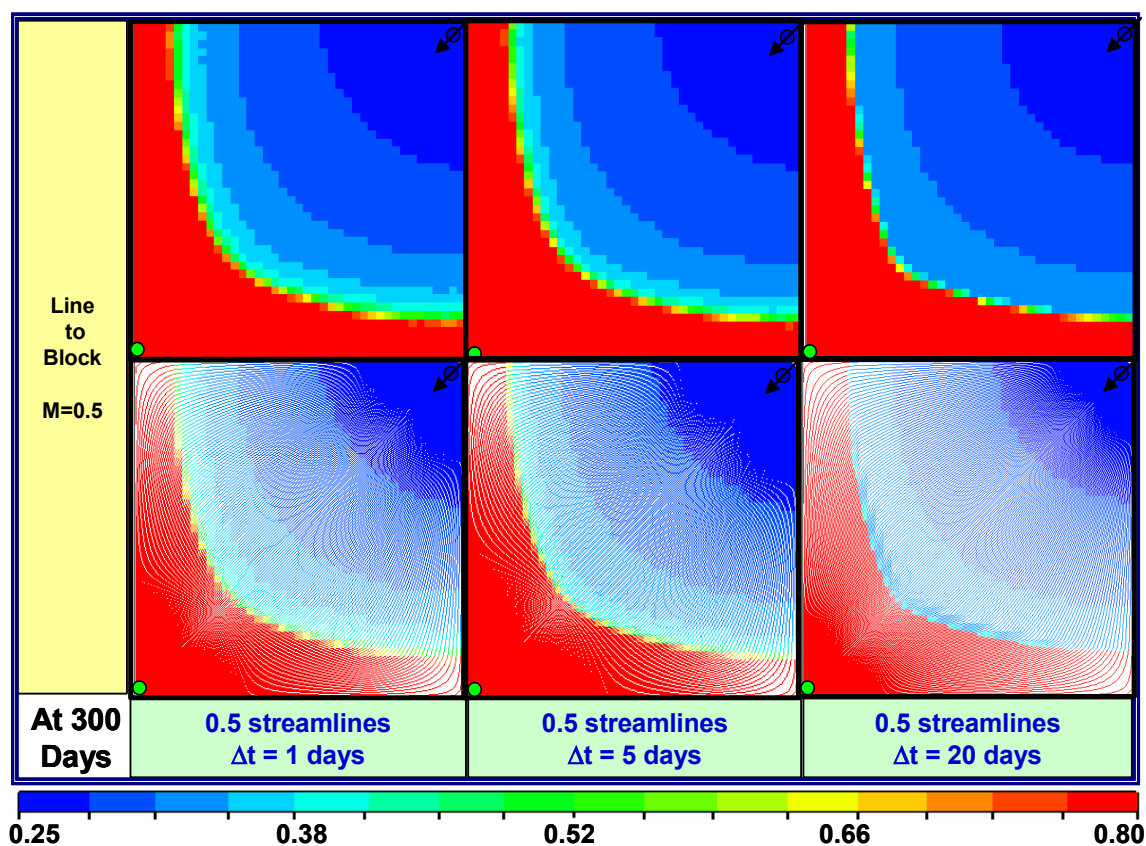


Fig. 4.24 Line to block mapping for 0.5 fraction of streamlines number and $M=0.5$ for homogeneous using different time step sizes at 300 days

In figures 4.22 to 4.24 we can see how the time step size affects the streamline solution depending on the number of streamline using in the model, apparently the effect is not very notorious but as the previous analysis we note that the larger time step of 20 days show a little bit different results than the 1 and 5 days time step size. Those results lead us to find that even changing the number of streamlines in the model the smaller time step can give better resolution and less accuracy errors.

Figure 4.25 and 26 show how saturation mapping methods can affects the saturation results depending on the number of streamlines used in the homogeneous model for the same $M=0.5$, same time step size and at 300 simulation days.

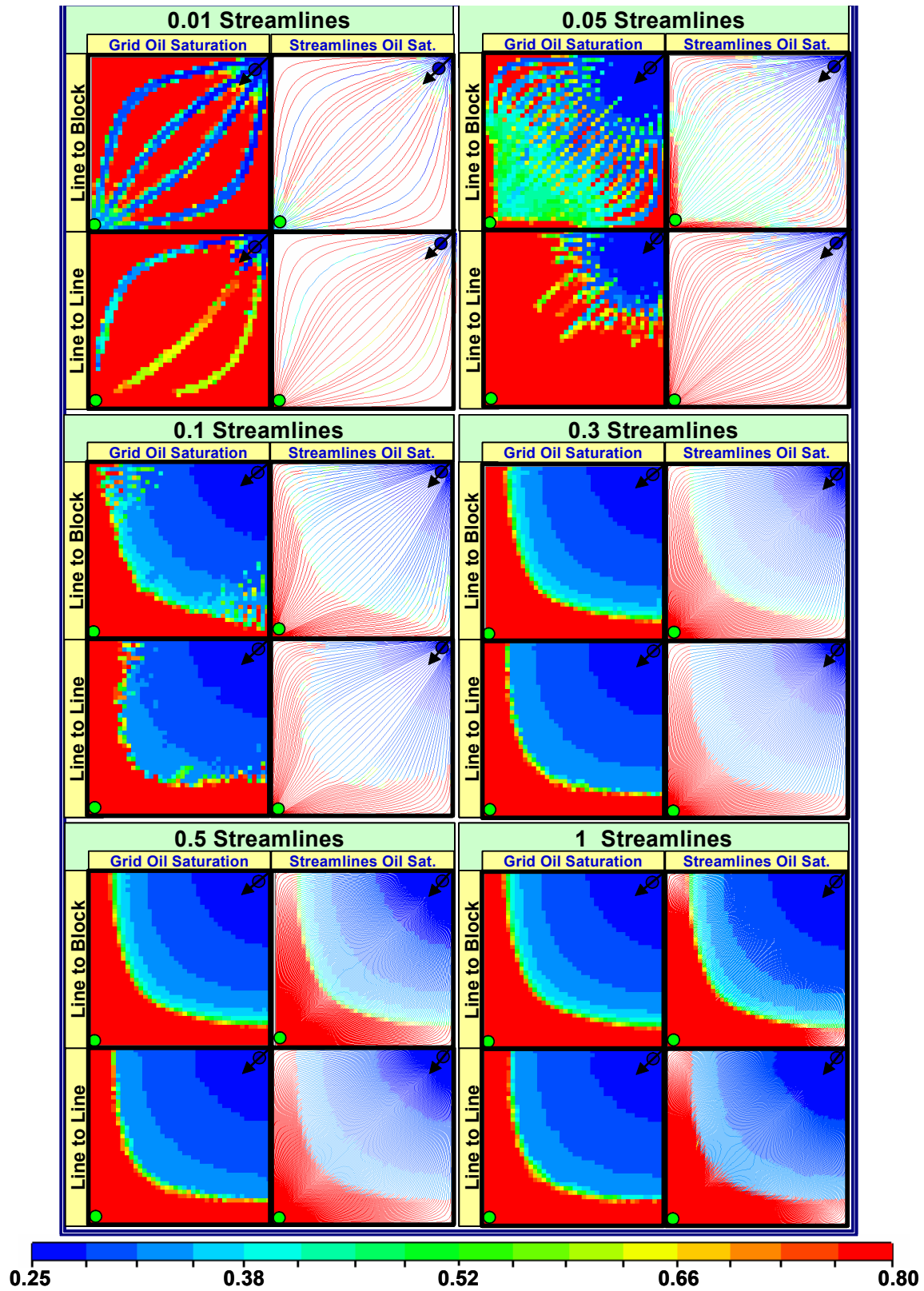


Fig. 4.25 Saturation mapping comparison by number of streamlines in homogeneous model for $\Delta t=1$ day

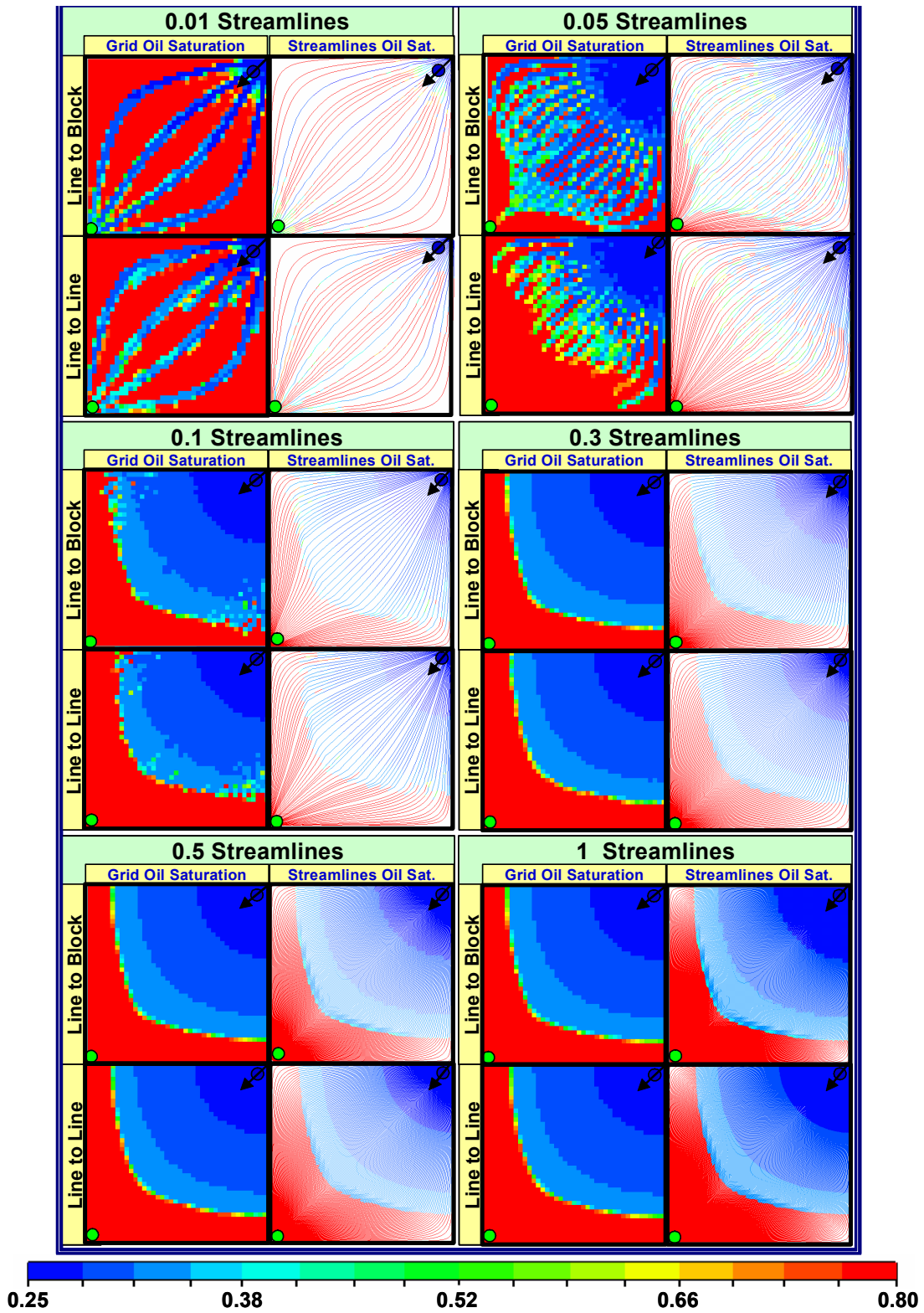


Fig. 4.26 Saturation mapping comparison by number of streamlines in homogeneous model for $\Delta t=20$ days

Also we compared the results based in the number of streamlines and the mobility ratios used in the model, for $M=0.5$ (favorable) and $M=10$ (less favorable). Likewise, we performed those exercises for line to block and line to line saturation mapping methods at different time step sizes (1, 5, and 20 days), and for all the cases, the specific time showed in all the simulation runs was 300 days, the results can be found in figures 4.27 to 4.37.

The result associated to this sensitivity analysis will show that any missed grid block is assigned a saturation based on tracing streamlines backwards in the velocity field from a missed grid block to one containing multiple streamlines and they corroborate the impacting effect of the number of streamlines in a simulation model³³.

Moreover, it can be mentioned that few streamlines lead to less resolution in the results, and also we can remark how the use of small number of lines (0.01, 0.05, 0.1, and 0.3) causes a loss of information in the corners where the streamlines are not crossing the grid blocks.

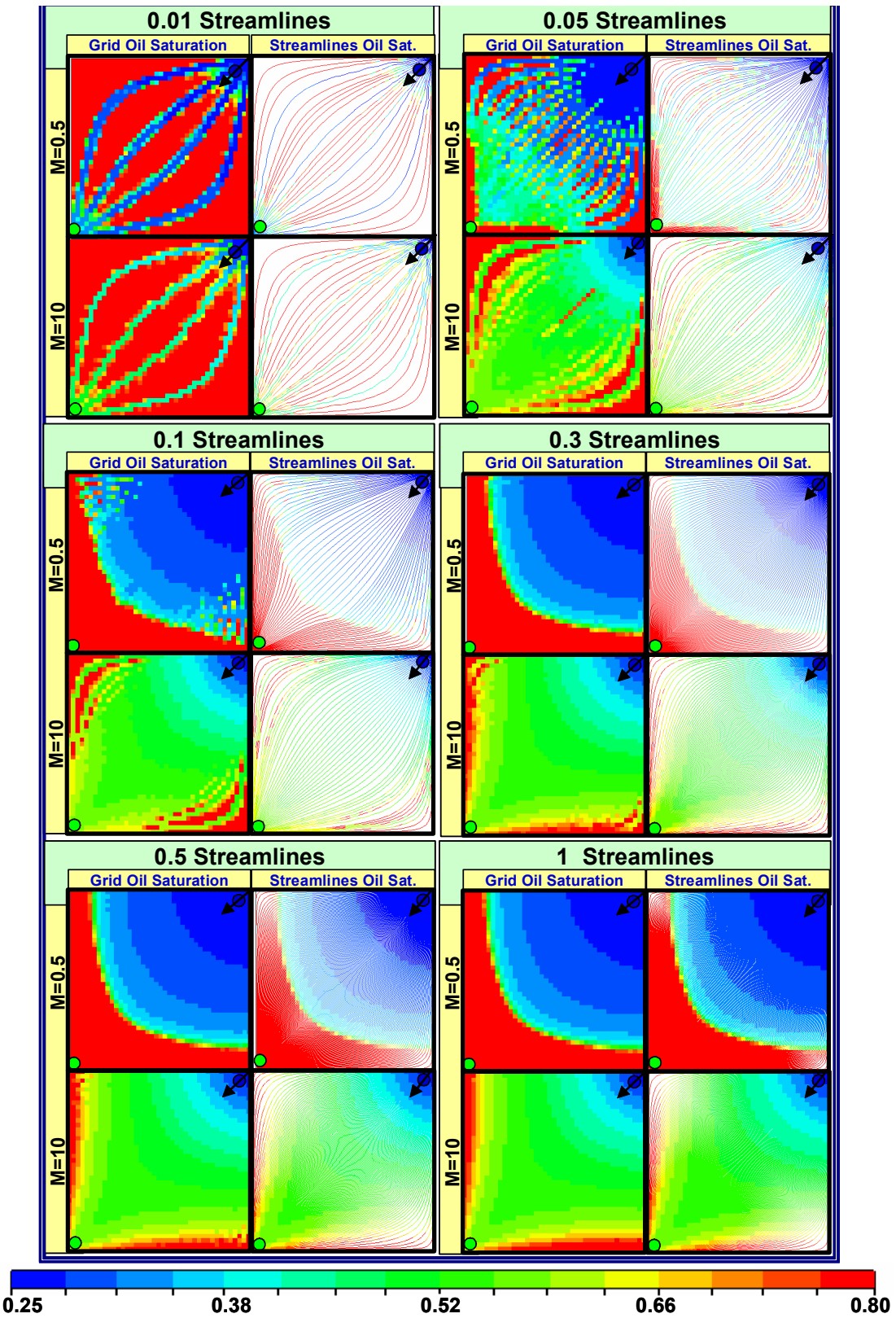


Fig. 4.27 Mobility comparison by streamlines number for line to block in homogeneous model at time step size of 1 day.

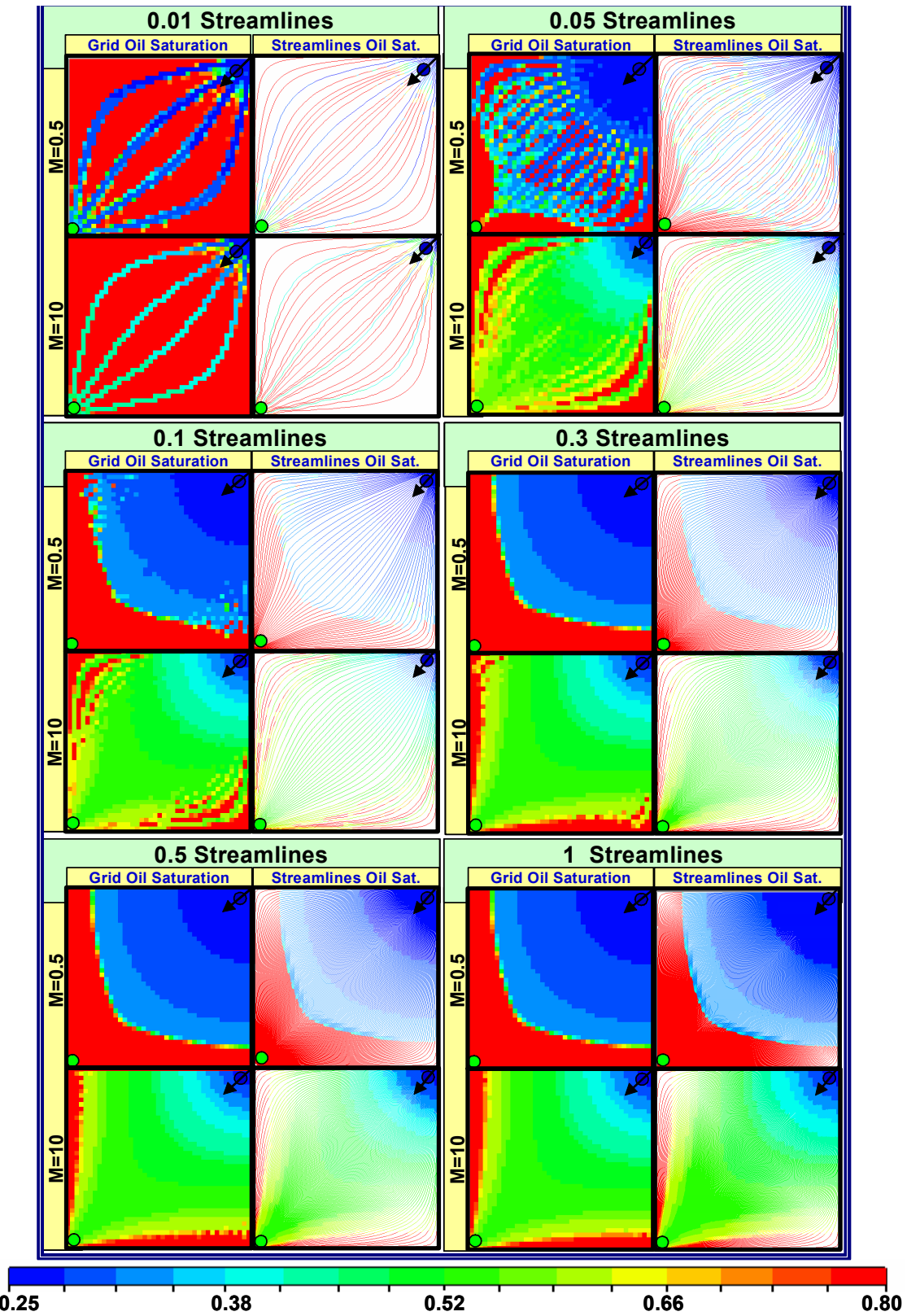


Fig. 4.28 Mobility comparison by streamlines number for line to block in homogeneous model at time step size of 20 days.

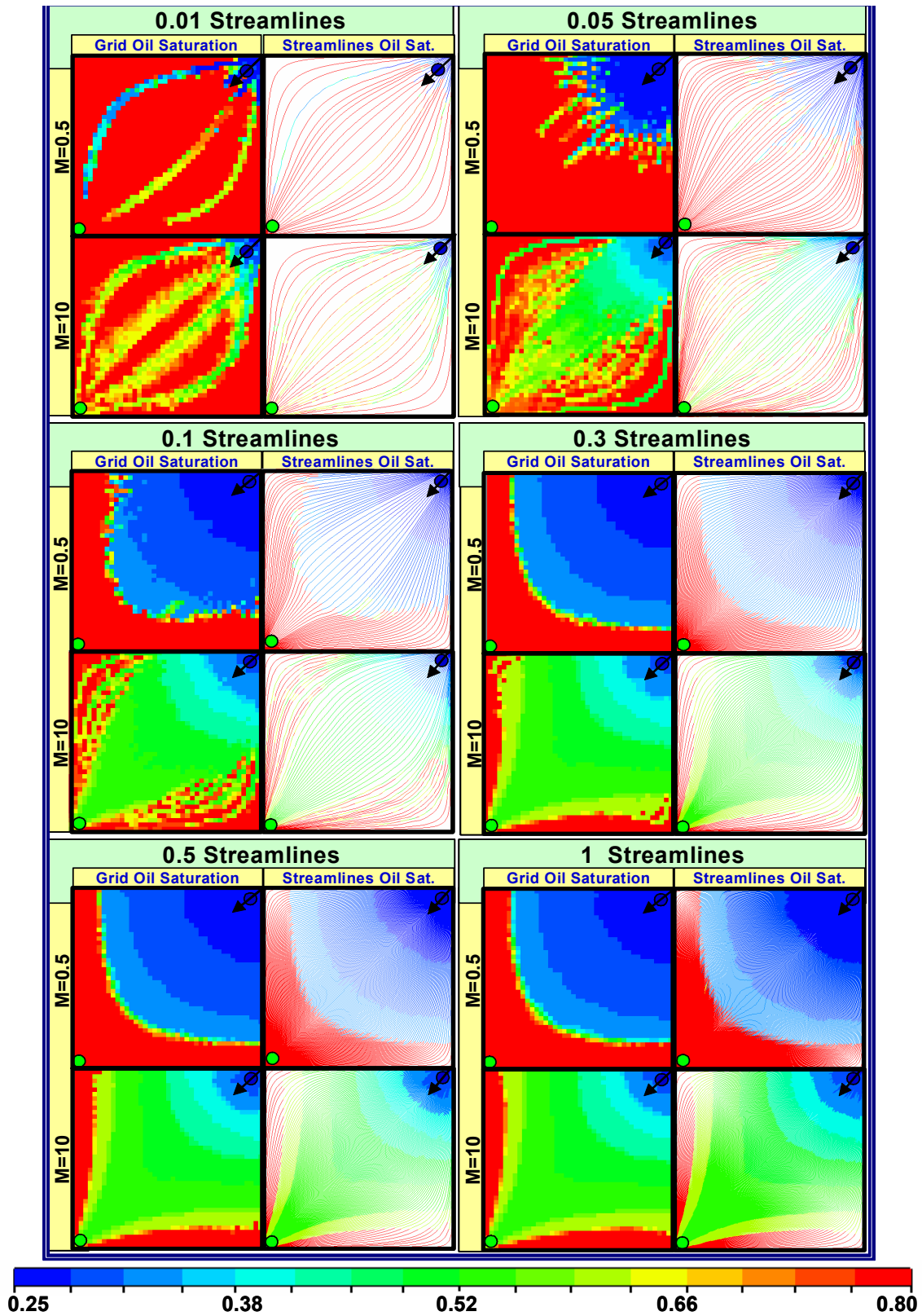


Fig. 4.29 Mobility comparison by streamlines number for line to line in homogeneous model at time step size of 1 day.

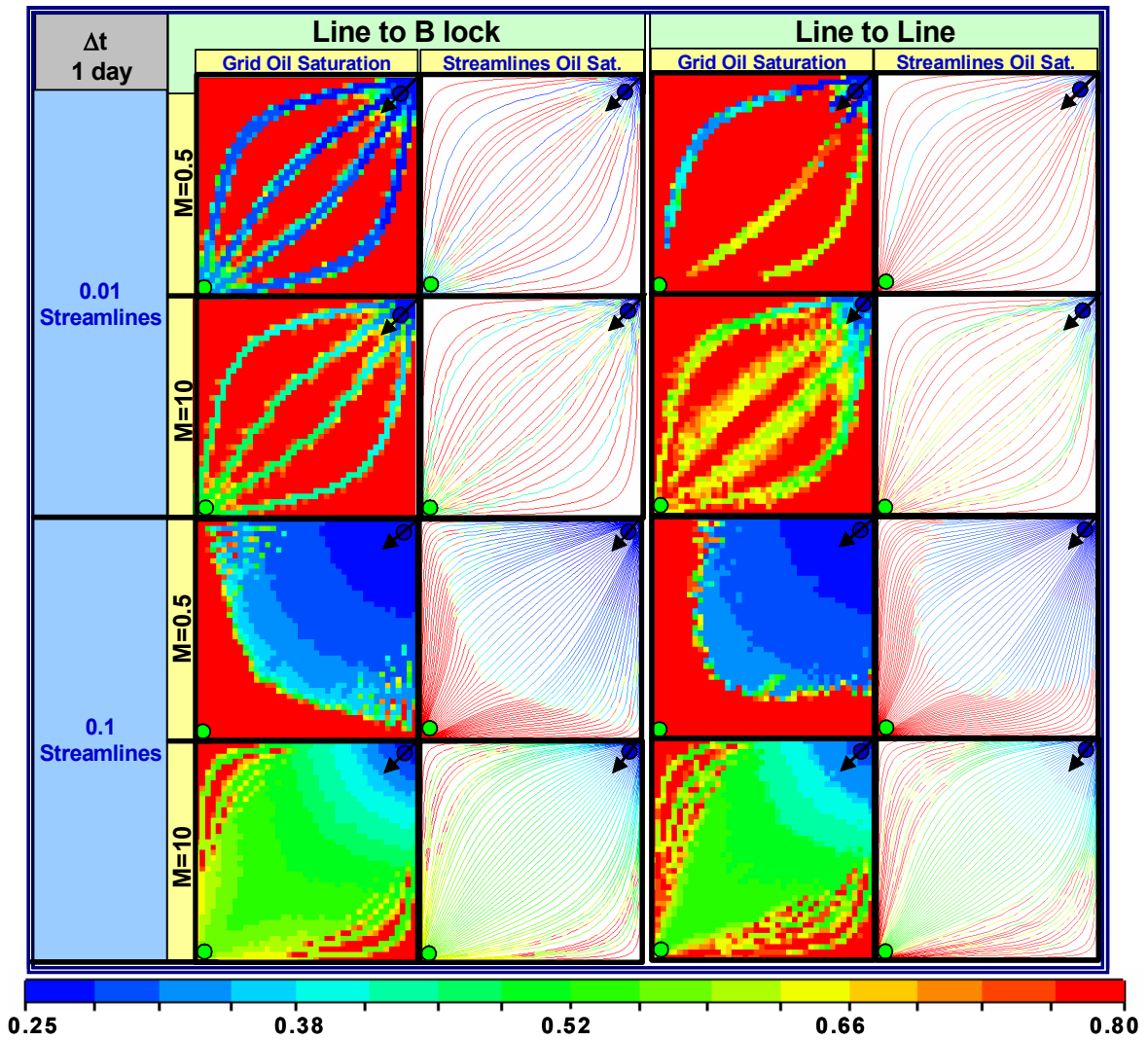


Fig. 4.30 Comparison using different numbers of streamlines in homogeneous model at time step size of 1 day (0.01 and 0.1 fractions)

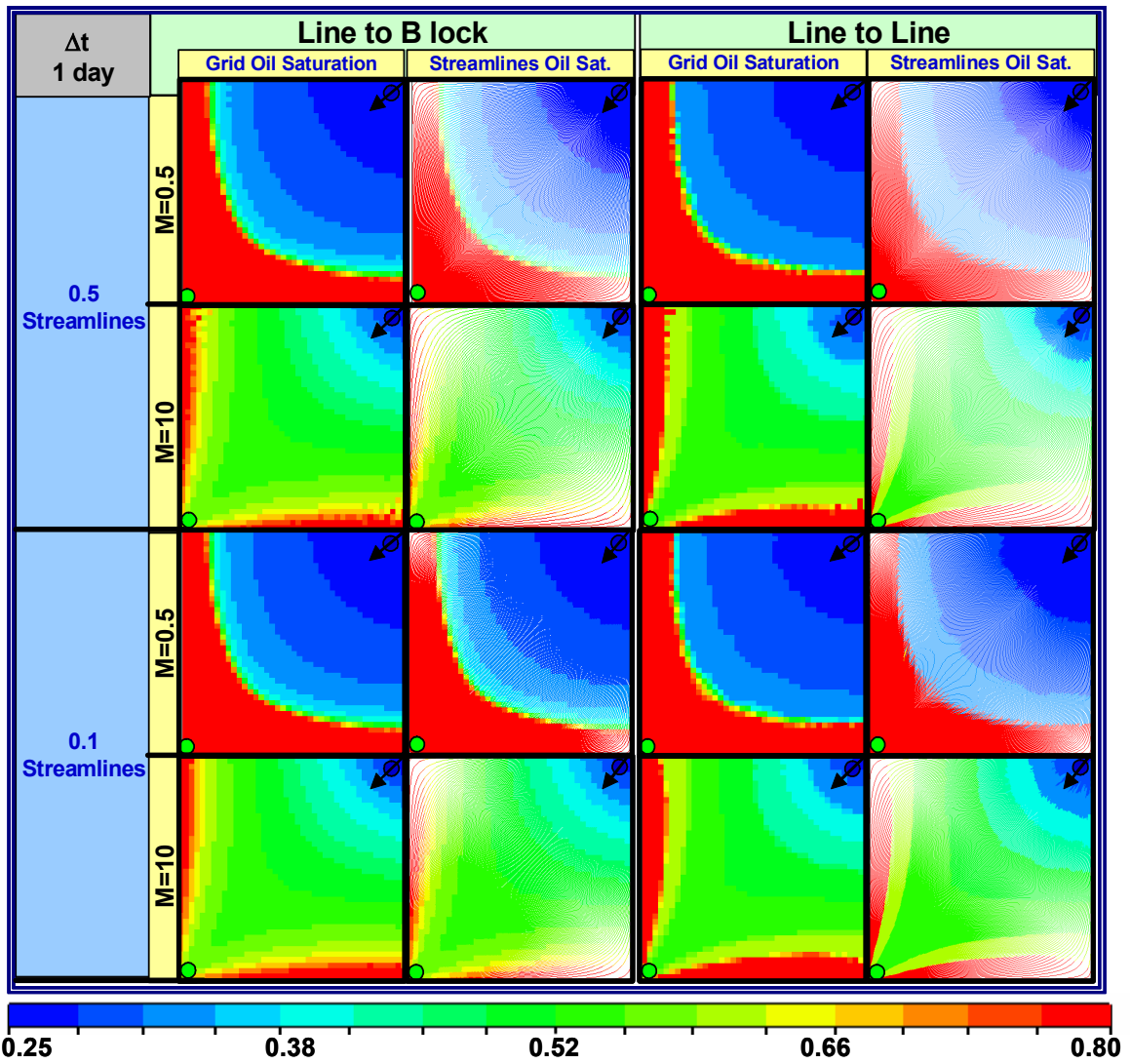


Fig. 4.31 Comparison using different numbers of streamlines in homogeneous model at time step size of 1 day (0.5 and 1 fractions)

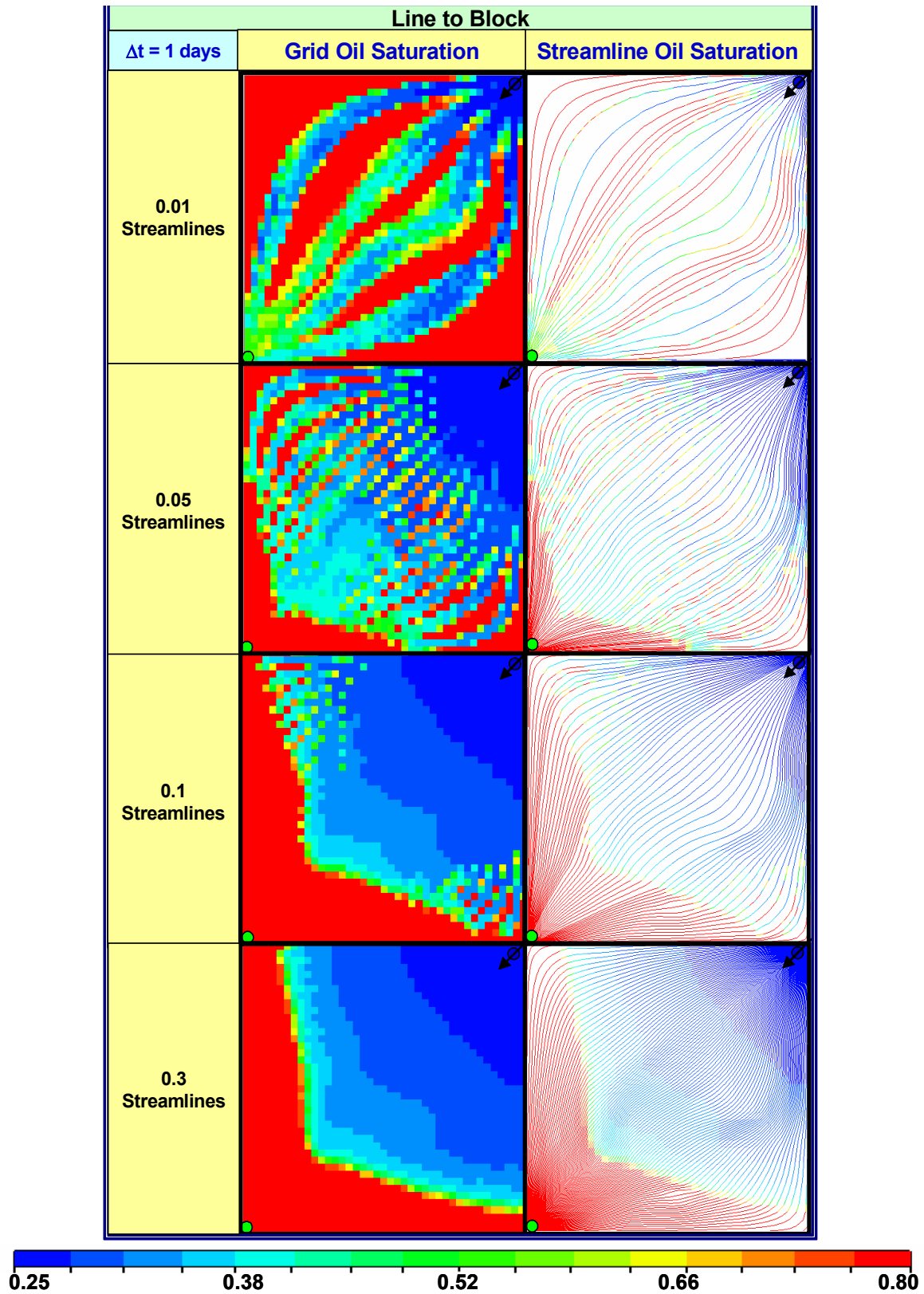


Fig. 4.32 Line to block saturation mapping for 0.01, 0.05, 0.1 and 0.3 fractions of streamlines number and $M=0.5$ for heterogeneous, $\Delta t=1$ day at 300 days

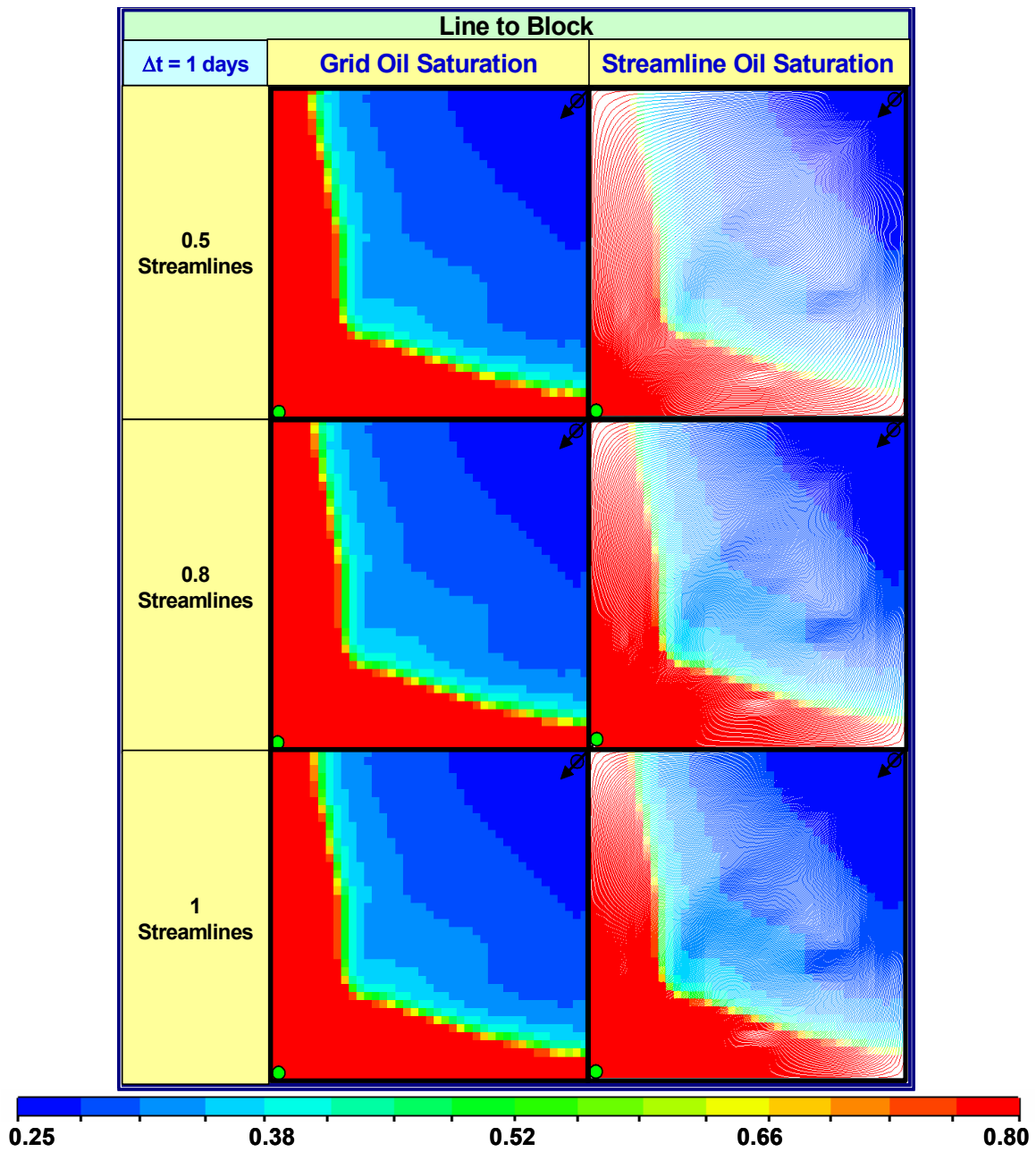


Fig. 4.33 Line to block saturation mapping for 0.5, 0.8, and 1 fractions of streamlines number and $M=0.5$ for heterogeneous, $\Delta t=1$ day at 300 days

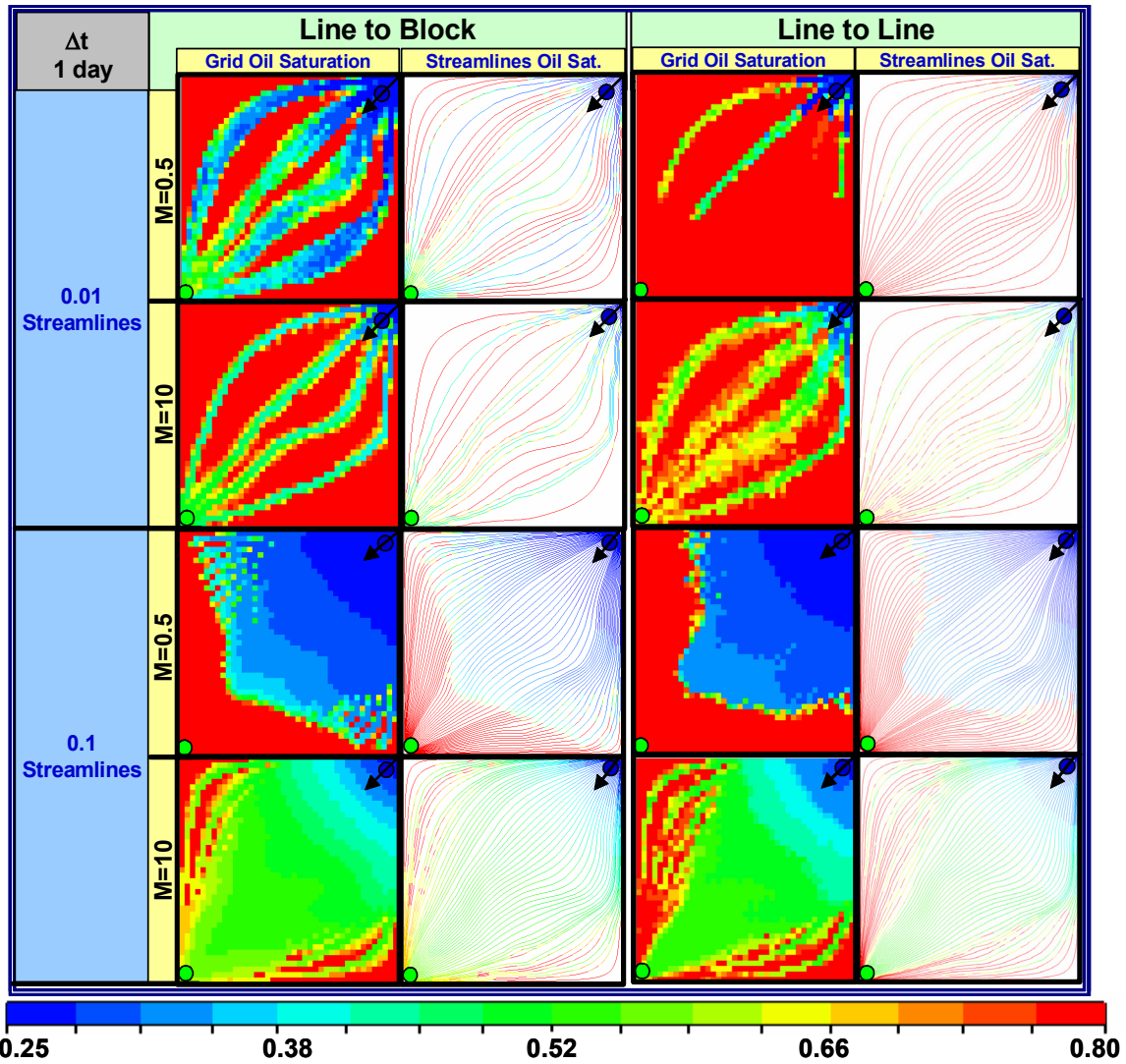


Fig. 4.34 Comparison by mobility ratios using different numbers of streamlines (0.01 and 0.1 fractions) in heterogeneous model at time step size of 1 day

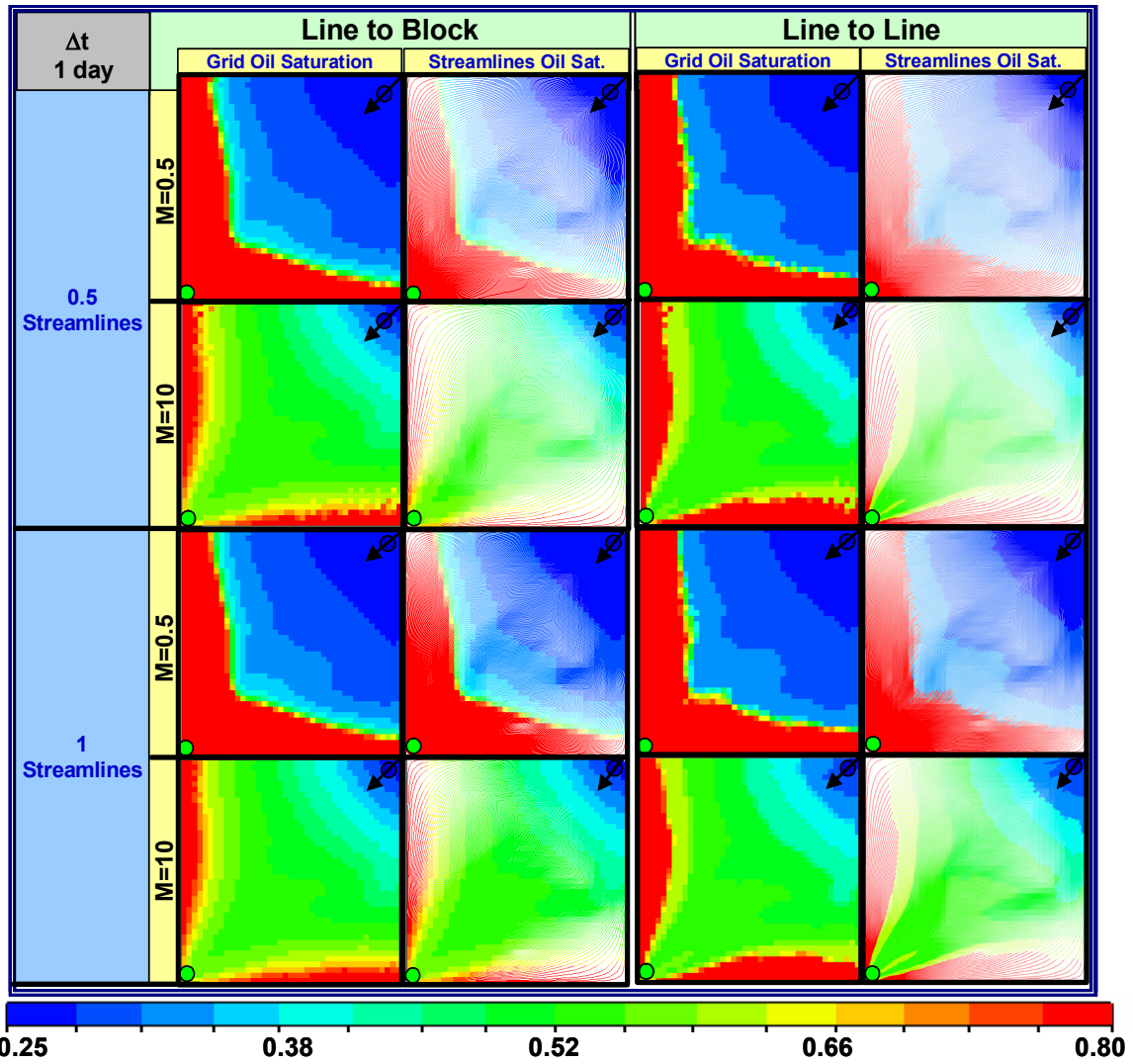


Fig. 4.35 Comparison by mobility ratios using different numbers of streamlines (0.5 and 1 fraction) in heterogeneous model at time step size of 1 day

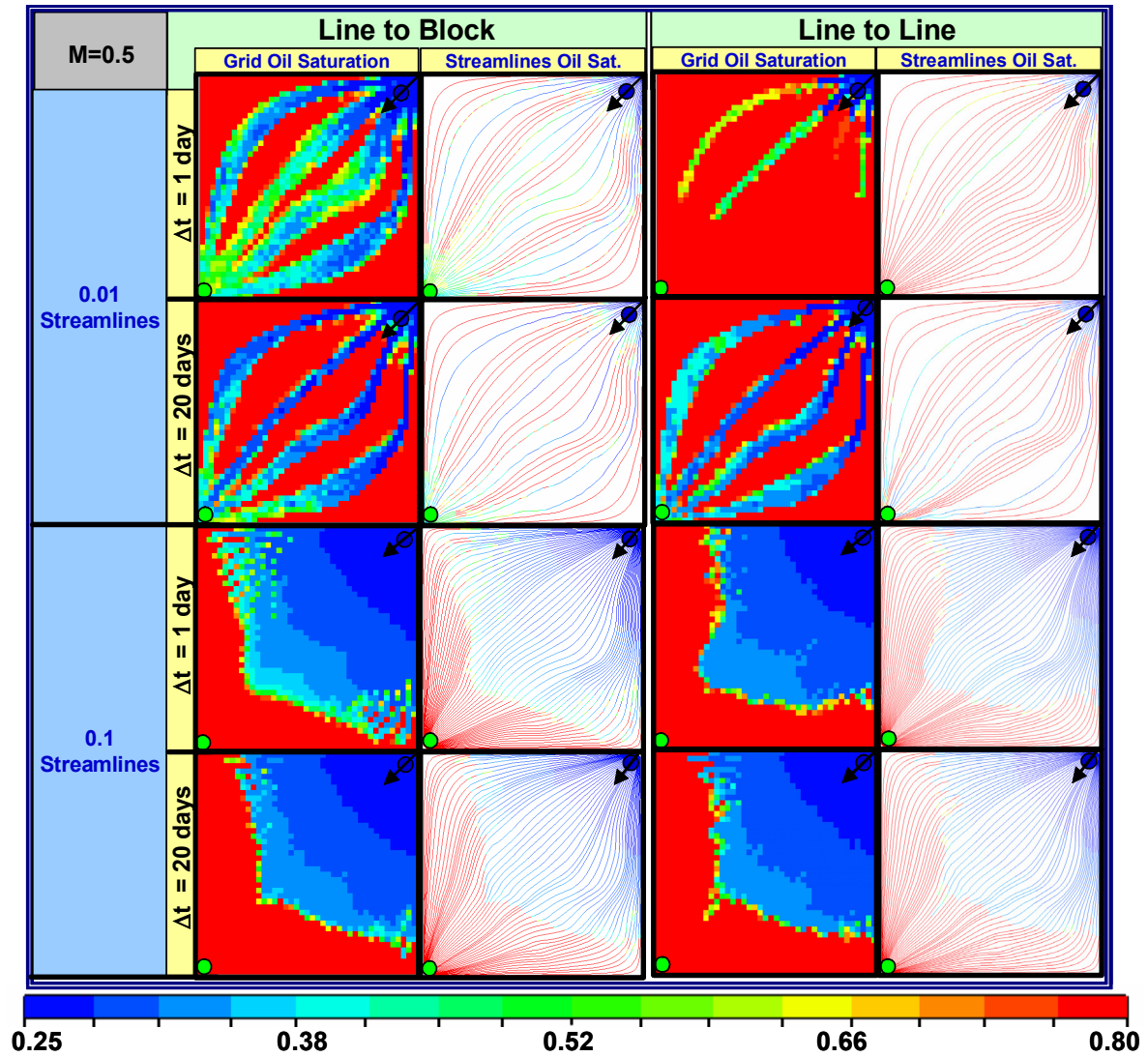


Fig. 4.36 Comparison by time step size using different numbers of streamlines (0.01 and 0.1 fractions) in heterogeneous with $M=0.5$

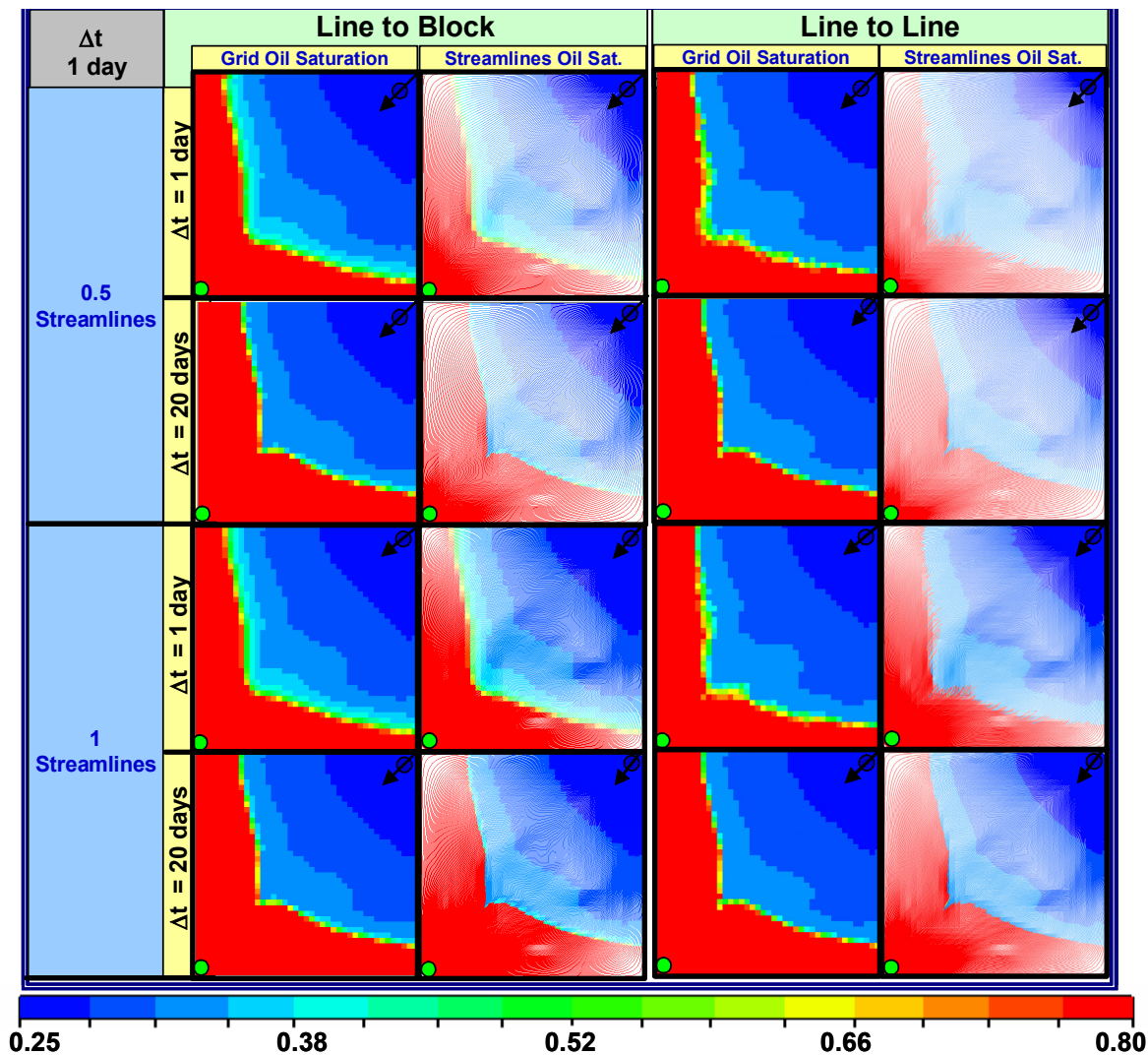


Fig. 4.37 Comparison by time step size using different numbers of streamlines (0.5 and 1 fractions) in heterogeneous with $M=0.5$.

Use Line to Line mapping of saturations minimizes numerical dispersion as it was demonstrated in previous sections but it does not guarantee the preciseness of the model until a reasonable and optimum number of streamline is defined. Line to Line requires more memory and increased CPU time.

Definitively, the results from the streamline method are highly dependent on the number of stream lines that are traced in a model. The greater number of streamlines that are launched in a model, the fewer number of grid blocks that are missed with the streamlines. For highly heterogeneous flows may be an infinite number of streamlines

may be needed to trace from injectors in order to intersect all grid blocks. However, recall that any missed grid block is assigned a saturation based on tracing streamlines backwards in the velocity field from a missed grid block to one containing multiple streamlines

Finally, from the extensive analysis performed in this section, now we can clearly assure the importance of the number of streamline to use in a simulation model, this mentioned element influences the solution in resolution and accuracy.

4.6 Effects of Gravity in Streamline Solution

The third stage involves the analysis and modeling of the gravity effects for the saturation solver in the homogeneous and heterogeneous synthetic models activating the gravity segregation option in the streamline based simulator. Here we are going to consider a cross section model with $N_z=50$ (50 layers) and $N_x=50$ (50 cells in I direction) but with $D_x=5$ ft and $D_z=2$ ft, defining also one producer and one injector well to study the effect. It is important to mention that for the sensitivities in this topic will be based on 2 phase fluid model, using two water injection rates of 10 and 50 Bbls/Day to show the gravity segregation behavior, also turning on the gravity effect in the saturation solver require to define a number of sub-iterations in the saturation solver to capture the segregation effect, due to this we consider cases of 1 and 4 iteration number (SegIT) for each case.

SegIT is defined as the frequency of segregation iterations within each time step, this is the number of times that the saturation is mapped from streamlines onto the gravity lines, allowing heavy fluids to move down and lighter fluids to move up. If the reservoir is very thin, or steeply dipping, or the fluids have little density contrast, then gravity segregation will not be a significant process in the reservoir.

Additionally, the sensitivities analysis will be carried out based on changes for the gravity number (N_g) and time step size for mobility ratio of 0.5. The fluid properties

between the miscible phases are mixed at the grid block scale. Using Darcy's law to determine the travel times, a dimensionless gravity number is defined by Tchelepi and Orr²⁰ as:

$$N_g = \frac{\bar{k}_v \Delta \rho g L^2}{\bar{k}_H (\Delta p_H) h} \quad (4.1)$$

where \bar{k}_v and \bar{k}_H are the permeability averages vertical and horizontal respectively, $\Delta \rho$ is the fluid density difference, Δp_H is the pressure drop in the horizontal direction, L the distance between the wells, and h is the model height.

Based on this definition, as density differences or model length increase, the gravity number increases, while if model height or horizontal flow rate increase (horizontal pressure drop increases), the gravity number decreases. N_g in Eq. 4.1 is only for strictly two-dimensional homogeneous permeability fields. For more complex displacements, all the parameters in Eq. 4.1 can vary in space, and the pressure drop can vary in time due to changes in the mobility Field. Thus, a single value of N_g cannot characterize a displacement.

Another important parameter in the gravity effect analysis is the K_v/K_h variation, which is varied in 1, 0.1 and 0.01 for the sensitivities analysis. For this simple 2D model K_v and K_h were determined from pressure solves using constant pressure and no-flow boundary conditions in each coordinate direction. Every grid block in the domain must contain a streamline. The complication of gravity is that some grid blocks will contain circulation streamlines, rather than streamlines passing from injectors to producers. As gravity forces are increased, this occurs in a greater percentage of grid blocks. Likewise, the pure fluid density difference ($\Delta \rho$) was taken into account in this stage changing the oil density (ρ_o) in 0.8 and 0.9 fractions of a specific water density (ρ_w) to model the effect in the streamlines. All the mentioned considerations were used for homogeneous and heterogeneous models, with $M=0.5$ and time step size of 5 and 20 days. At the end of

this sensitivities analysis 192 cases were generated and compared to determine the studied effect. Table 4.3 presents the final cases distribution in this stage.

Table 4.3 Cases distribution for gravity effect analysis

Saturation Mapping Method Line to Block, and Line to Line Homogeneous and Heterogeneous Model							
kv/kh	ρ_w	ρ_o Calculated	ρ_o	Delt	Qwinj (STB/D)	M	Iteration for Segregation
1 0.1 0.01	62.5	$\rho_o = \rho_w^{0.8}$	50	5 days	10	0.5	1
1 0.1 0.01		$\rho_o = \rho_w^{0.9}$	56.25				
1 0.1 0.01	62.5	$\rho_o = \rho_w^{0.8}$	50	20 days			
1 0.1 0.01		$\rho_o = \rho_w^{0.9}$	56.25				
1 0.1 0.01	62.5	$\rho_o = \rho_w^{0.8}$	50	5 days	10	0.5	4
1 0.1 0.01		$\rho_o = \rho_w^{0.9}$	56.25				
1 0.1 0.01	62.5	$\rho_o = \rho_w^{0.8}$	50	20 days			
1 0.1 0.01		$\rho_o = \rho_w^{0.9}$	56.25				
1 0.1 0.01	62.5	$\rho_o = \rho_w^{0.8}$	50	5 days	50	0.5	1
1 0.1 0.01		$\rho_o = \rho_w^{0.9}$	56.25				
1 0.1 0.01	62.5	$\rho_o = \rho_w^{0.8}$	50	20 days			
1 0.1 0.01		$\rho_o = \rho_w^{0.9}$	56.25				
1 0.1 0.01	62.5	$\rho_o = \rho_w^{0.8}$	50	5 days	50	0.5	4
1 0.1 0.01		$\rho_o = \rho_w^{0.9}$	56.25				
1 0.1 0.01	62.5	$\rho_o = \rho_w^{0.8}$	50	20 days			
1 0.1 0.01		$\rho_o = \rho_w^{0.9}$	56.25				

To calibrate the model, a base case with no gravity effect and line to block saturation mapping was performed, the results are showed in figure 4.38.

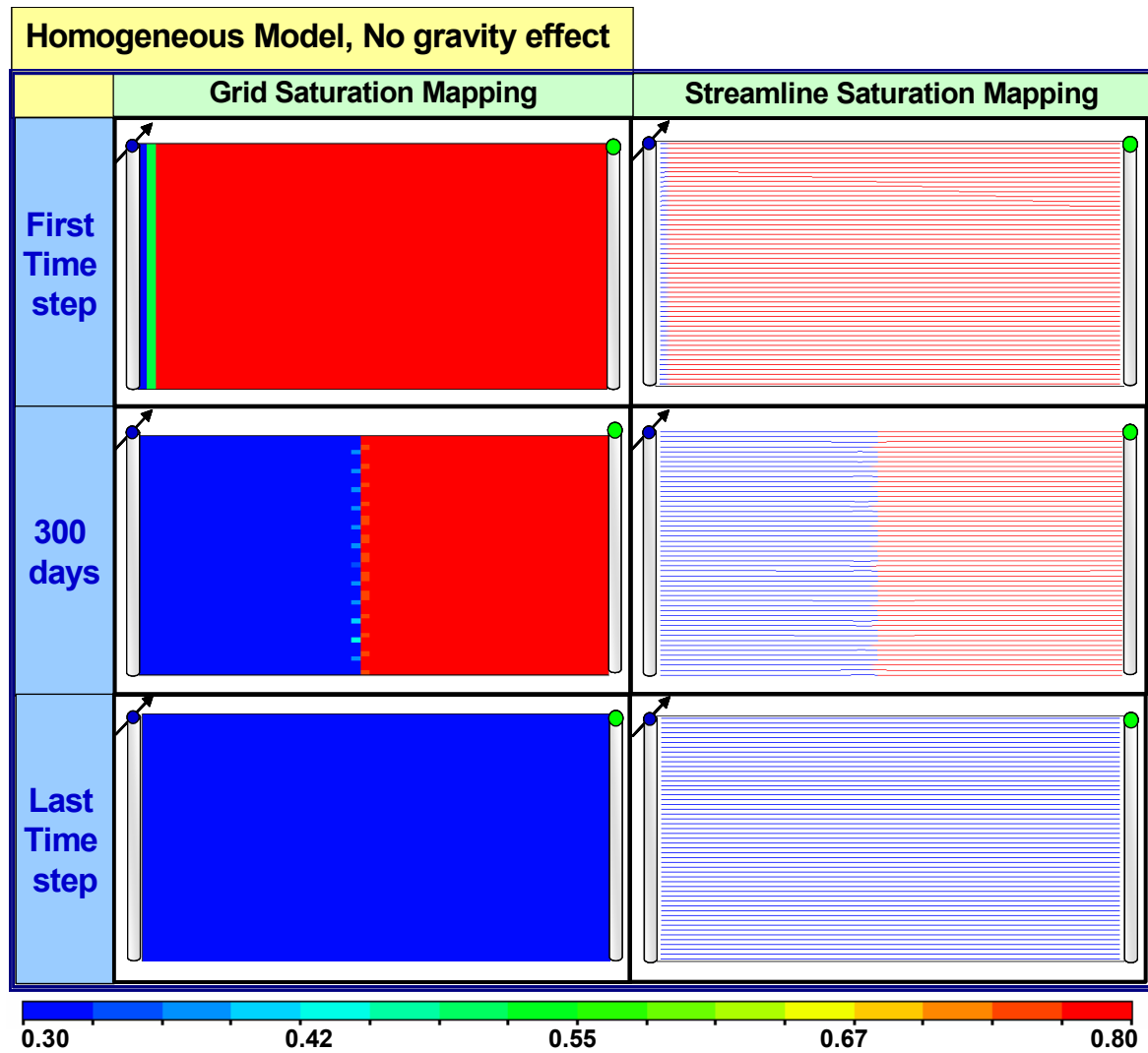


Fig. 4.38 Homogeneous line to block case without gravity effect and $M=0.5$.

The calibration of the model is correct because it does not show any segregation gravity effect in figure 4.38.

The gravity numbers are based in the K_v/K_h ratio and they are computed and presented in table 4.4.

Table 4.4 Gravity number (N_g) based in K_v/K_h for gravity effect analysis

$\rho_o = \rho_w * 0.8$		$\rho_o = \rho_w * 0.9$	
K_v/K_h	N_g	K_v/K_h	N_g
1	868	1	434
0.1	86.8	0.1	43.4
0.01	8.6	0.01	4.3

Results of Line to block saturation mapping, varying K_v/K_h , using $\rho_o = \rho_w * 0.8$ with $\Delta t = 20$ days are demonstrated in Fig. 4.39.

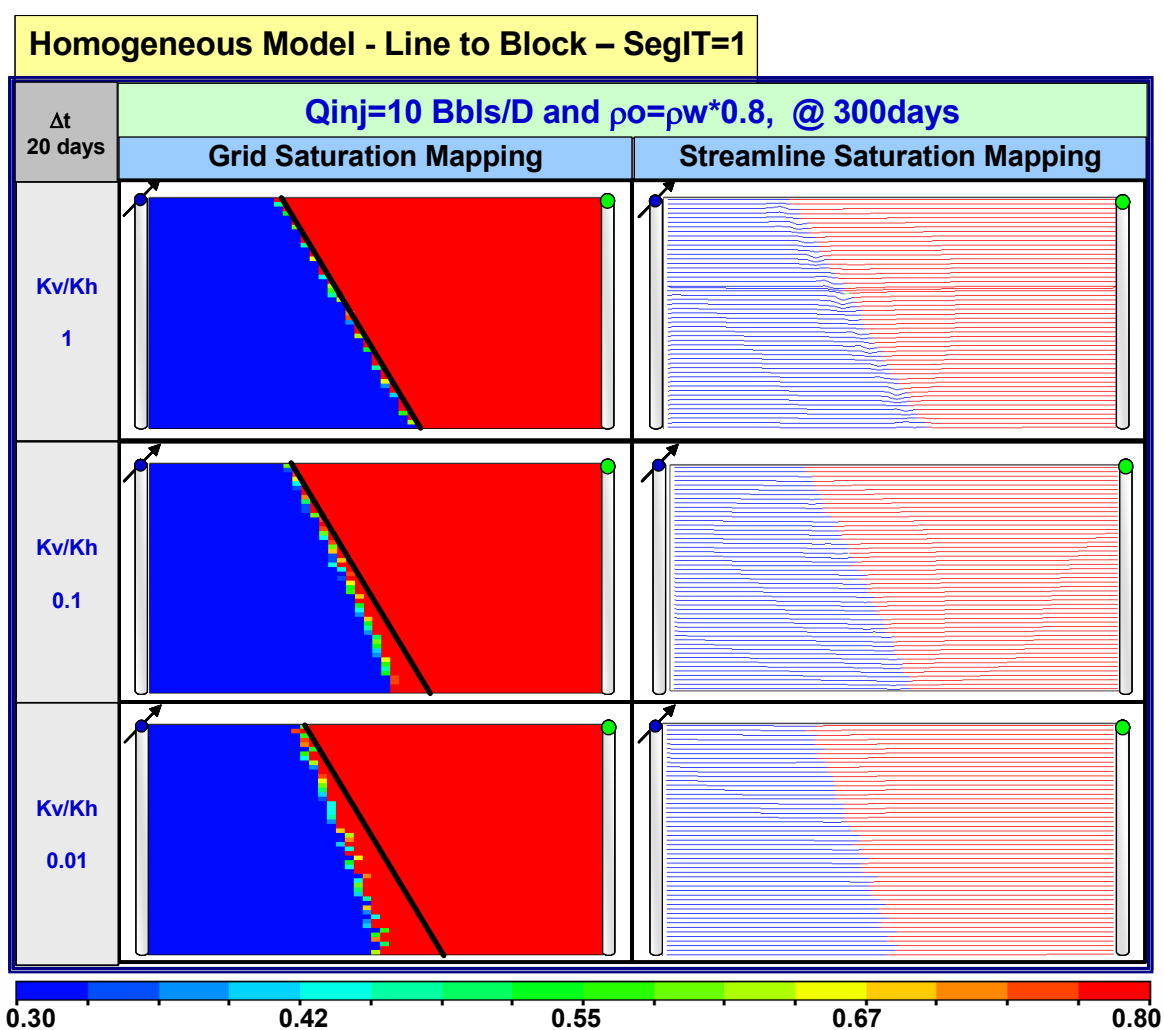


Fig. 4.39 Homogeneous line to block varying K_v/K_h using $\rho_o = \rho_w * 0.8$ at $\Delta t = 20$ days

Fig. 4.39 clearly demonstrates the variation effect produced by the gravity segregation altogether with the K_v/K_h variation at the same $\Delta \rho = 12.5$, same $\Delta t = 20$ days

and same simulation running time of 300 days. The black line traced intentionally correspond to the injection front displacement for the $K_v/K_h=1$, it can be seen that for $K_v/K_h = 0.1$ and 0.01 the front displacement are different, this is resulting of the gravity segregation effect where higher values of K_v/K_h induce major impact in the gravity of the streamline model.

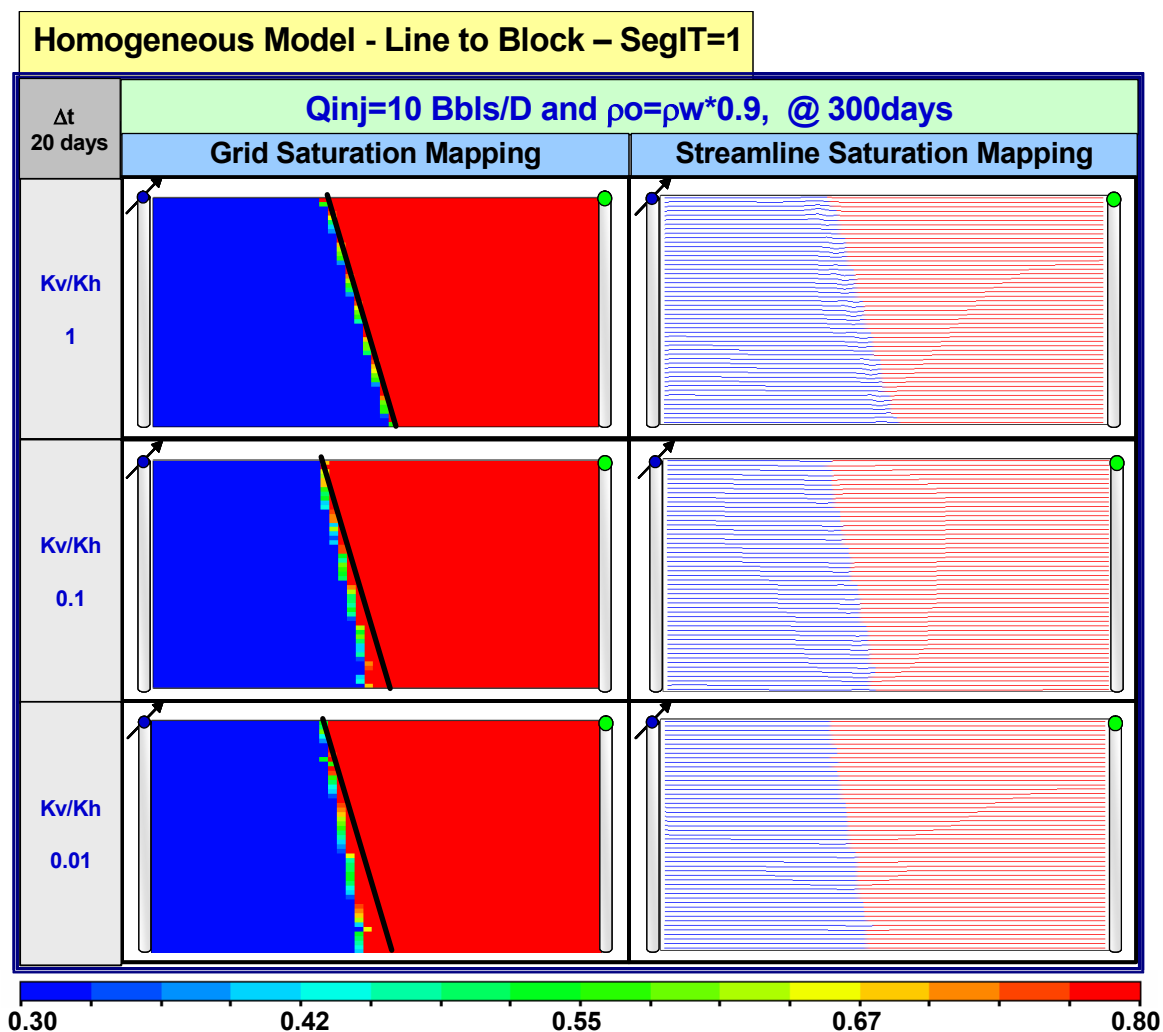


Fig. 4.40 Homogeneous line to block varying K_v/K_h using $\rho_o=\rho_w*0.9$ at $\Delta t=20$ days

In Fig. 4.40 also is demonstrated the variation effect produced by the gravity segregation based in K_v/K_h changes, defining a new $\Delta\rho=6.25$ constant, same $\Delta t = 20$ days, and same simulation running time of 300 days. The black line traced intentionally correspond to the injection front displacement for the $K_v/K_h=1$ again, it can be seen that

for $K_v/K_h = 0.1$ and 0.01 the front displacement are different again but in a lower grade than the previous $\Delta\rho=12.5$ cases, then $\Delta\rho$ and K_v/K_h can cause different behavior in the solution obtained from the gravity segregation option in SL models. Higher $\Delta\rho$ values introduce major impact in the results based on this gravity conditions.

Figures 4.41 and 4.42 manifest the results concerning to the same previous presented in Fig. 4.39 and Fig. 4.40, but using a different time step size of $\Delta t = 5$ days.

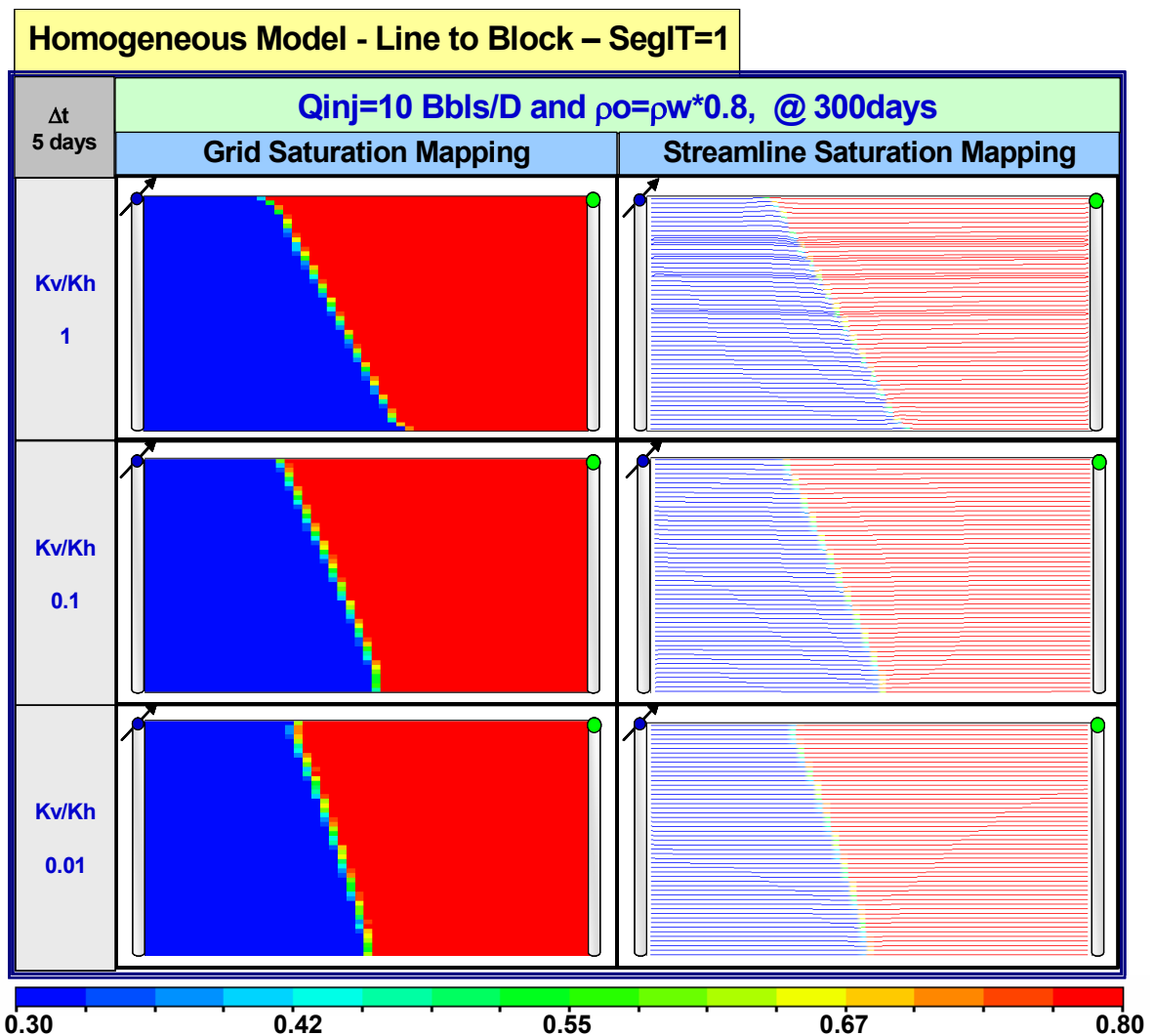


Fig. 4.41 Homogeneous line to block varying K_v/K_h and using $\rho_o=\rho_w*0.8$ at $\Delta t=5$ days

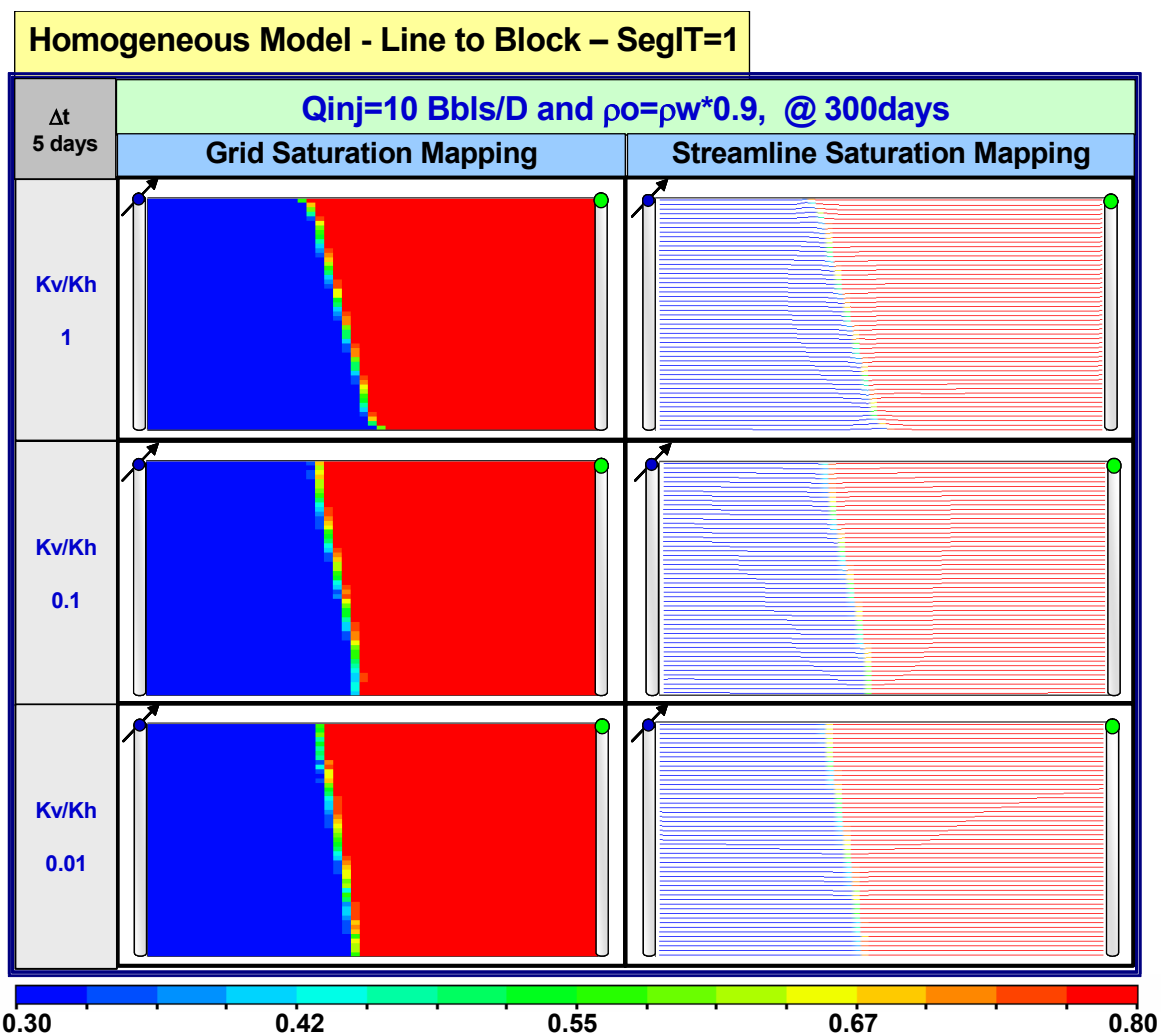


Fig. 4.42 Homogeneous line to block varying Kv/Kh and using $\rho_o = \rho_w * 0.9$ at $\Delta t = 5$ days

The results in last figures 4.41 and 4.42 show the same performance concerning to the gravity segregation effect but with better resolution in the saturation mapping due to the small time step size.

Figure 4.43 to 4.45 exhibit the comparison between the previously presented case but grouping by Kv/Kh ratios. These pictures permit to validate the mentioned facts about the $\Delta\rho$, Kv/Kh, and Δt impact when gravity segregation is considered in SL models.

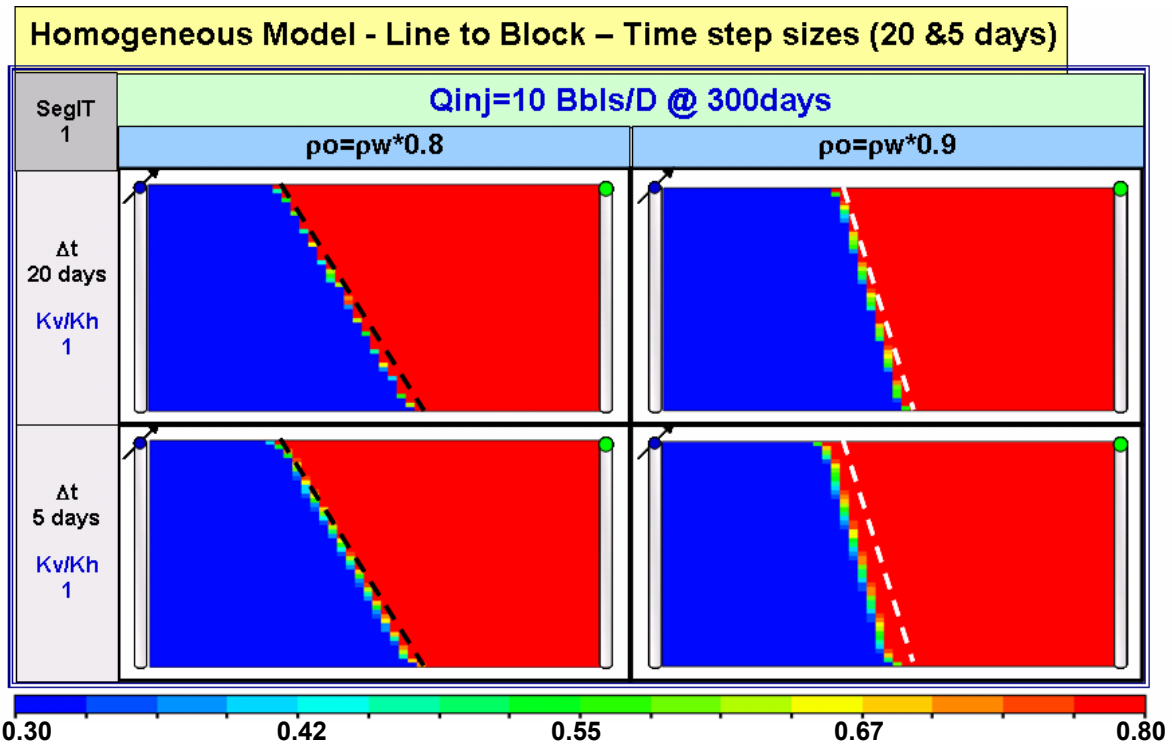


Fig. 4.43 Homogeneous line to block for $K_v/K_h=1$ using different ρ_o and varying Δt

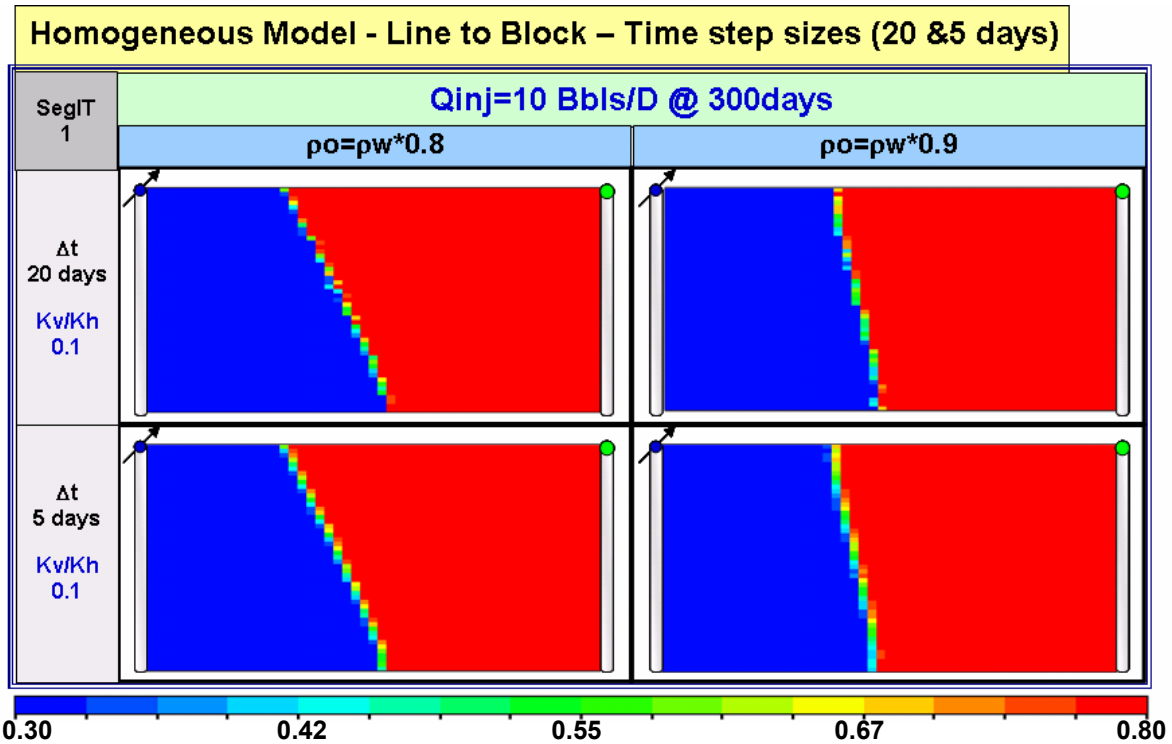


Fig. 4.44 Homogeneous line to block for $K_v/K_h=0.1$ using different ρ_o and varying Δt

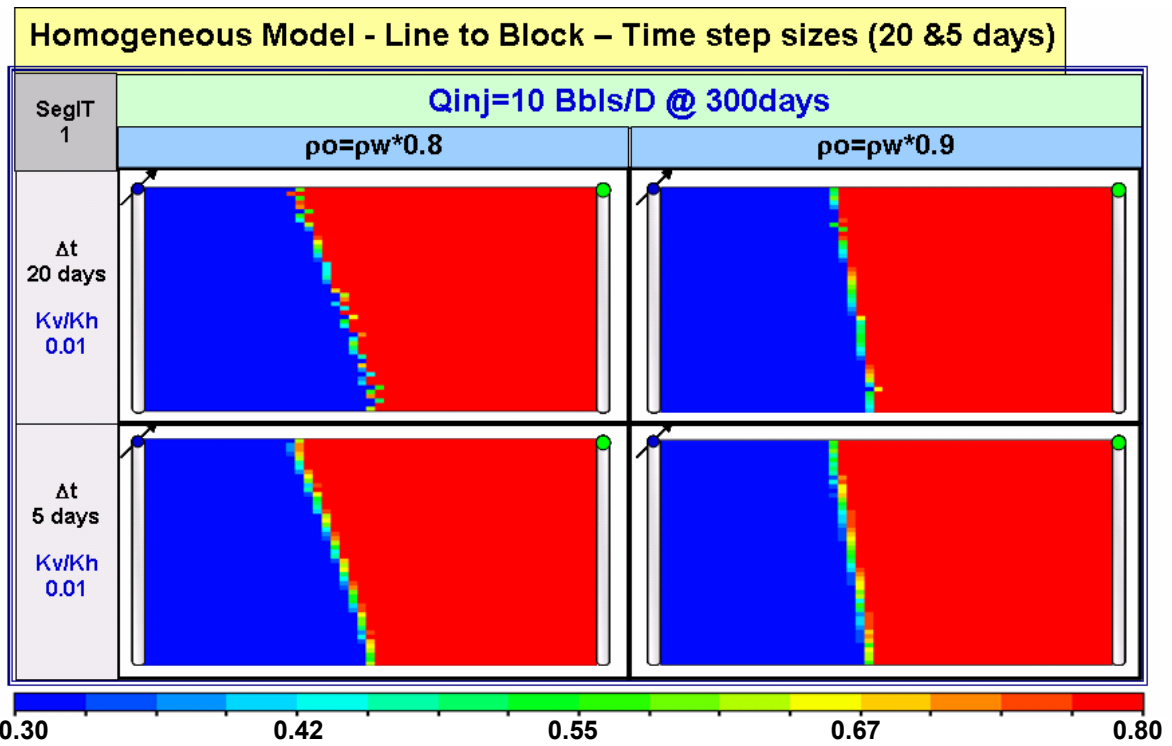


Fig. 4.45 Homogeneous line to block for $K_v/K_h=0.01$ using different ρ_o and varying Δt

The next results are obtained from some cases used to determine the influence of the SegIT in the SL solution.

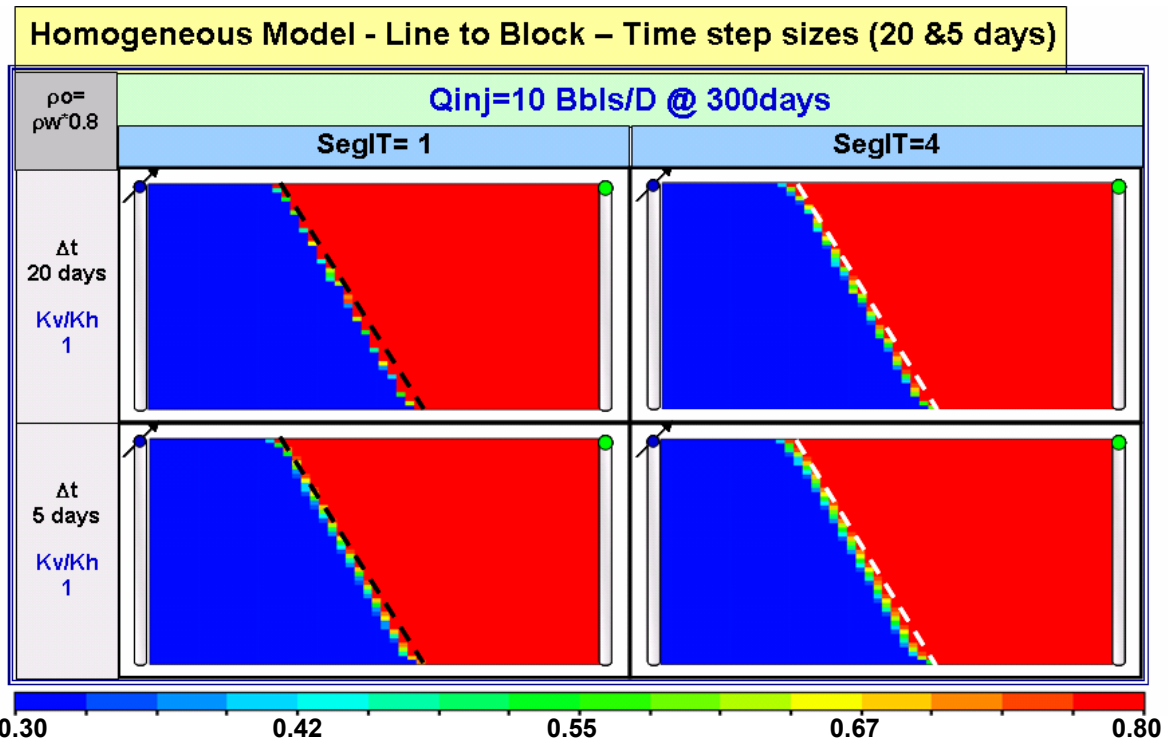


Fig. 4.46 Homogeneous line to block for $K_v/K_h=1$ using different SegIT and varying Δt

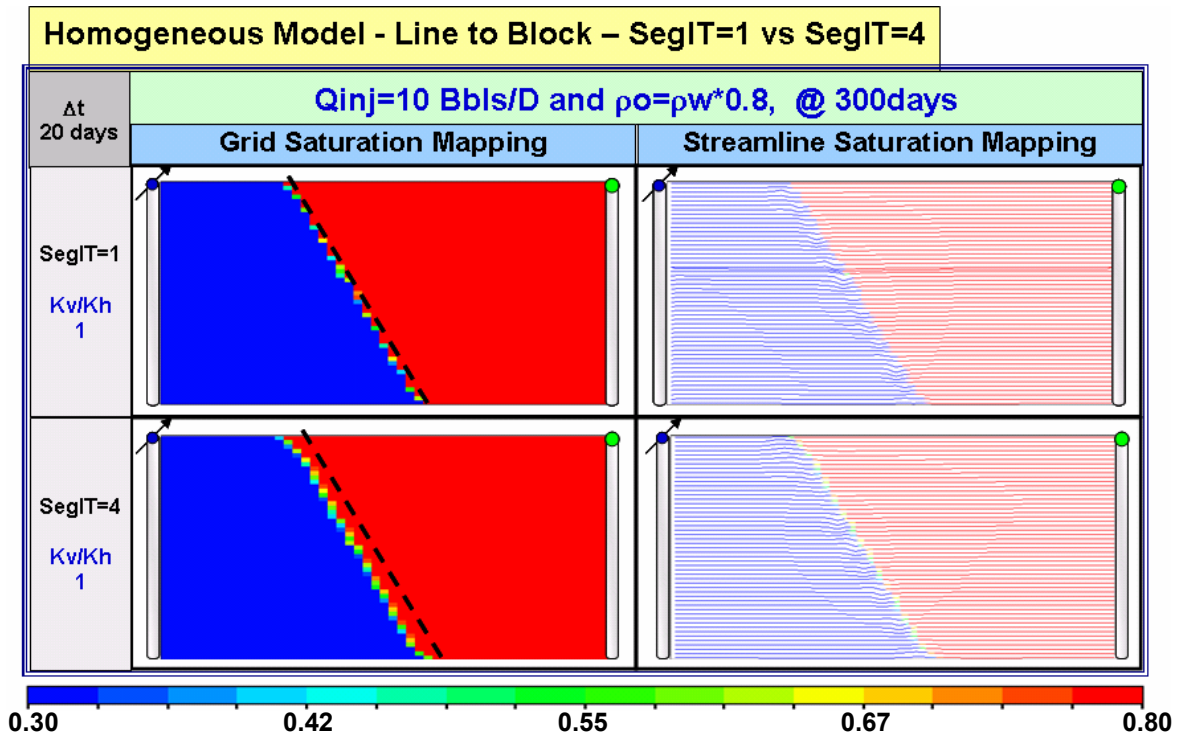


Fig. 4.47 Homogeneous line to block for $K_v/K_h=1$ using different SegIT at $\Delta t=20$ days

Figure 4.46 indicates that SegIT effect is not impacting at different time step sizes but Fig. 4.47 show some later displacement in the front with higher frequency of segregation iterations (SegIT=4). Moreover, the same behavior is presented using K_v/K_h 0.1 and 0.01.

Figures 4.48 and 4.49 summarize the comparison between the Line to Block SL mapping cases with different SegIT's, $\Delta\rho$'s, and K_v/K_h ratios for the same $\Delta t=20$ days.

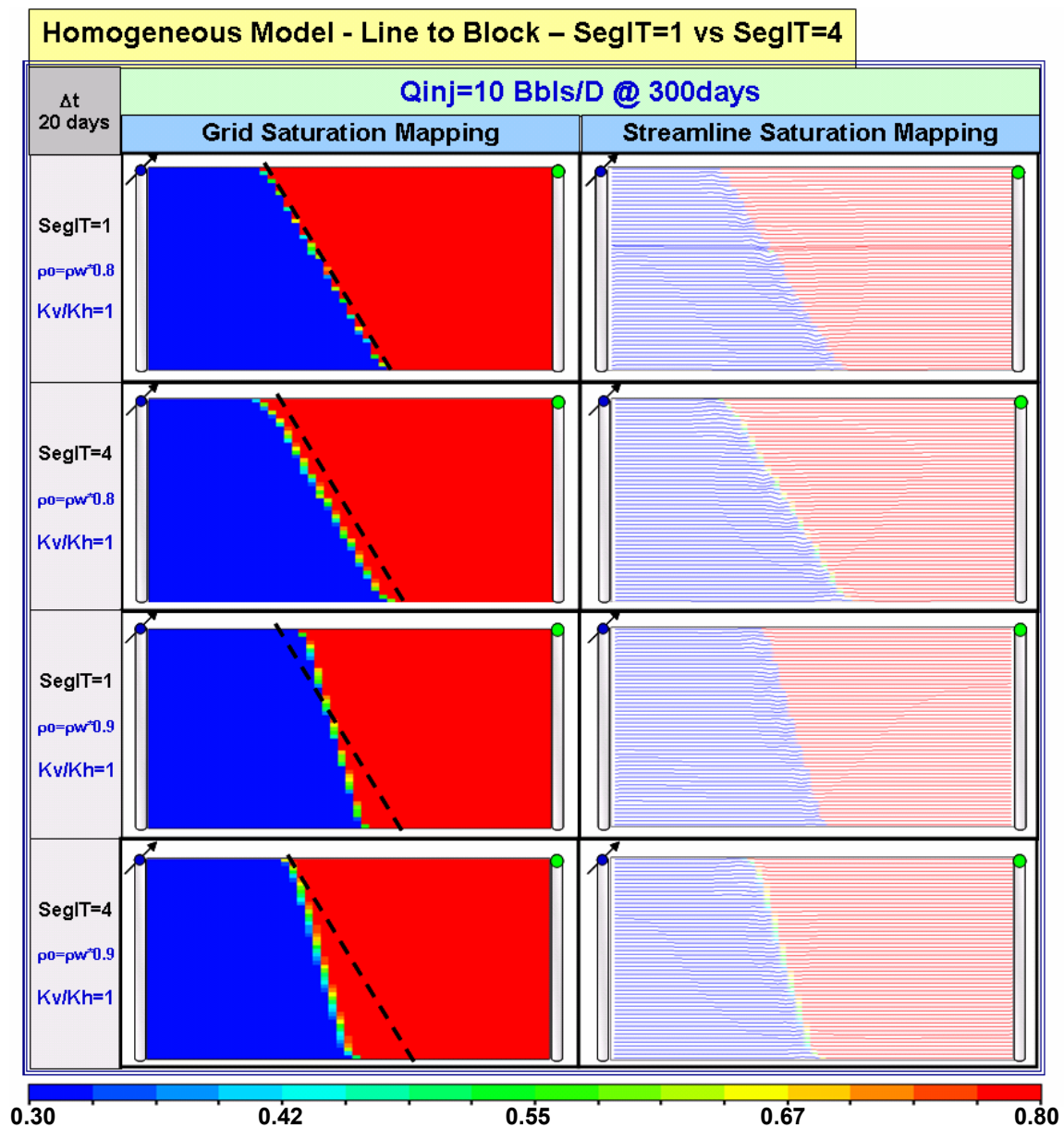


Fig. 4.48 Homogeneous line to block for $K_v/K_h=1$ varying SegIT and ρ_0 at $\Delta t=20$ days

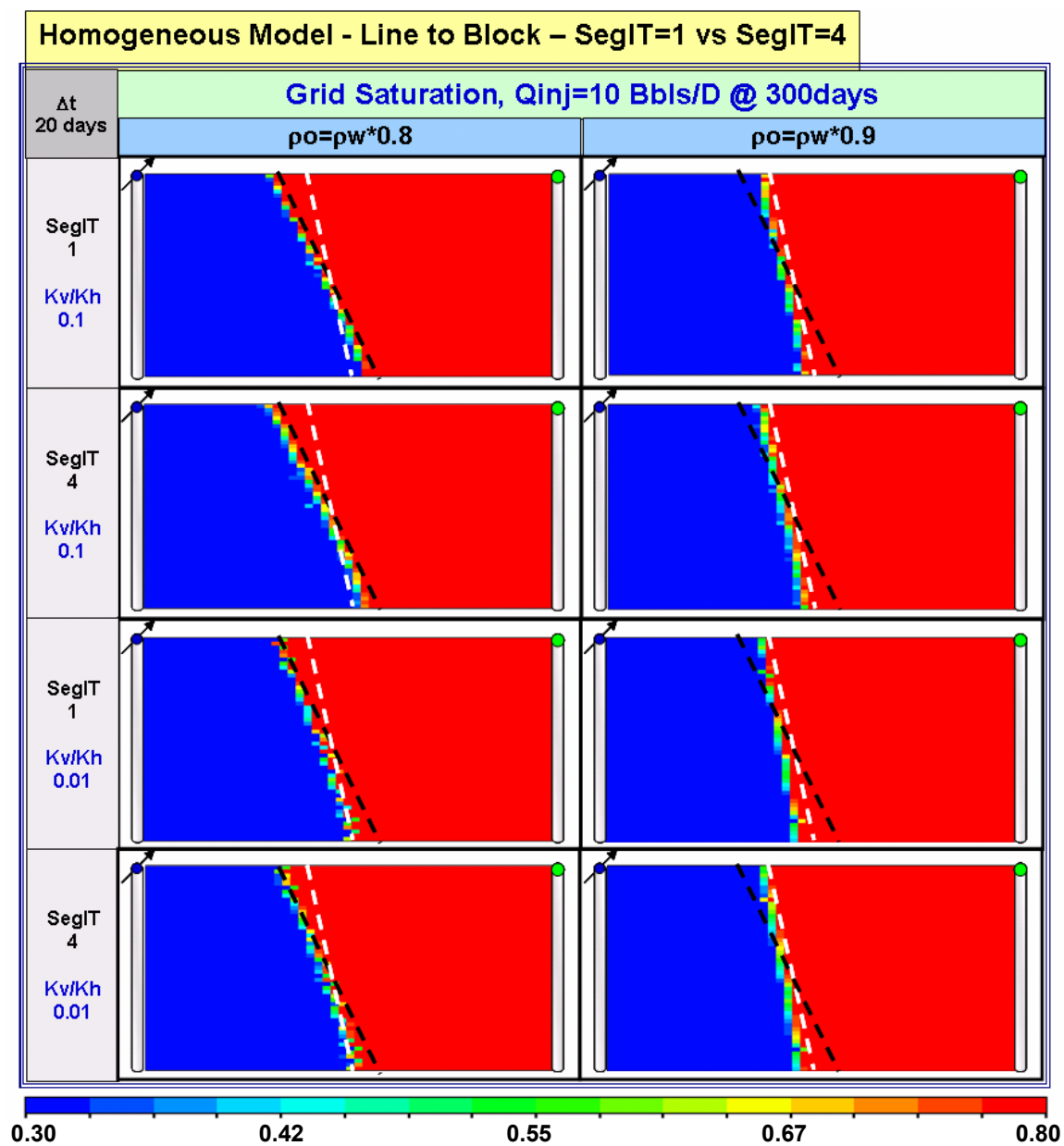


Fig. 4.49 Homogeneous line to block general comparison for $\Delta t=20$ days

Using Line to block to mapping saturation solutions to the streamlines can be suitable to model the gravity effect. The commercial SL simulator (FRONTSIM) does not recommend the use of Line to line method with the gravity segregation option activated. Though, been aware of this warning, it is used this numerical mapping option to continue with the research plan.

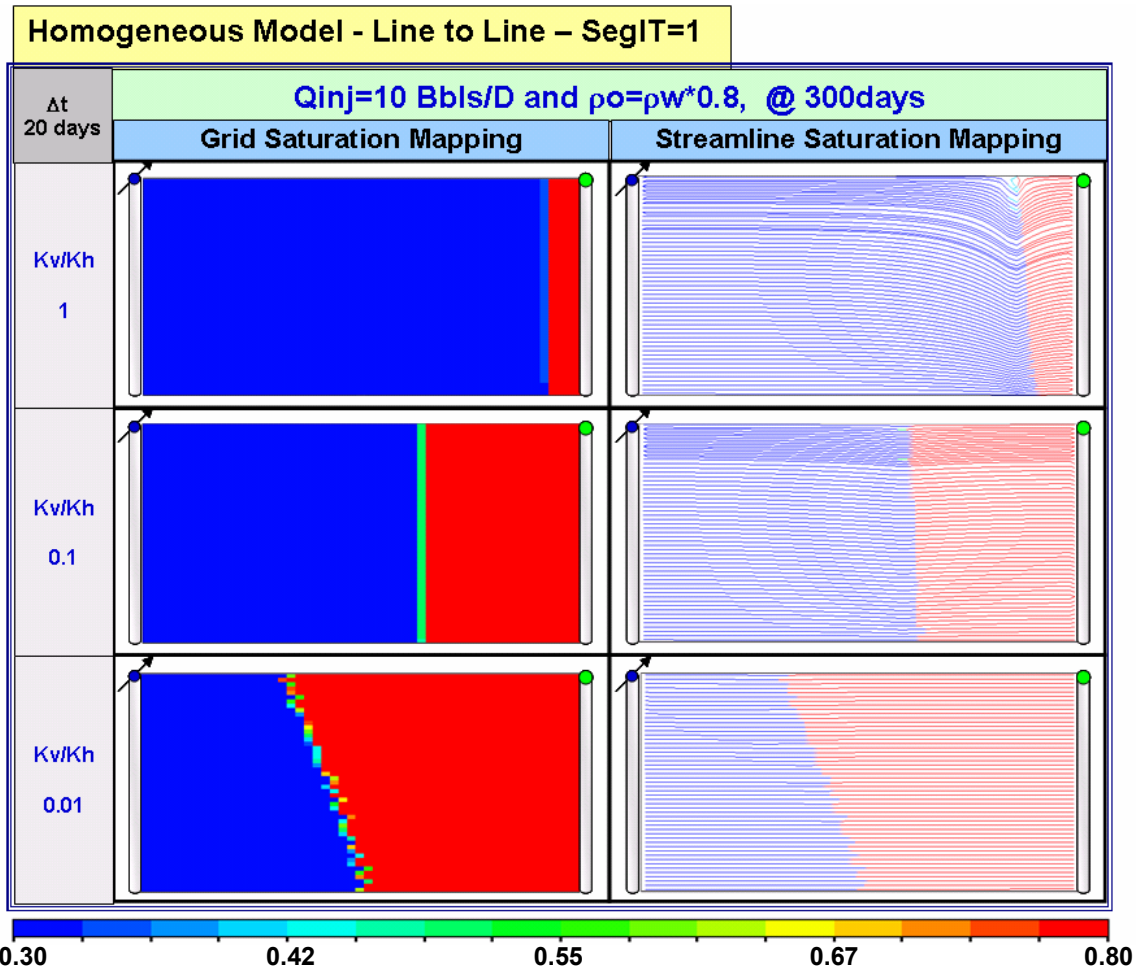


Fig. 4.50 Homogeneous line to line varying K_v/K_h and using $\rho_o=\rho_w*0.8$ at $\Delta t=20$ days

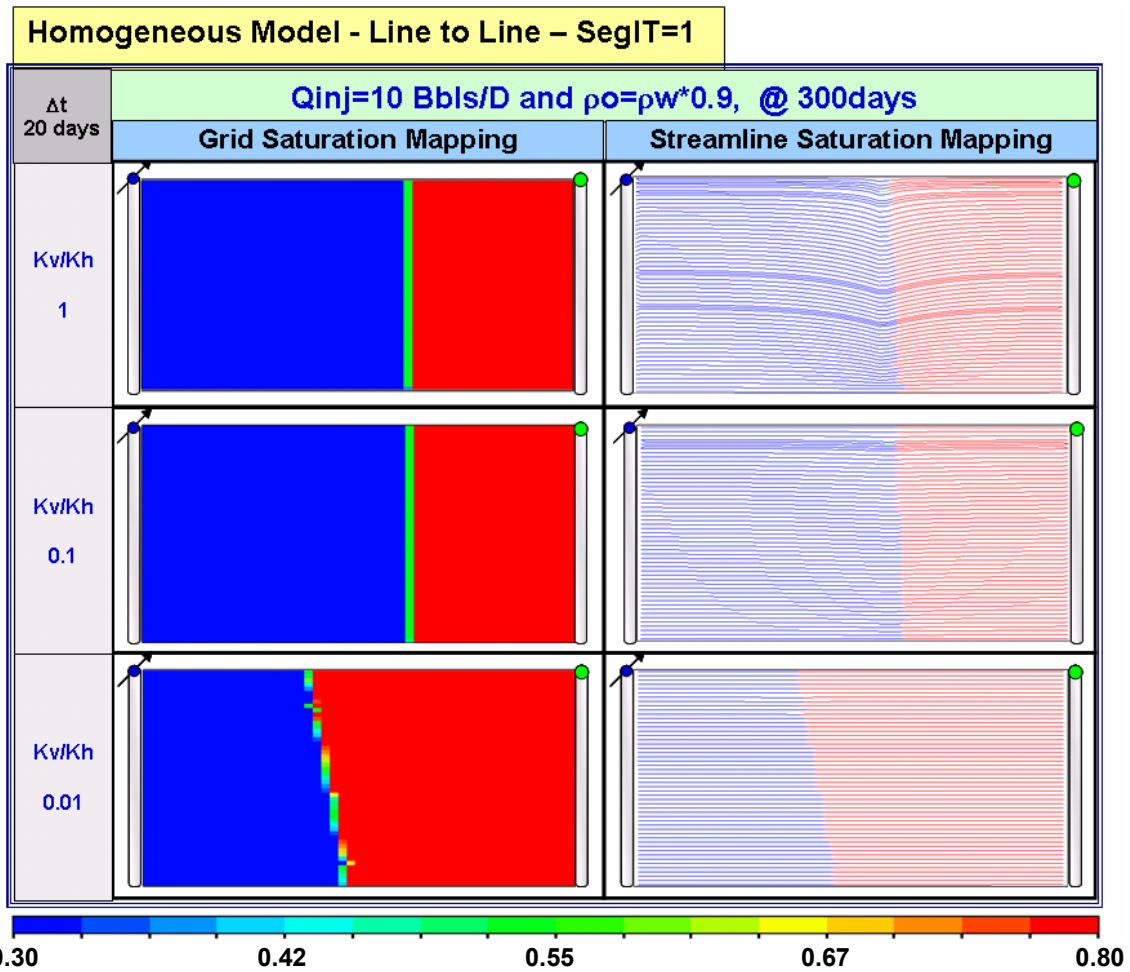


Fig. 4.51 Homogeneous line to line varying K_v/K_h and using $\rho_o = \rho_w * 0.9$ at $\Delta t = 20$ days

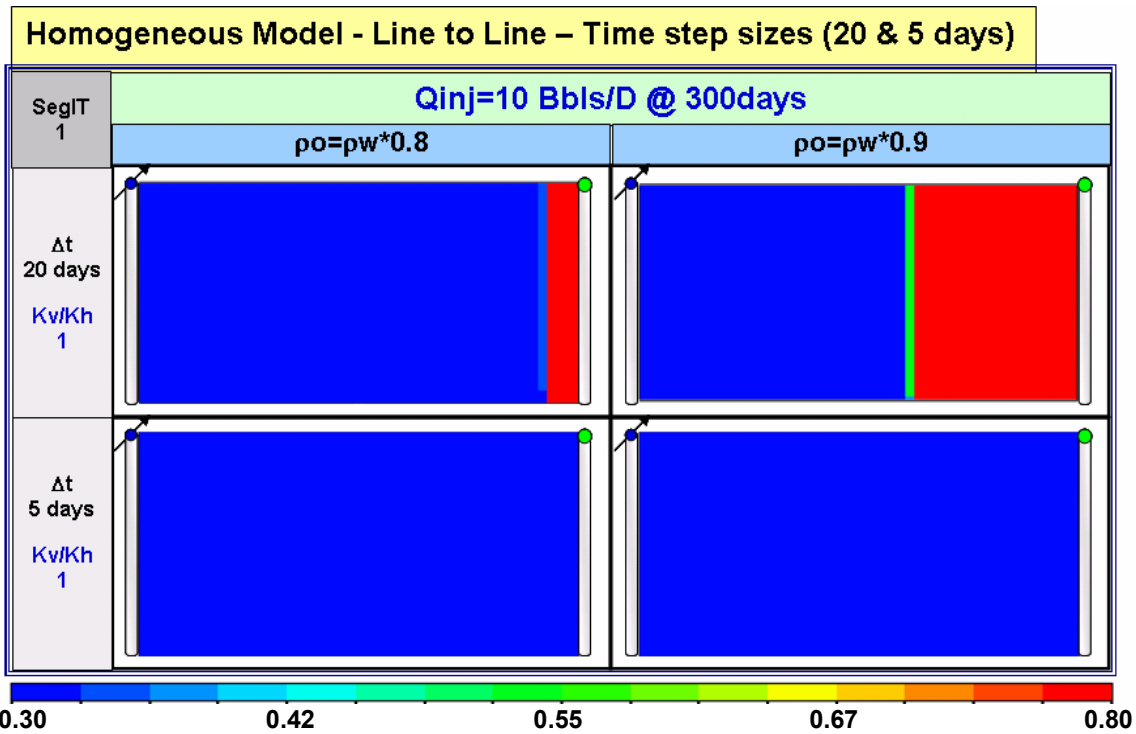


Fig. 4.52 Homogeneous line to line for $K_v/K_h=1$ and varying ρ_o and Δt

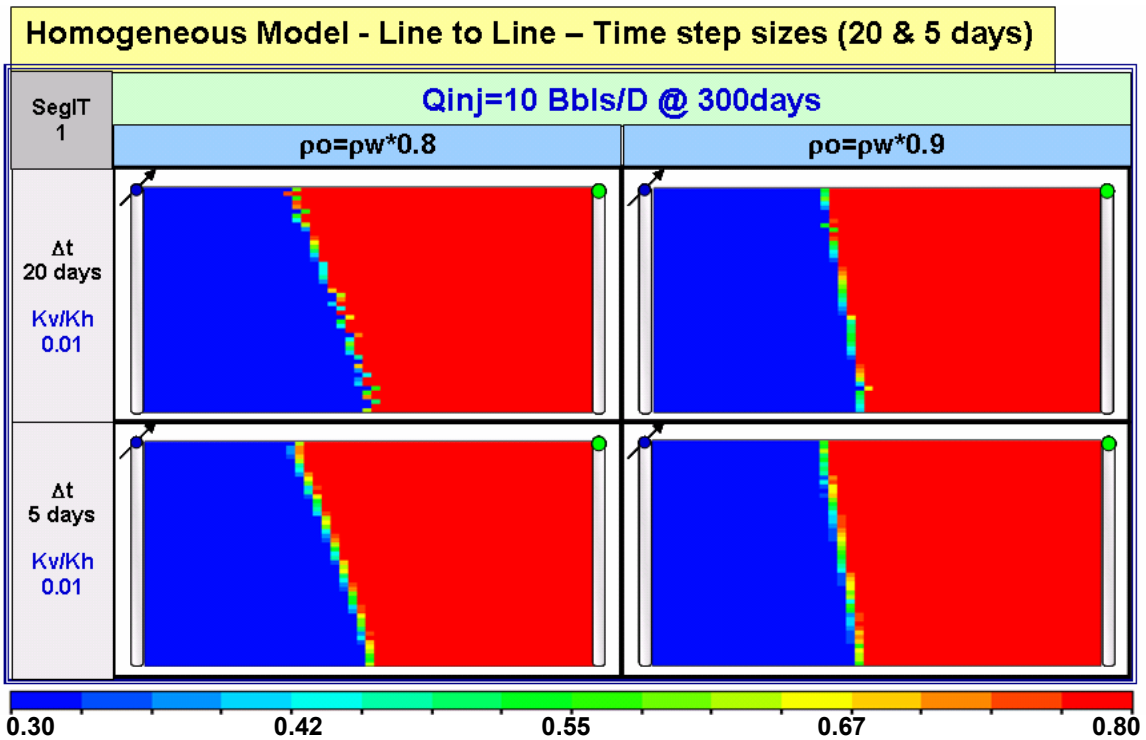


Fig. 4.53 Homogeneous line to line for $K_v/K_h=0.01$ and varying ρ_o and Δt

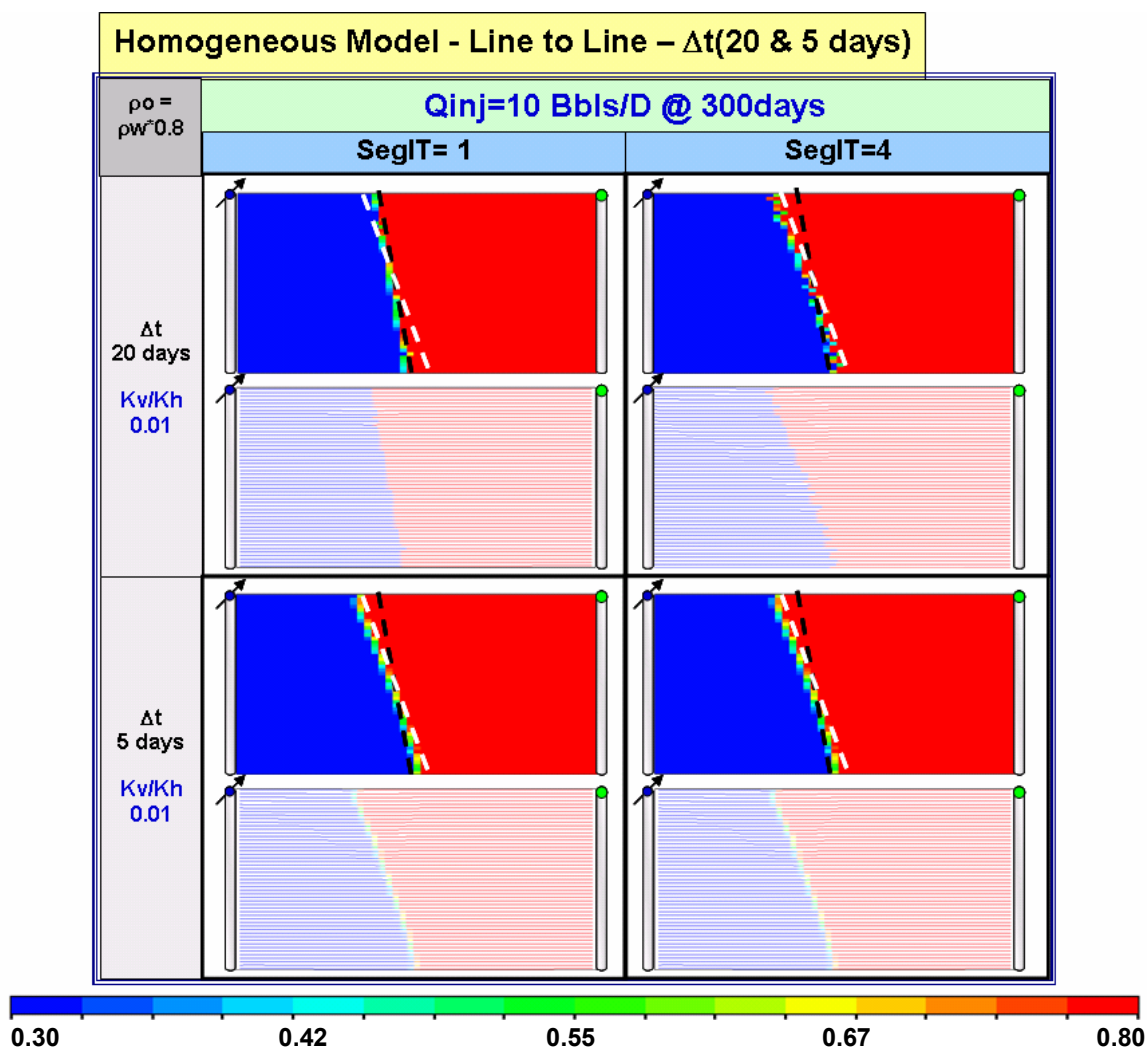


Fig. 4.54 Homogeneous line to line for $K_v/K_h=0.01$ at different Δt

The latest results presented in figures 4.50 to 4.54 did not introduce major visual effects for $K_v/K_h= 1$ or $K_v/K_h=0.1$ due the high MBE errors generated to get the solution. Thus, using low gravity number like in $K_v/K_h =0.01$ case can let the use of the Line to Line method. The results are pretty similar with ones obtained from the Line to Block experiments. See Fig 4.55.

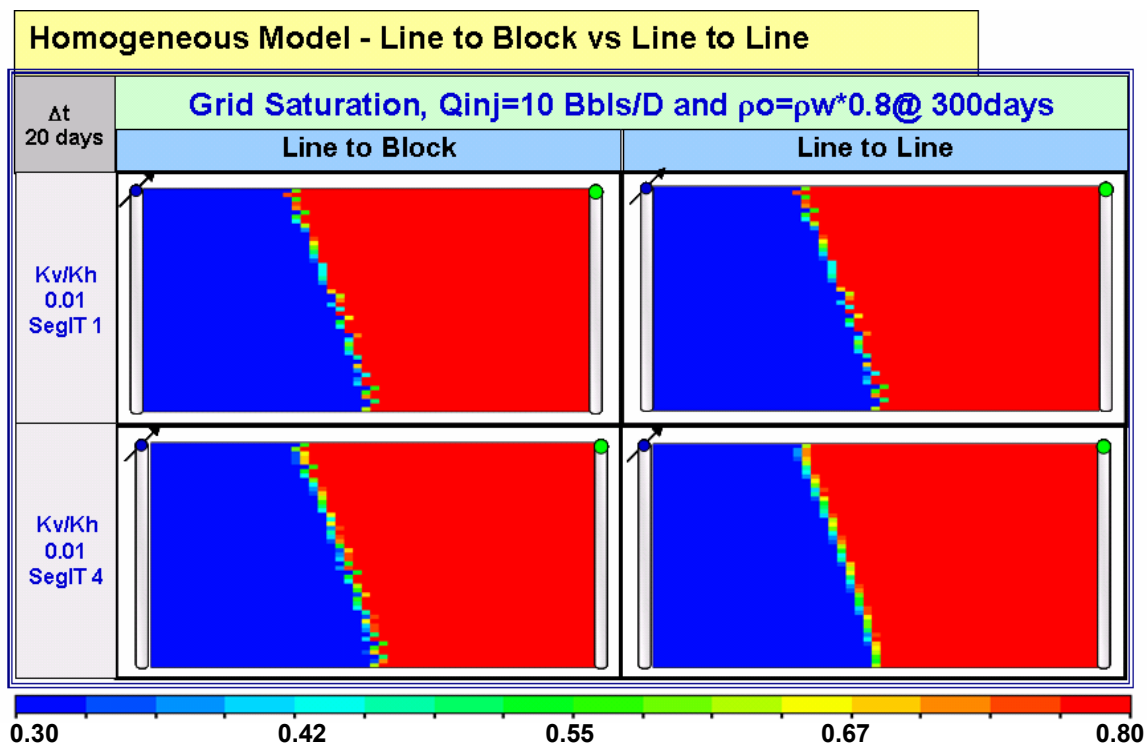


Fig. 4.55 Homogeneous saturation mapping comparison varying SegIT

The same behavior was noted for $\rho_o=\rho_w*0.9$. Also, varying the SegIT is not affecting the solution answer but the resolution. We can see here that increasing the number of sub iteration (SegIT) in Line to Line method makes smoother solution as in Line to Block.

The next bunch of numerical experiments are based in the injection of more fluid but at the same simulation time where the same pore volume injected (PVI) is reached. In this part the water injection rate is increased to 50 bbls/d from the original of 10 Bbls/d, also the simulation time for the new cases are at 60 days instead the previous 300 days, likewise the PVI are the same from the first part of this section to study the gravity segregation effect. See figures 4.56 to 4.61.

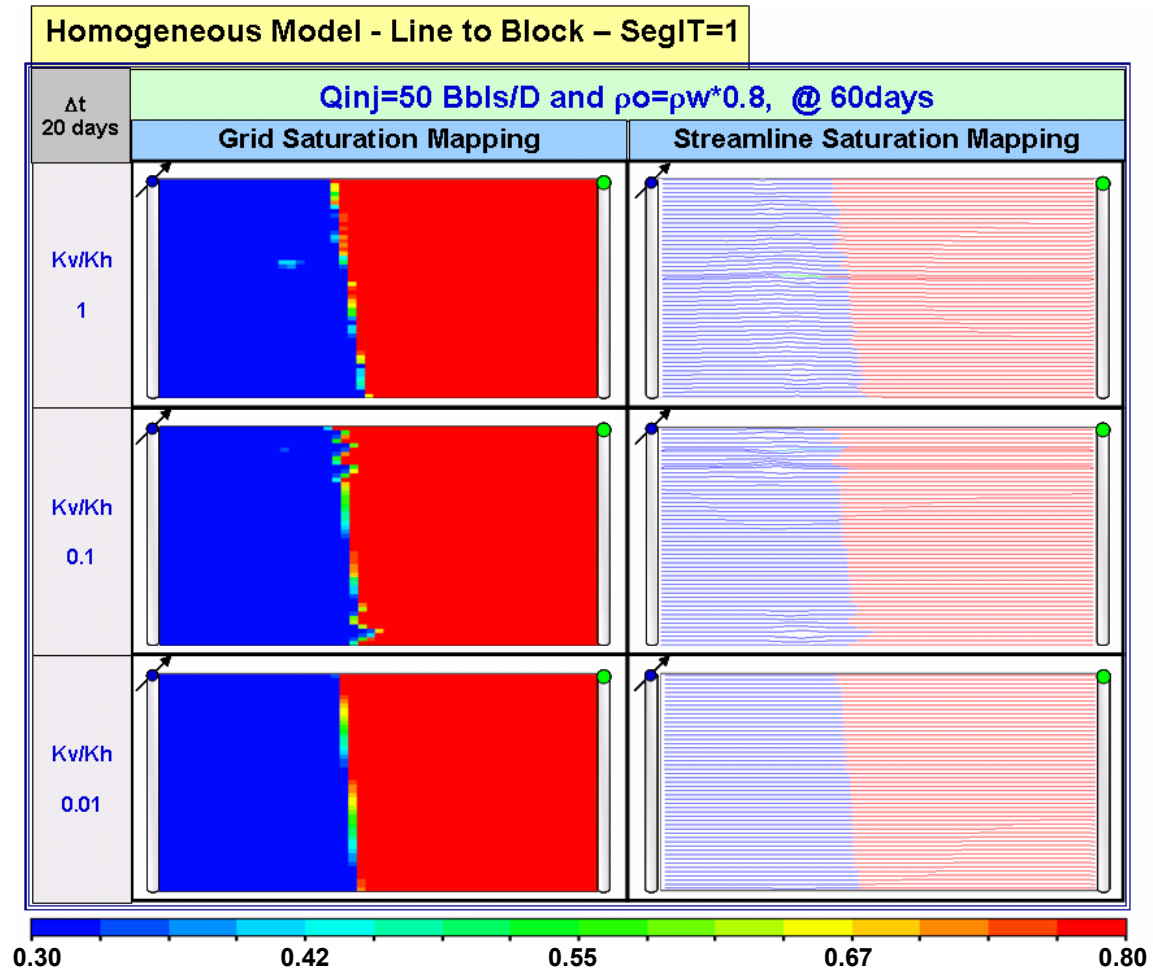


Fig. 4.56 Homogeneous with $Q_{inj}=50$ Bbls/D varying Kv/Kh.

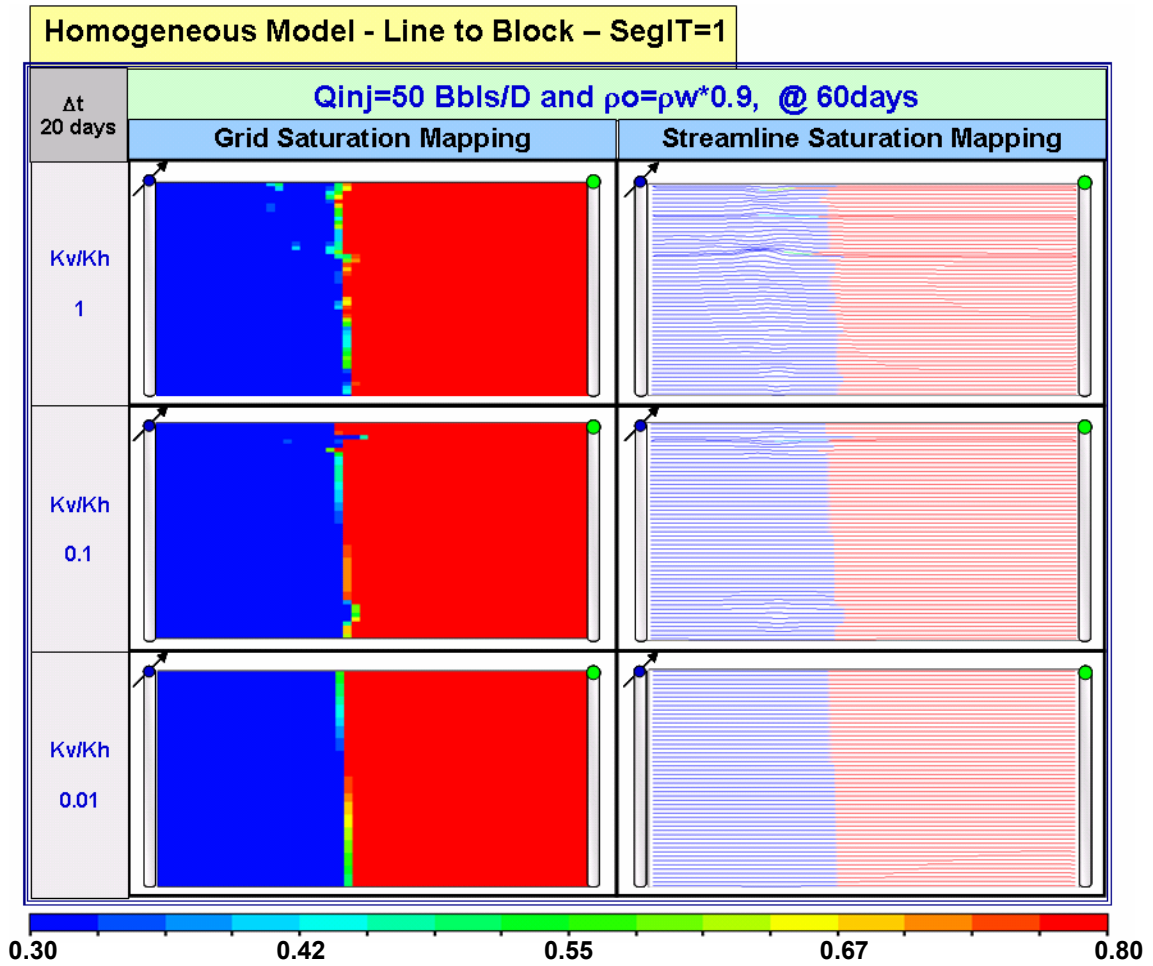


Fig. 4.57 Homogeneous with $Q_{inj} = 50$ Bbls/D varying K_v/K_h and $\rho_o = \rho_w * 0.9$

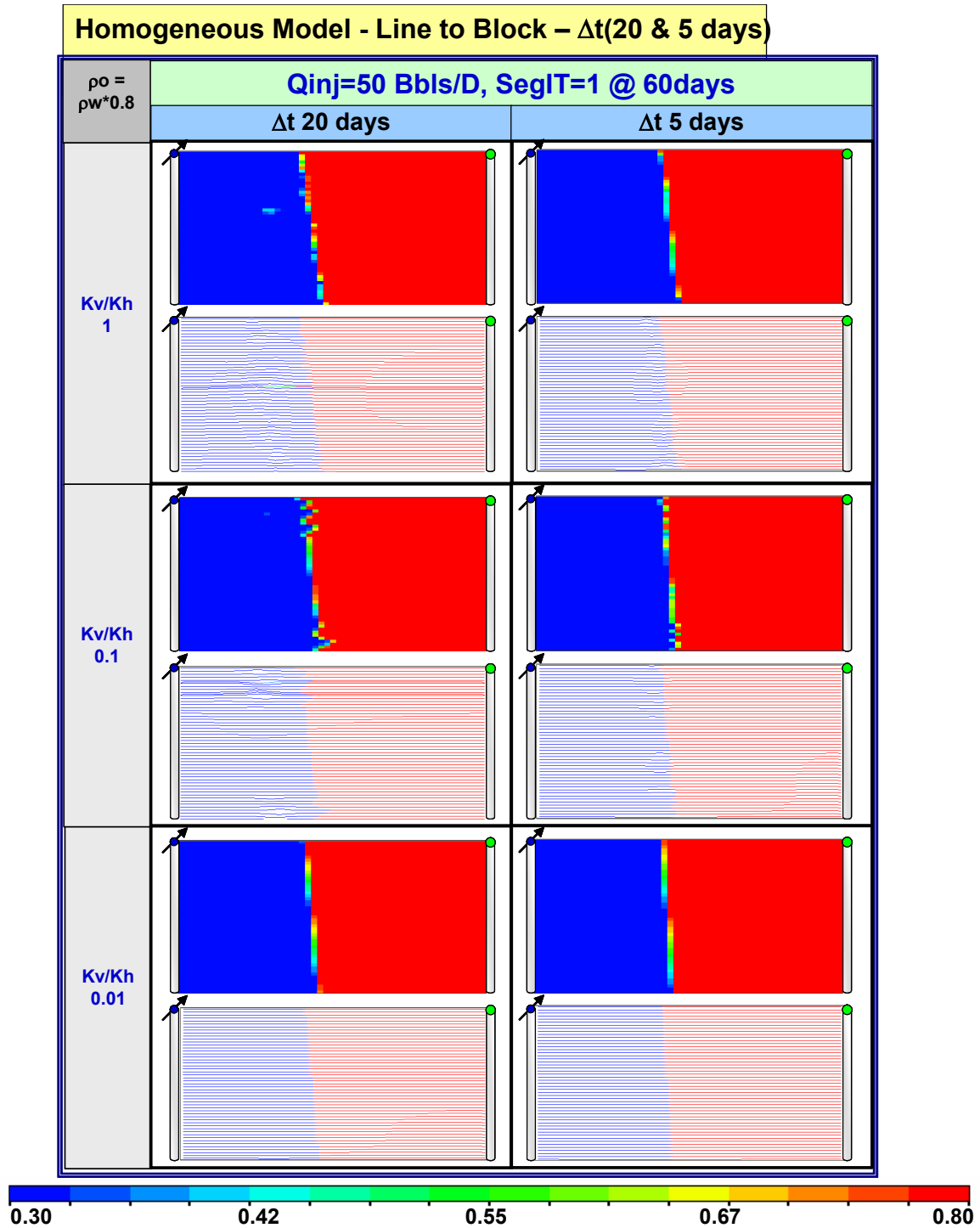
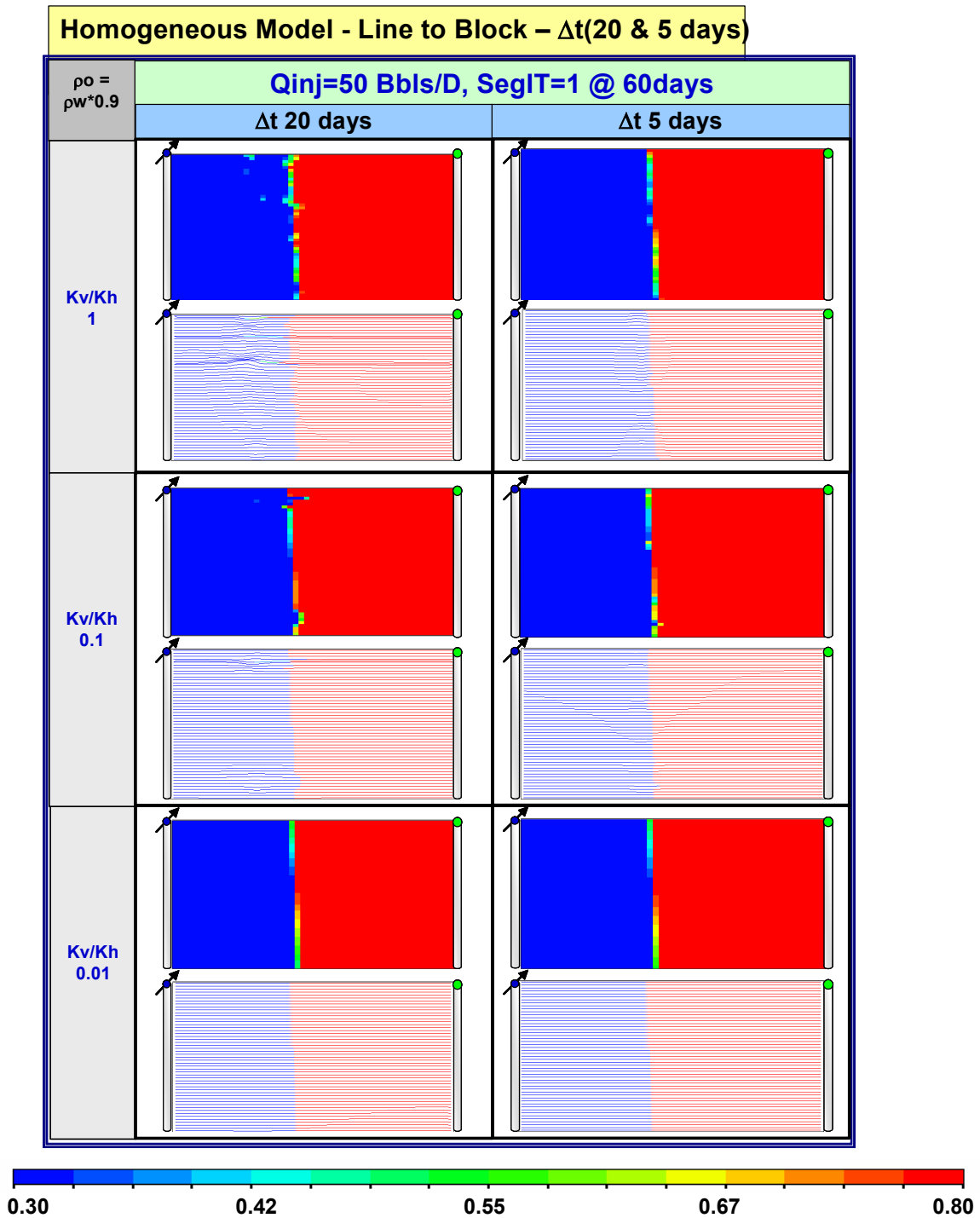


Fig. 4.58 Homogeneous with $Q_{inj}=50 \text{ Bbls/D}$ varying time step size

The significant issue that can be seen here is that time step size affects the smearing of the solution, making it more smooth in smaller $\Delta t=5 \text{ days}$ than in the bigger one $\Delta t=20 \text{ days}$. But the gravity effect is not appreciated because the high injection rate.



*Fig. 4.59 Homogeneous with $Q_{inj}=50 \text{ Bbls/D}$ varying time step size at $\rho_o = \rho_w^{*0.9}$*

In the last case presented in Fig. 4.59, the ρ_o was changed to a higher value and the response is similar to the previous sensitivities. Figure 4.60 shows the response of the model when the SegIT is varied.

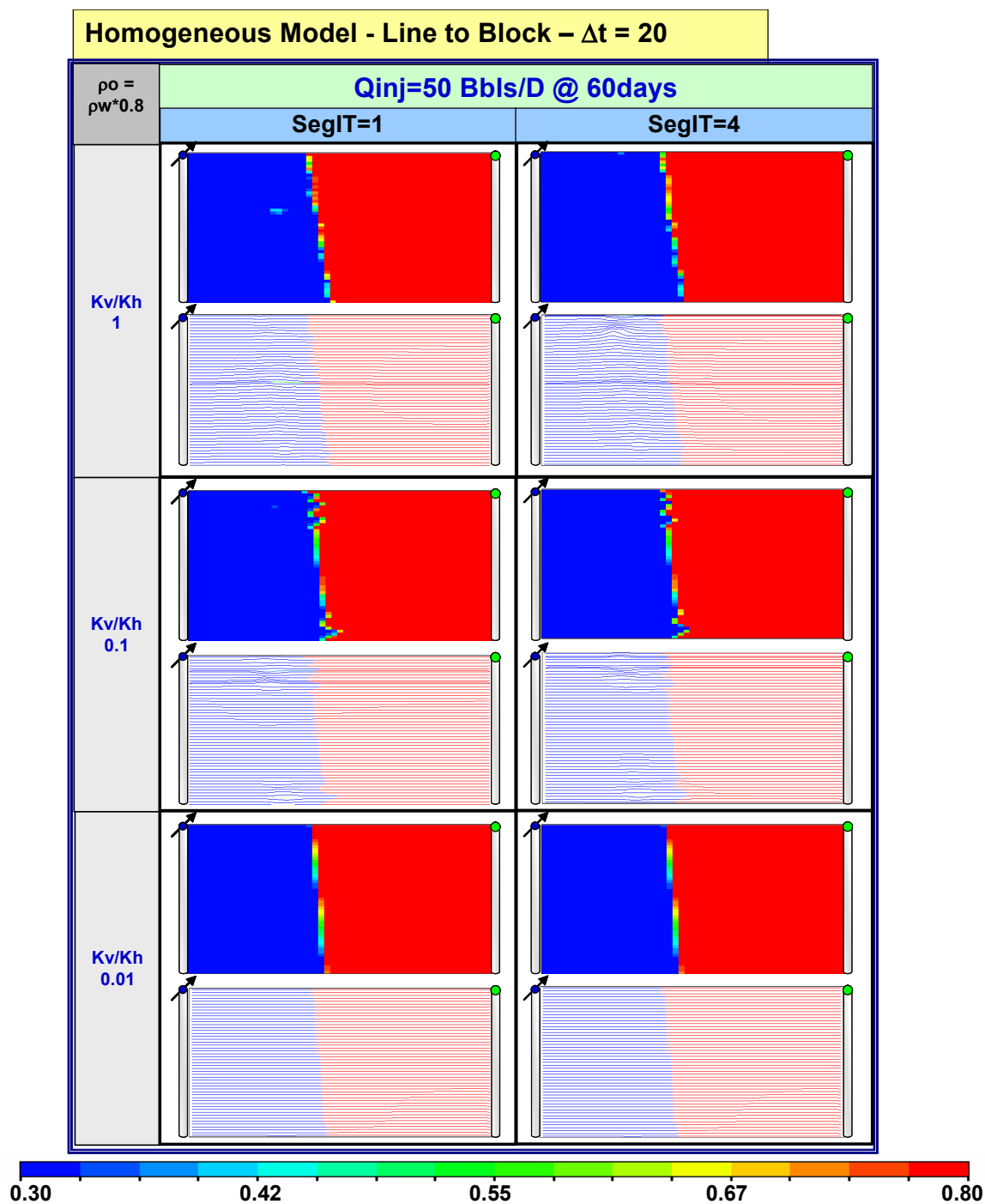


Fig. 4.60 Homogeneous with $Q_{inj} = 50$ Bbls/D varying SegIT value

Fig. 4.60 shows a line to block case for Homogeneous model but performed for SegIT values of 1 and 4, it is demonstrated that the SegIT is not affecting very much the results. Similar sensitivities were also performed for a different (higher) ρ_o value and the results were the same. Thus, number of iterations on the segregation option doesn't have

an important effect in the streamline model solution for high injection rate or different ρ_o or time step size when using a high injection rate. Additionally, the following cases will show the results for a Line to Line saturation mapping varying K_v/K_h in Homogeneous Model at different Δt and using a high injection rate (50 Bbls/D).

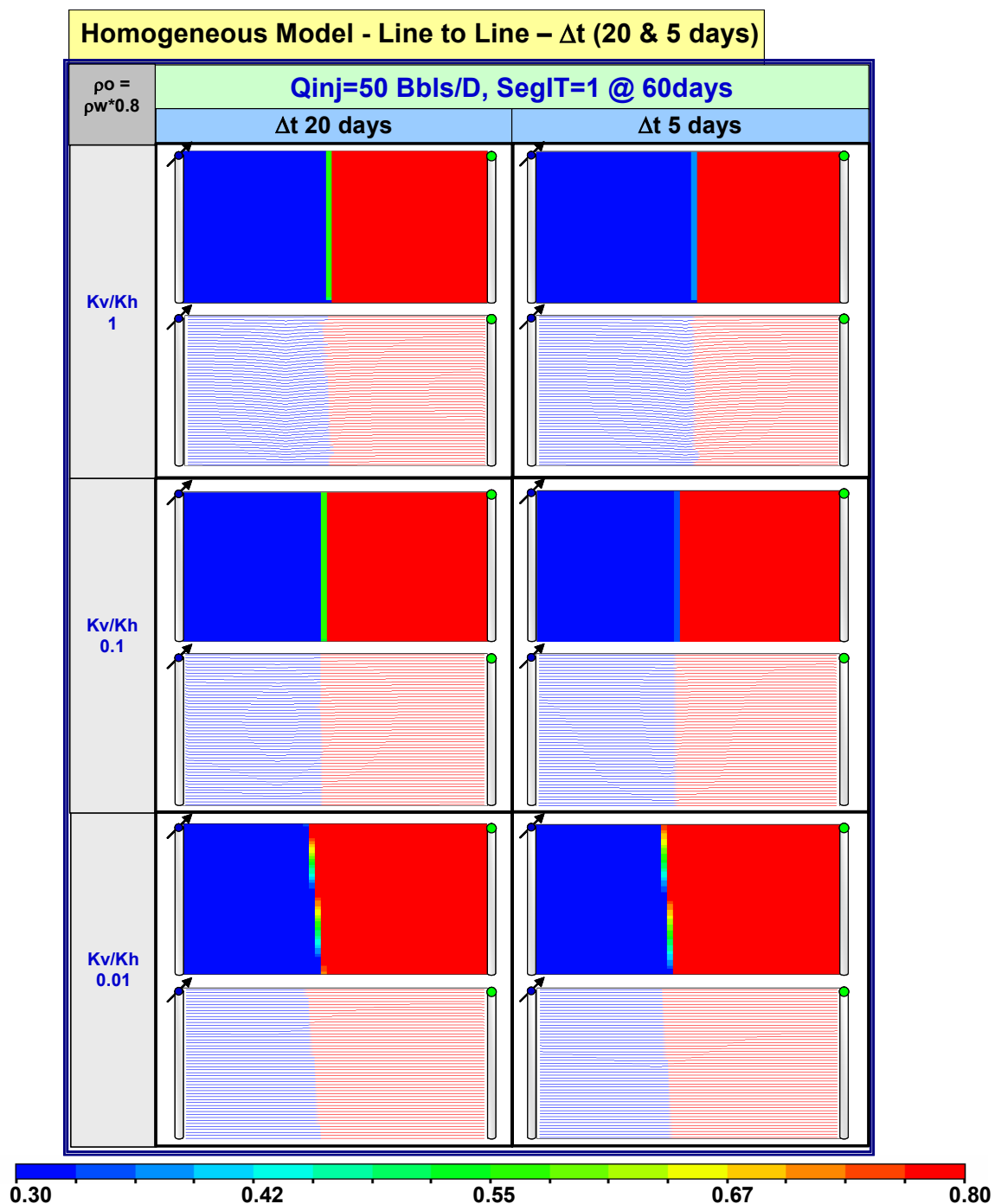


Fig. 4.61 Homogeneous line to line with $Q_{inj}=50$ Bbls/D using different Δt .

Fig 4.61 shows the results obtained from the sensitivity analysis in a Line to line saturation mapping method for the streamline model using time step sizes of 20 and 5 days, the results have the same behavior for both Δt 's but using K_v/K_h values of 1 and 0.1 shows the similar results in both cases but using a smaller $K_v/K_h=0.1$ it shows different and more reliable results, it means that high values of K_v/K_h do not impact in the streamline solution when is used a Line to line approach.

The following pictures display some comparisons of the results obtained for the developed cases for $Q_{inj}=10$ Bbls/d and $Q_{inj}=50$ Bbls/d, using Line to Block method to mapping the saturation solution for the SL model. These cases are compared at the time when the same injected pore volume (PVI) is obtained.

The reason of the mentioned comparisons is based on the fact that if we are using different injection rate in a reservoir model, we must also consider the same amount of injected fluid to simulate the same condition, then is calculated the PVI for each cases and compared at the same point.

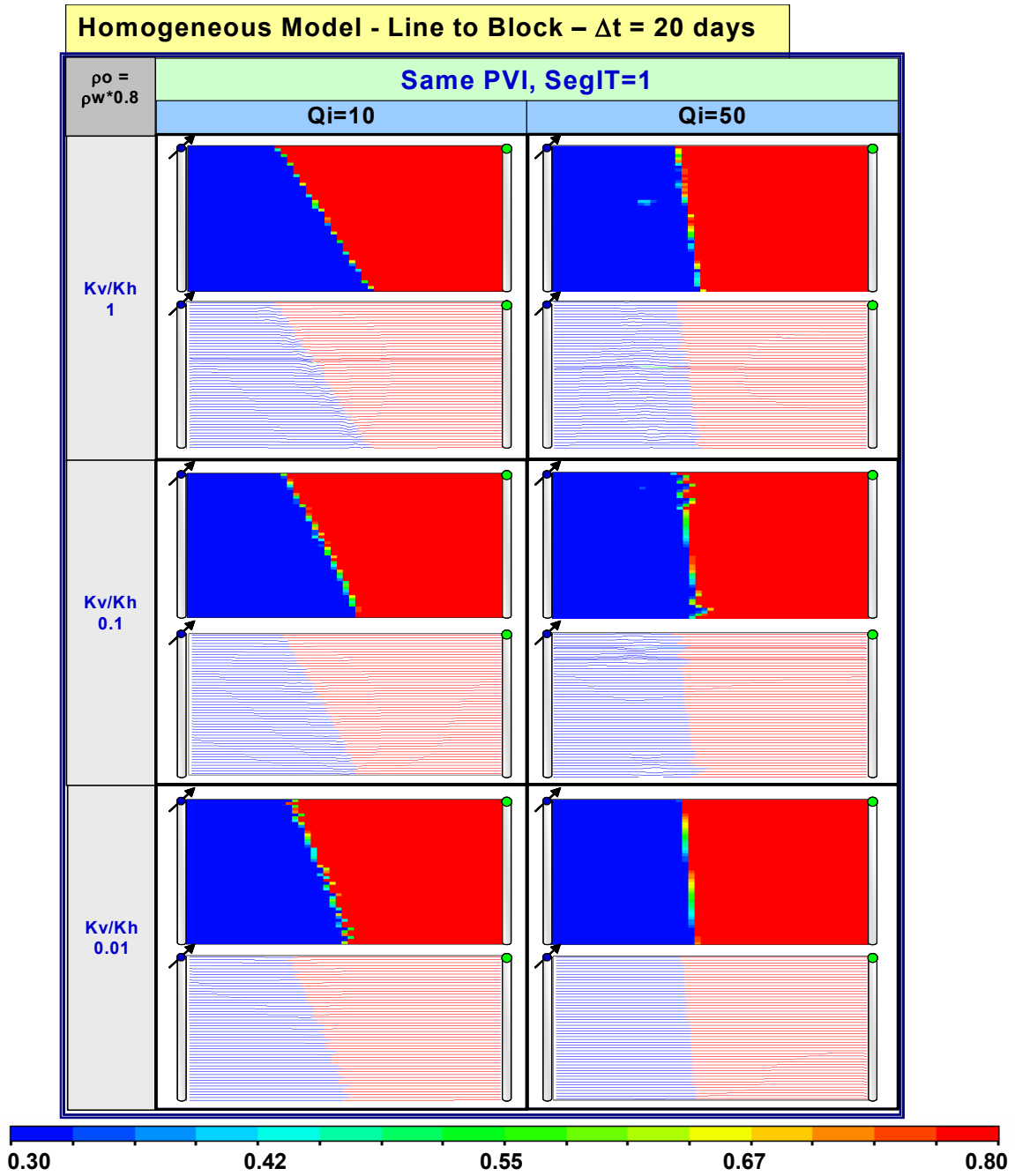


Fig. 4.62 Homogeneous line to block at same PVI using $\Delta t=20$ days.

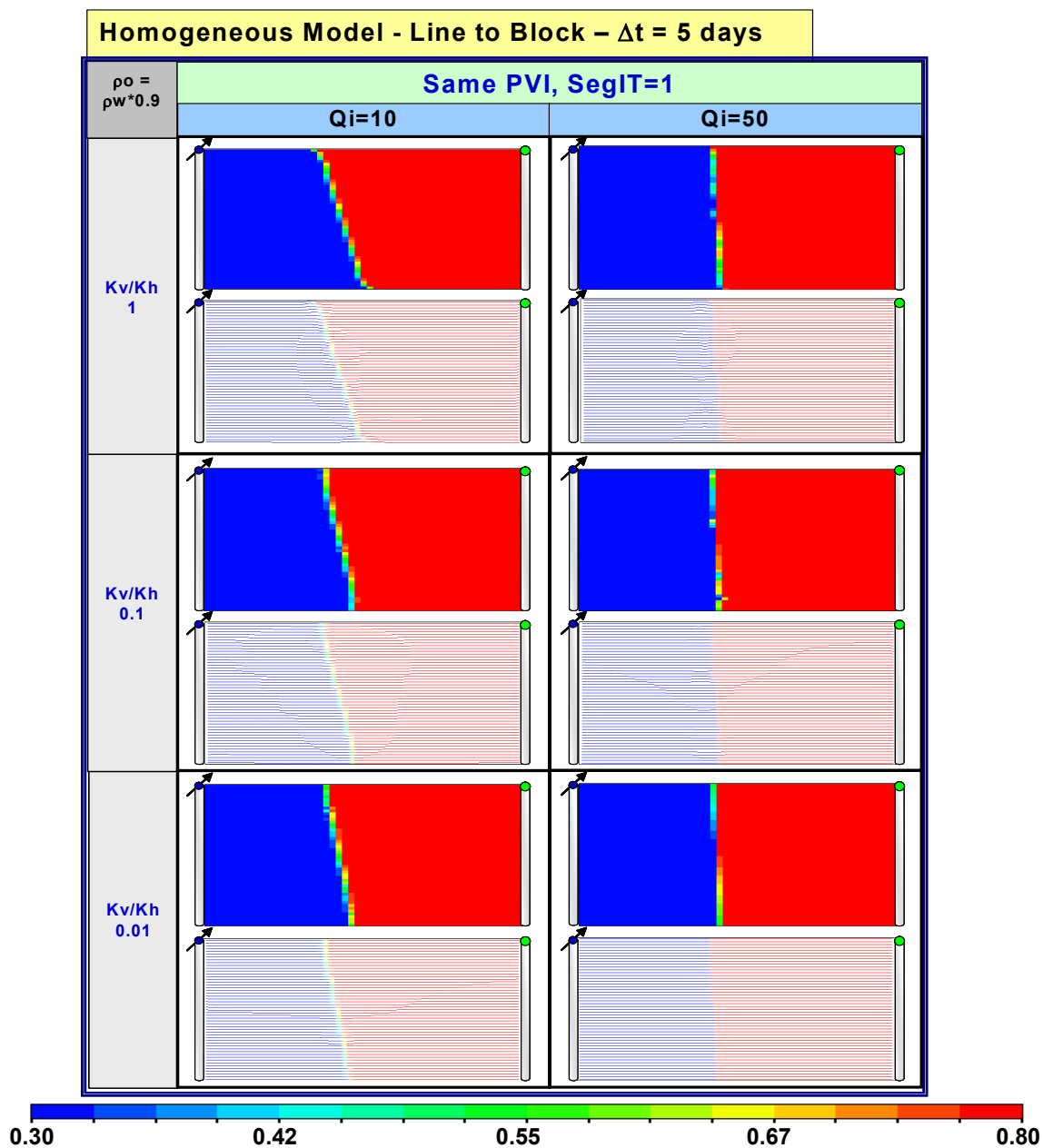


Fig. 4.63 Homogeneous line to block at same PVI using $\Delta t=5$ days.

The results shown in the last figures 4.62 and 4.63, determine that a high injection rate can not allow modeling the segregation gravity effect during streamline simulation.

As we mentioned before, additional sensitivities were performed to taking into account the gravity effect in a heterogeneous model during SL simulation, the results of those numerical exercise are presented in figures 4.65 to 4.76.

The heterogeneous permeability distribution is shown in the following Fig 4.64.

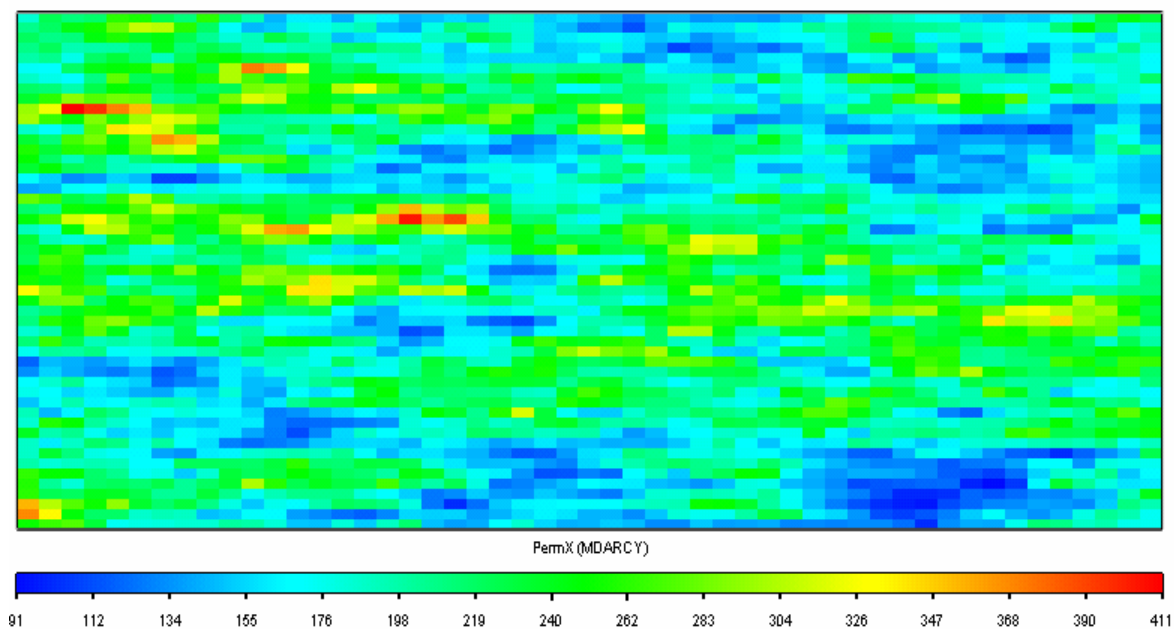


Fig. 4.64 PermX distribution for heterogeneous model in gravity cases.

The results of Line to block saturation mapping for heterogeneous model, varying K_v/K_h , using $\rho_o = \rho_w * 0.8$ ($\Delta\rho = 12.5$) with $\Delta t = 20$ days are shown in Fig. 4.65. The premises applied to the model but using different $\Delta\rho$ of 6.25 is shown in Fig. 4.66.

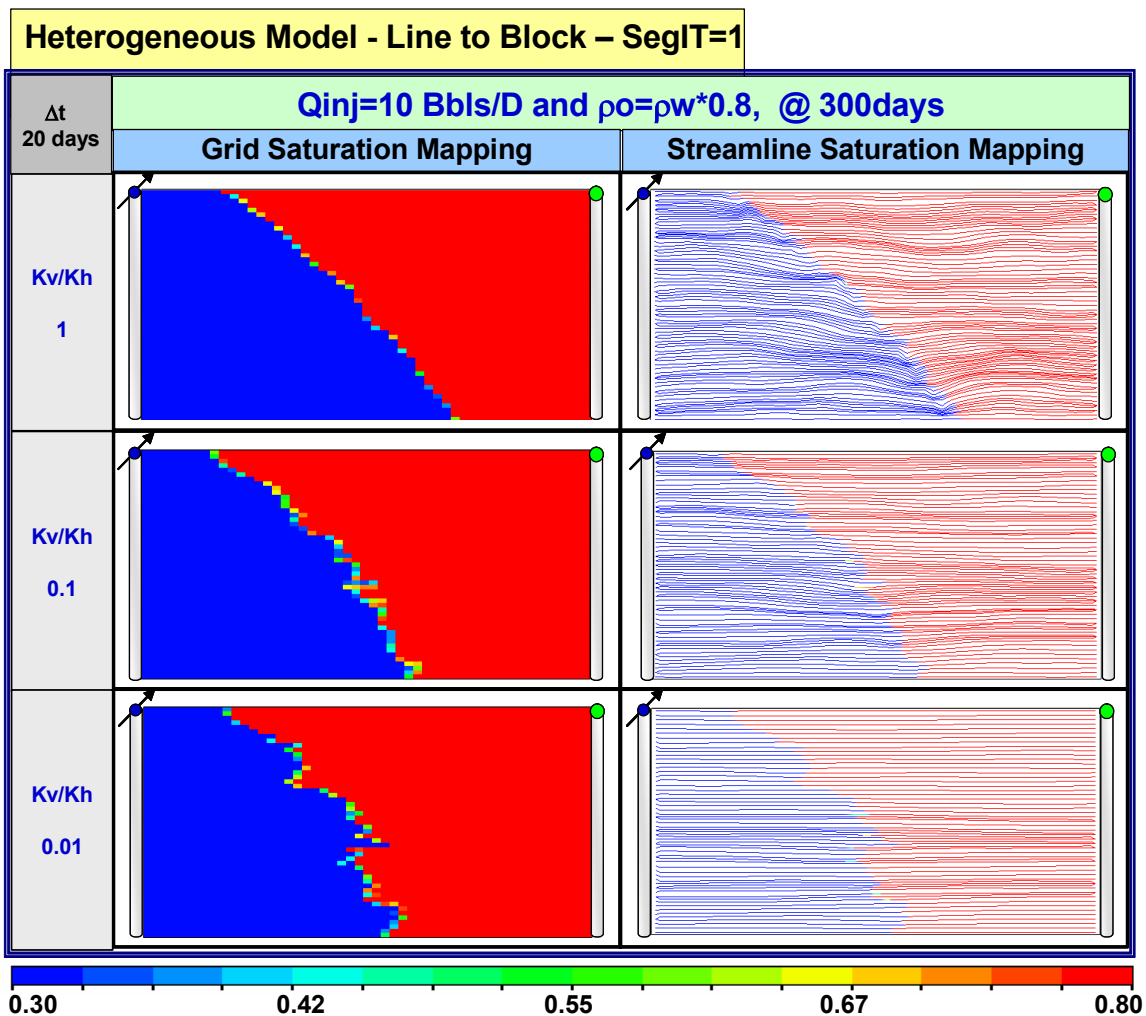


Fig. 4.65 Heterogeneous line to block varying K_v/K_h and using $\rho_o = \rho_w * 0.8$ at $\Delta t = 20$ d.

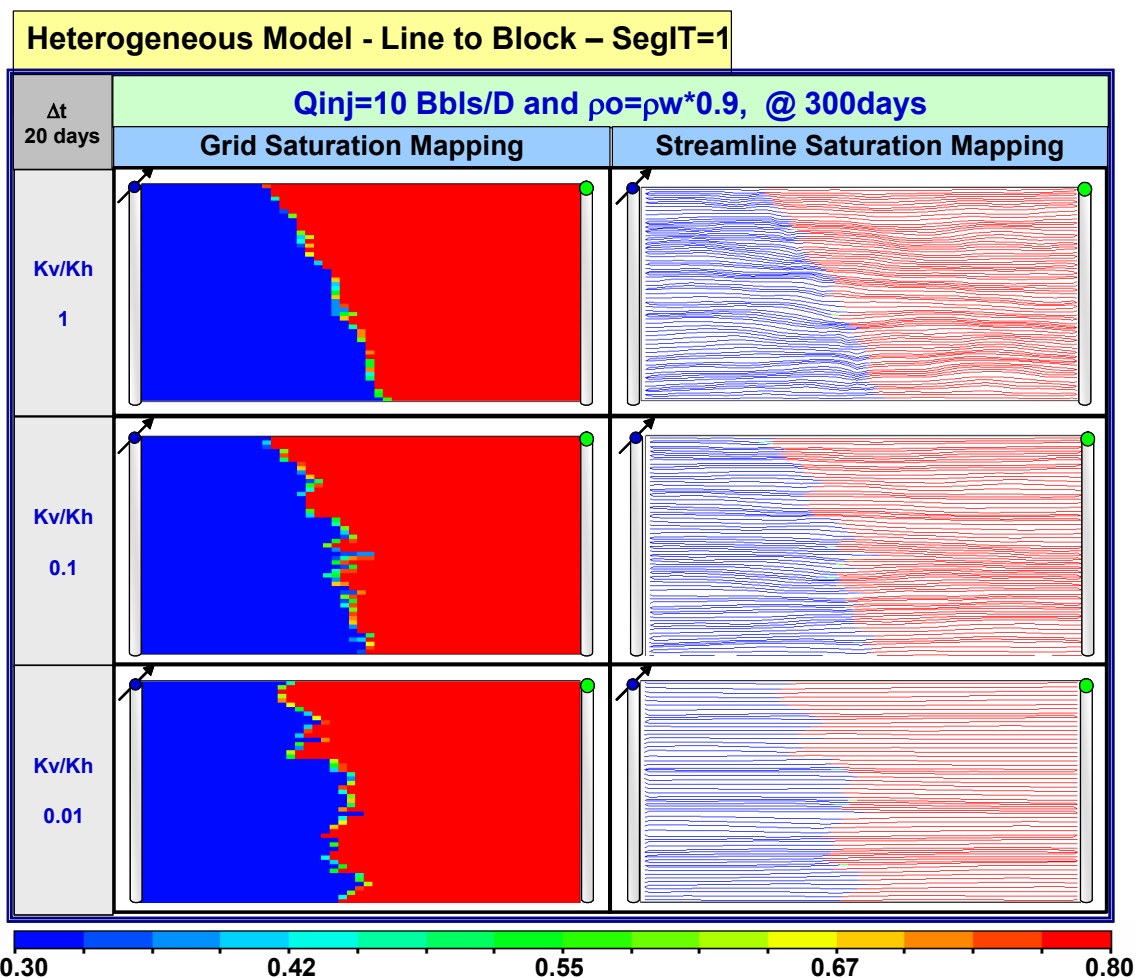


Fig. 4.66 Heterogeneous line to block varying Kv/Kh and using $\rho_o=\rho_w*0.9$ at $\Delta t=20$ d.

Last two figures demonstrated that the variation effect produced by the gravity segregation based in Kv/Kh changes and $\Delta\rho$ variation. As expected, the parameters $\Delta\rho$ and Kv/Kh can cause different behavior in the solution obtained from the gravity segregation option in SL models. Higher $\Delta\rho$ values introduce major influence in the results based on this gravity conditions. Moreover, lower Kv/Kh values introduce more smearing in the results.

Figure 4.67 describes the effect caused by changing the time step sizes, and figures 4.68, 4.69, and 4.70 consider the changes in the SegIT parameter, those results lead to ensure that Δt and SegIT are not an impacting element during SL in heterogeneous model.

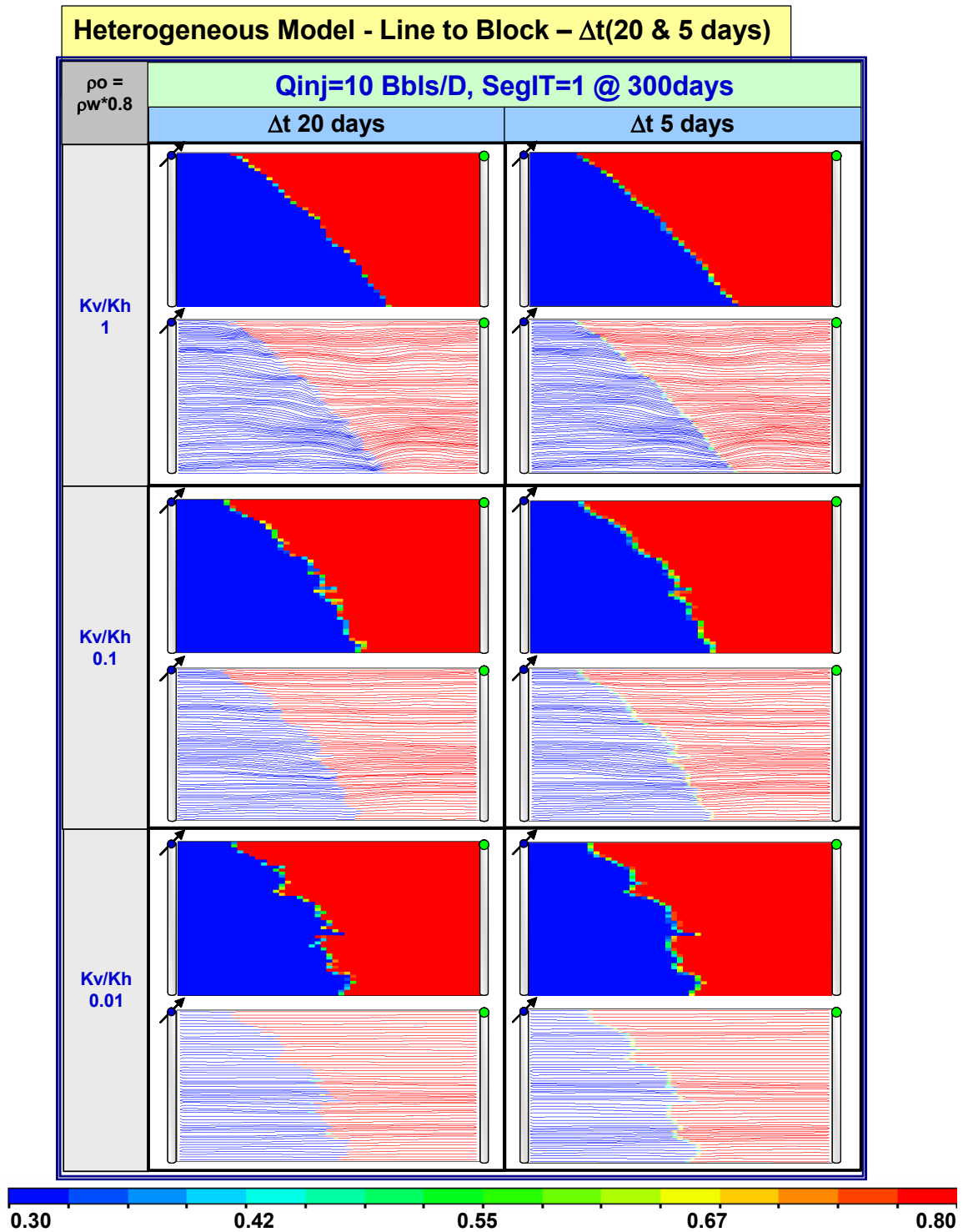


Fig. 4.67 Heterogeneous line to block varying K_v/K_h and Δt .

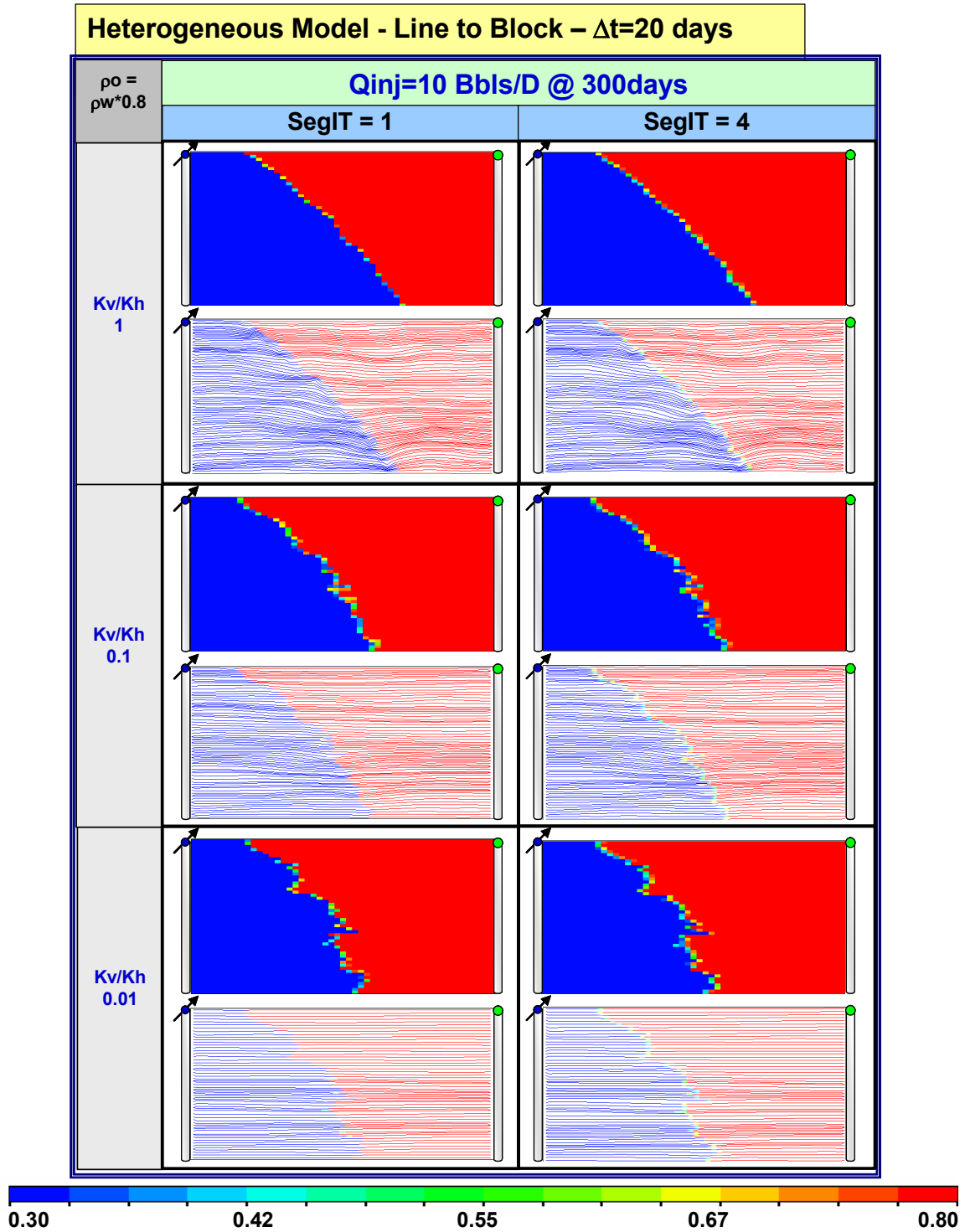


Fig. 4.68 Heterogeneous line to block varying K_v/K_h and SegIT for $\Delta t=20$ days.

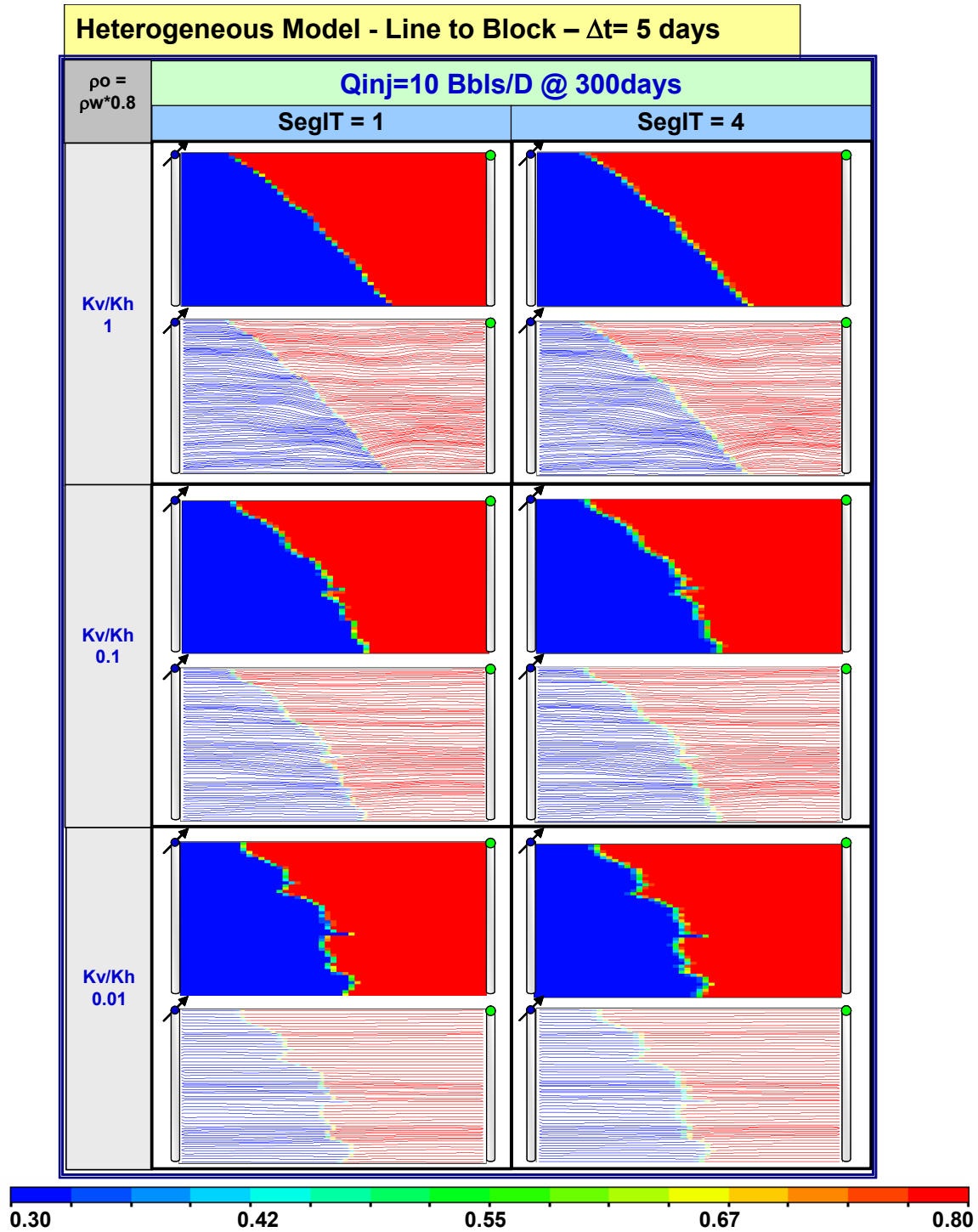


Fig. 4.69 Heterogeneous line to block varying K_v/K_h and SegIT for $\Delta t = 5$ days

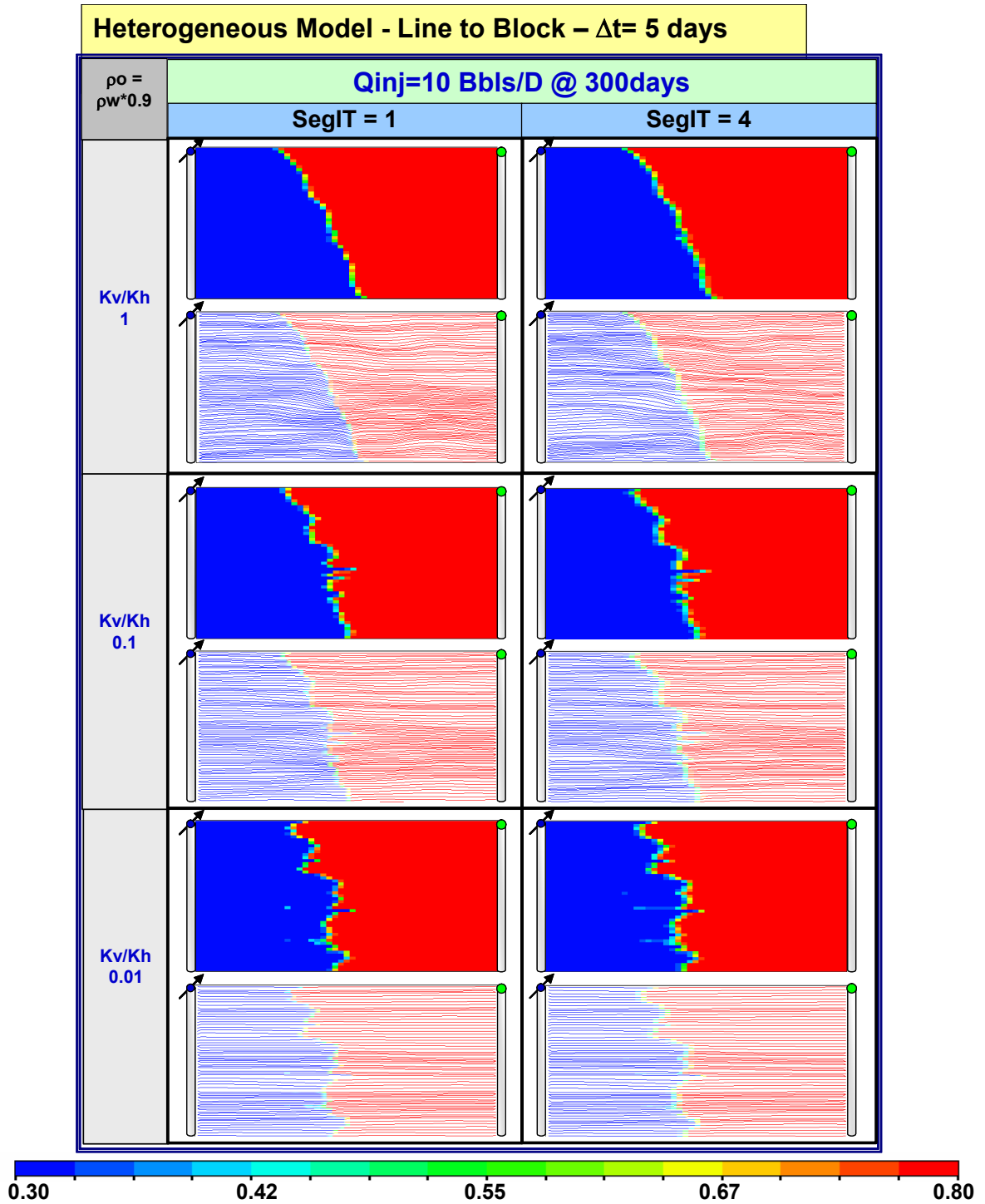


Fig. 4.70 Heterogeneous line to block using $\rho_o = \rho_w * 0.9$ and varying SegIT for $\Delta t = 5$ d.

Concerning to the other mapping saturation method (Line to Line), the results shown worst solution than the Line to block, even for small values of Kv/Kh (0.01) which in previous experiment exhibited an acceptable solution. Definitely, Line to line

approach is not recommended to be applied during SL simulation of for Heterogeneous pattern. Comparative results on this topic are presented in figures 4.71 to 4.72.

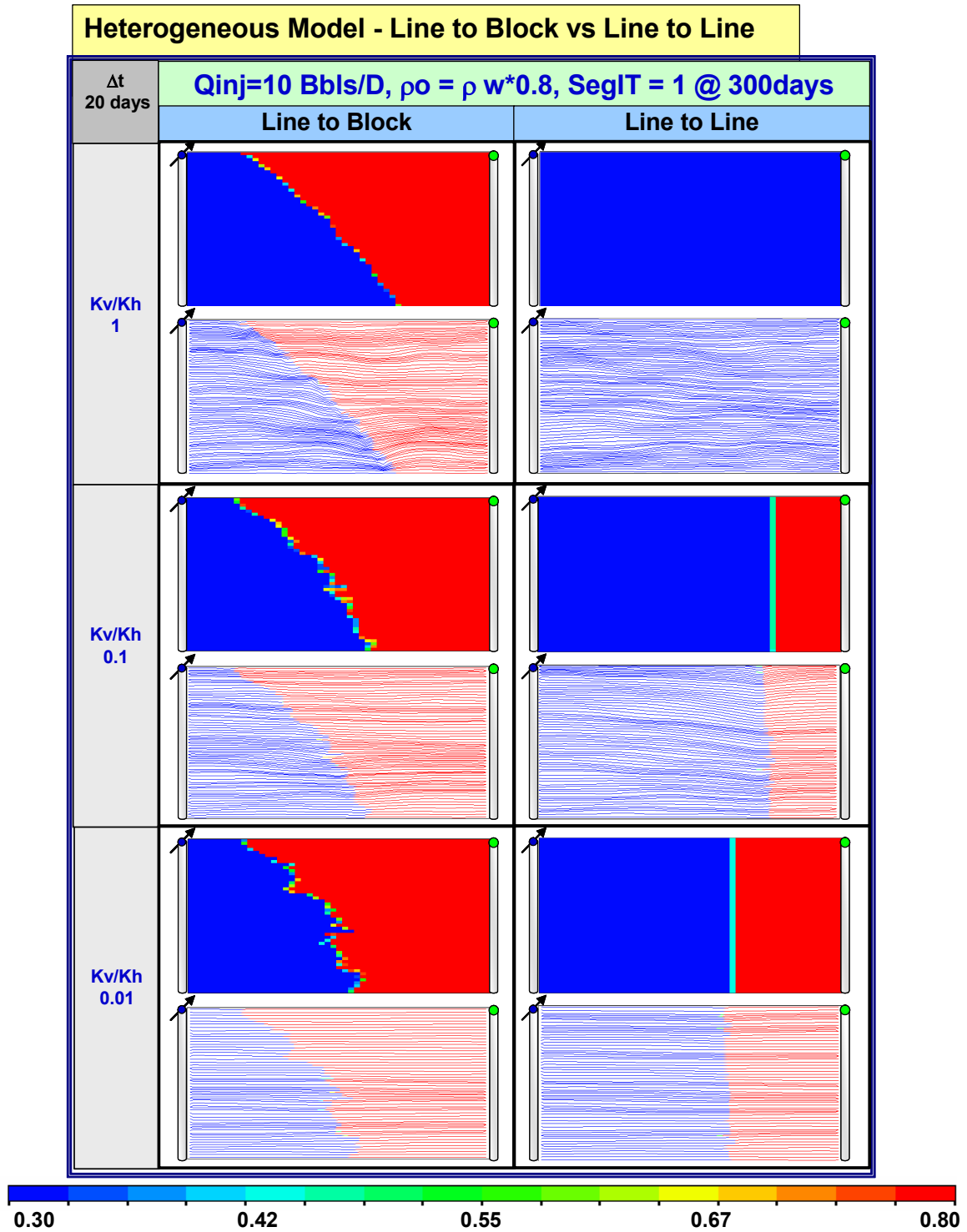


Fig. 4.71 Heterogeneous saturation mapping comparison varying Kv/Kh

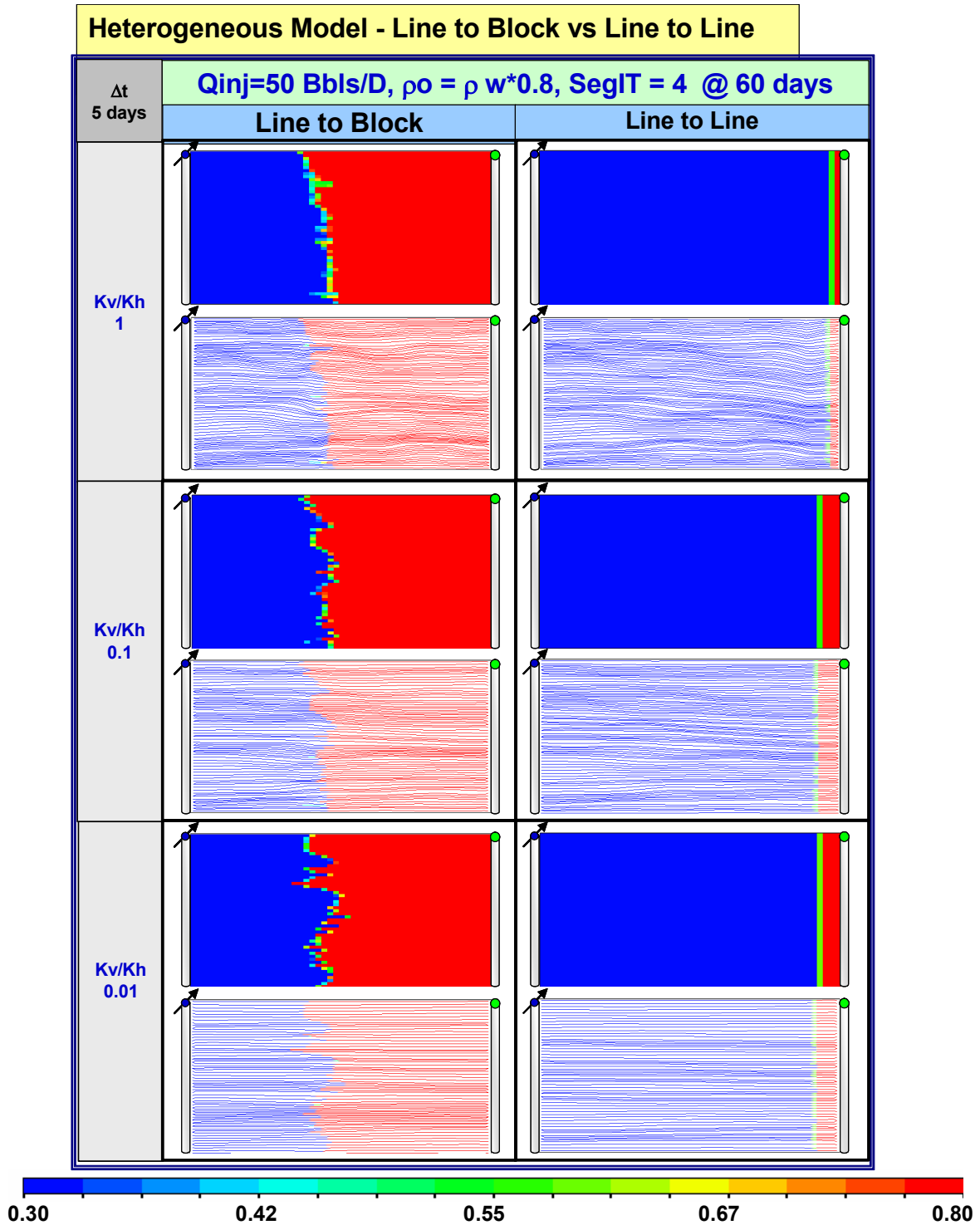


Fig. 4.72 Heterogeneous saturation mapping comparison for a higher injection

For displacements dominated by heterogeneity taking into account gravity segregation, the injection front movement shown that the numerical streamline method does not converge very well and present stability problems for the solution. Additionally, the Line to Line method is very inconvenient to model heterogeneities cases and consider gravity effect in SL.

Two-phase gravity problems used to be more difficult to model with the streamline method. However, the new advances in this subject permit to develop field models that can count gravity effects in multiphase flow.

In comparison with conventional simulation methods, the streamline method still retains orders-of-magnitude speed-ups and accuracy. The speed-up depends on the size of the gravity number, the model size, and the type of displacement process. Thereby, SL method is considered as a very applicable, modern, innovative and useful technology in the reservoir simulation area.

CHAPTER V

CONCLUSIONS AND RECOMMENDATIONS

5.1. Conclusions

- Line to Block saturation mapping provides crosswise communication among the streamlines in the grid block scale. Moreover, the averaging computation used in this approach leads to loss of the sub-grid resolution in saturation, thus negating an important advantage of streamline simulation. Also, the mapping will introduce material balance error that will depend on the difference between the grid block pore volume and the volume covered by the streamlines crossing through the grid block.

- Line to line mapping method preserves the displacement front. However, mapping of saturation from line to line is computationally more demanding but reduces numerical dispersion because there is no mixing of streamlines at the grid block scale. The mapping can lead to mass balance errors higher than the Line to block method.

- Higher mobility ratio (less favorable) displacement problem can be solved more easily and accurately using SL method compared to lower mobility (favorable) displacement.

- Pressure time step size is an important element to consider in the accuracy of streamlines model. This element can affect the homogeneous and heterogeneous displacement in similar way. Optimization of the number of pressure updates during streamline simulation not only to improve the computational efficiency but also to reduce the mapping errors.

- Streamline simulation results are highly dependent on the number of stream lines that are traced in a model. The greater the number of streamlines that are launched

in a model, the fewer number of grid blocks that are missed with the streamlines, resulting in improved accuracy in solution.

- Gravity segregation effect is influenced by the gravity number N_g , K_v/K_h ratio, gravity segregation time step Δt , and density difference $\Delta\rho$ showing different behavior in the solution during SL using Line to Block mapping in homogeneous displacements. Higher $\Delta\rho$ values introduce major impact in the results. Use of low gravity number or low K_v/K_h values allows Line to Line mapping without significant loss in accuracy.
- The gravity segregation effect is not significant when a high injection rate is used, the number of iterations on the segregation option doesn't have an important effect in the streamline model solution for high injection rate or different $\Delta\rho$ or time step size when using a high injection rate.
- For displacements dominated by heterogeneity and in the presence of significant segregation, the injection front movement shows that the numerical streamline method does not converge very well and present stability problems for the solution.
- Comparison with the conventional simulation methods shows that the streamline method provides better speed-ups and accuracy, for two-phase water-oil flow and in the presence of moderate gravitational effects.

5.2. Recommendations

The sensitivity analysis performed using streamline models are based on synthetic cases. It's highly recommended to run some field cases in order to have real field results.

Three phase flow analysis using streamline simulation is an excellent additional issue to continue this research. There are too many unresolved issues in this matter.

REFERENCES

1. Kulkarni, K., Datta-Gupta, A. and Vasco, D.: "A Streamline Approach to Integrating Transient Pressure Data into High Resolution Reservoir Models," *SPE Journal* (September 2001) **6**, No. 3, 273-280.
2. Thiele, M., Batycky, R., Blunt, M., and Orr, J.: "Simulating Flow in Heterogeneous Systems Using Streamtubes and Streamline," paper SPE 27834 presented at the 1994 SPE Improved Oil Recovery Symposium, Tulsa, OK, 17-20 April.
3. Muskat, M.: *Flow of Homogeneous Fluids Through Porous Media*. Intl. Human Resources Development Corp., Boston, MA (1982).
4. LeBlanc, J. and Caudle, B.: "A Streamline Model for Secondary Recovery," *SPEJ* (March 1971) **9**, No. 1, 7-12.
5. Martin, J. and Wegner, R.: "Numerical Solution of Multiphase Two-Dimensional Incompressible Flow Using Streamtube Relationships," *SPE Journal* (October 1979) **3**, No. 13, 267.
6. Bratvedt, F., Bratvedt, K., Buchholz, C. F., Gimse, T., Holden, H., Holden, L. and Datta-Gupta A. and King M.J.: "A Semianalytic Approach to Tracer Flow Modeling in Heterogeneous Permeable Media," *Adv. in Water Resources* (1995), **18**, No. 1, 9.
7. Emanuel, A. and Miliken, J.: "The Application of Streamtube Techniques to Full Field Waterflood Simulation," paper SPE 30758 presented at the 1995 SPE Annual Meeting, Dallas, TX, 3-5 October.
8. King, M. J. and A. Datta-Gupta: "Streamline Simulation: A Current Perspective", *In Situ* (1998), **22**, No. 1, 91-140.
9. Bratvedt, F., Gimse, T. and Tegnander, C.: "Streamline Computations for Porous Media Flow Including Gravity," *Transport in Porous Media* (1996), **25**, 63.
10. Pollock, D.: "Semi-Analytical Computation of Path Lines for Finite Difference Models," *Ground Water* (November/December 1988) **26**, No. 6, 743.
11. Shafer, J.: "Reverse Pathline Calculation of Time-Related Zones in Nonuniform Flow," *Ground Water* (May/June 1987) **25**, No. 3, 283.

12. Fay, C. and Prats. M.: "The Application of Numerical Methods to Cycling and Flooding Problems," *Proc.*, Third World Petroleum Congress, The Hague, Netherlands (1951) 555.
13. Datta-Gupta A. and King M.J.: "A Semianalytic Approach to Tracer Flow Modeling in Heterogeneous Permeable Media," *Adv. in Water Resources* (1995), **18**, No. 1, 9.
14. Batycky, R., Blunt, M. and Thiele, M.: "A 3D Field Scale Streamline-Based Reservoir Simulator," paper SPE 36726 presented at the 1997 SPE Annual Technical Conference and Exhibition, Denver, CO, 6-9 October.
15. Blunt, M., Lui, K., Thiele, M.: "A Generalized Streamline Method to Predict Reservoir Flow," *Petroleum Geoscience* (1996) **2**, 259-269.
16. Samier, P., Quettier, L. and Thiele, M.: "Applications of Streamline Simulations to Reservoir Studies," paper SPE 66362 presented at the 2001 SPE Reservoir Simulation Symposium, Houston, TX, 11-14 February.
17. Lolomari, T., Bratvedt, K. and Crane, M.: "The Use of Streamline Simulation in Reservoir Management: Methodology and Case Studies," paper SPE 63157 presented at the 2000 SPE Annual Technical Conference and Exhibition, Dallas, TX, 1-4 October.
18. Baker, R., Kuppe, F., Bora, R., Chugh, S., Stojanovic, S. *et al.*: "Full-Field Modeling Using Streamline-Based Simulation: Four Case Studies," paper SPE 77172 presented at the 2001 SPE Reservoir Simulation Symposium, Houston, TX, 11-14 February.
19. Peddibhotla, S., Datta-Gupta, A. and Xue, G.: "Multiphase Streamline Modeling in Three Dimensions: Further Generalizations and a Field Application," paper SPE 38003 presented at the 1997 SPE Reservoir Simulation Symposium, Dallas, TX, 8-11 June.
20. Tchelepi, H. and Orr, F.: "Interaction of Viscous Fingering, Permeability Heterogeneity, and Gravity Segregation in Three Dimensions," *SPHERE* (November 1994) **1**, 266.
21. King, M., Blunt, M., Mansfield, M. and Christie, M.: "Rapid Evaluation of the Impact of Heterogeneity on Miscible Gas Injection," paper SPE 26079 presented at the 1993 SPE Western Regional Meeting, Anchorage, AK, 26-28 May.
22. Ingebrigsten, L. , Bratvedt, F. and Berge, J.: "A Streamline Based Approach to Solution of Three-Phase Flow," paper SPE 51904 presented at the 1999 SPE Reservoir Simulation Symposium, Houston, TX, 14-17 February.

23. Aziz, K. and Settari, A.: *Petroleum Reservoir Simulation*, Applied Science Publishers, Essex, England (1979).
24. Ponting, D.: "Hybrid Streamline Methods," paper SPE 39756 presented at the 1998 Asia Pacific Conference on Integrated Modeling, Kuala Lumpur, Malaysia, 23-24 March.
25. Gonzalez, P., Kindelan, M. and Mustieles, F.: "Streamline Methodology Using an Efficient Operator Splitting for Accurate Modeling of Capillarity and Gravity Effects," paper SPE 79693 presented at the 2003 SPE Reservoir Simulation Symposium, Houston, TX, 2-5 February.
26. Osako, I., Datta-Gupta, A. and King, M.: "Timestep Selection During Streamline Simulation via Transverse Flux Correction," paper SPE 79688 presented at the 2003 SPE Reservoir Simulation Symposium, Houston, TX, 3-5 February.
27. Mallison, M., Gerritsen, M. and Matringe, S.: "Improved Mappings for Streamline-Based Simulation," paper SPE 89352 presented at the 2004 SPE Symposium on Improved Oil Recovery, Tulsa, OK, 17-21 April.
28. Jessen, K. and Orr, F.: "Gravity Segregation and Compositional Streamline Simulation," paper SPE 89448 presented at the 2004 SPE Symposium on Improved Oil Recovery, Tulsa, OK, 17-21 April.
29. Schlumberger Geoquest: *FRONTSIM User guide 2003A*, Schlumberger Information Solution, Texas A&M University, College Station, TX (2003).
30. Berenblyun, R., Saphiro, A., Jessen, K., Stenby, E. and Orr, F.: "Black Oil Streamline Simulator with Capillary Effects," paper SPE 84037 presented at the 2003 SPE Annual Technical Conference and Exhibition, Denver, CO, 5-8 October.
31. Schlumberger Geoquest: *ECLIPSE 100 Reference Manual 2003A*, Schlumberger Information Solution, Texas A&M University, College Station, TX (2003).
32. Sabir K.: "Velocity Models, Material Balance and Solution Convergence in Streamline-Based Simulation", MS thesis, Texas A&M University, College Station, TX.
33. Datta-Gupta, A.: "Streamline Simulation: A Technology Update," paper SPE 65604 *SPE Distinguished Author Series*, December 2000.

VITA

Fady Ruben Chaban Habib
Petroleum Eng. Dept.
3116 TAMU
College Station, TX USA, 77843
Ph: (979)847-8797
chabanf@yahoo.com

PROFILE

Reservoir engineer with nine years of experience in reservoir characterization and simulation engineering. Specific knowledge in reservoir simulation optimization, integrated reservoir characterization, research and development of new reservoir simulation technologies, Design and analysis of exploitation schemes for reservoir performance. Currently, involved in research concerning to streamline simulation. Special interest in development of new reservoir characterization procedures, application of high-resolution numerical schemes for reservoir simulation, reservoir data analysis techniques, and streamline simulation subject.

EDUCATION

Master of Science. Petroleum Engineering. Texas A&M University. December 2004

Bachelor of Science. System Engineering. Universidad Bicentenario de Aragua.
July 1995

EXPERIENCE

Texas A&M University. Graduate Student. 2002-2004

PDVSA Intevp. Researcher in Reservoir Simulation. 1995-2002